Insitu Measurement of Pavement Distress and Causal Mechanisms in Expansive Soil along Alabama Highway 5

by

Dan T. Jackson

A thesis submitted to the Graduate Faculty of
Auburn University
in partial fulfillment of the
requirements for the Degree of
Master of Science

Auburn, Alabama
December 10, 2016

Keywords: expansive clay, instrumentation, pavement

Copyright 2016 by Dan T. Jackson

Approved by

J. Brian Anderson, Ph.D., P.E., Chair, Associate Professor of Civil Engineering
David Timm, Ph.D., P.E., Brasfield & Gorrie Professor of Civil Engineering
Jack Montgomery, Ph.D., Assistant Professor of Civil Engineering

ABSTRACT

Alabama Highway 5 is a farm-to-market road built directly on an expansive clay subgrade. Moisture fluctuations cause the soil to shrink and swell, resulting in severe pavement distress. Laboratory testing has been performed to characterize the shrink-swell behavior of the subgrade soil. Swell pressures of up to 1500 psf have been observed in the laboratory. Several remediation strategies have been implemented at AL-5 in an attempt to reduce the need for pavement maintenance. These techniques include increased drainage, vertical moisture barriers, lime stabilization, and paved shoulders. To evaluate the performance of these test sections and further characterize the soil behavior, field instrumentation has been installed including soil moisture sensors, soil suction sensors, pore water pressure sensors, and asphalt strain gages. Monitoring is ongoing and will continue for the next two years.

ACKNOWLEDGMENTS

I would like to thank the Alabama Department of Transportation for their continued support of this research project. I would also like to thank my committee chair, Dr. J. Brian Anderson for his guidance and support. I would also like to acknowledge the other members of my committee, Dr. David Timm and Dr. Jack Montgomery. I would also like to thank the following people for their hard work with this project: Dylan Jones, Elizabeth Stallings, Jeremy Herman, Lester Lee, Pavlo Voitenko, Justin McLaughlin, Jonathan Hogan, Matt Barr, and Andy Weldon. Finally, I would like to thank my family, but especially my wife, Olivia. Above all these, I would like to thank my Lord Jesus Christ, and acknowledge that the fear of the Lord is the beginning of wisdom, and the love of the Lord is what makes life worth living.

TABLE OF CONTENTS

LIST OF TABLES

LIST OF FIGURES

LIST OF ABBREVIATIONS AND SYMBOLS

AADT	Average Annual Daily Traffic
AL	Alabama
AL-5	Alabama Highway 5
ALDOT	Alabama Department of Transportation
a_m	Coefficient of Compressibility with respect to Change in Matric Suction
ASG	Asphalt Strain Gage
ASTM	American Society of Testing and Materials
a_t	Coefficient of Compressibility with respect to Change in Net Normal Stress
a_v	Coefficient of Compressibility
b_m	Coefficient of Water Content Change with respect to Change in Matric Suction
b_t	Coefficient of Water Content Change with respect to Change in Net Normal Stress
CBR	California Bearing Ratio
cm	centimeters
dBd	Antenna Gain with respect to a Dipole Antenna
de	Incremental Change in Void Ratio
dw	Incremental Change in Water Content
$d(u_a - u_w)$	Incremental Change in Matric Suction
$d(\sigma_{mean} - u_a)$	Incremental Change in Net Normal Stress

e	Void Ratio
ECH_2O	Capacitance Moisture Content Sensor
FHWA	Federal Highway Administration
ft	feet
g	grams
G_s	Specific Gravity of Solids
HAE	High Air Entry
hr	Hours
IAEA	International Atomic Energy Agency
in	Inches
IRI	International Roughness Index
IWP	Inside Wheel Path
KHCTR	Korean Highway Corporation Test Road
kPa	Kilopascals
LL	Liquid Limit
m	Meters
MP	Mile Point
mS/m	Millisemens per Meter
mV	Millivolts
NCAT	National Center for Asphalt Technology
NCHRP	National Cooperative Highway Research Program
No.	Number
OWP	Outside Wheel Path

pcf	Pounds per Cubic Foot
PCI	Pavement Condition Index
PI	Plasticity Index
psf	Pounds Per Square Foot
s	seconds
SWCC	Soil Water Characteristic Curve
TDR	Time Domain Reflectometry
TS	Test Section
T_s	Surface Tension
u_a	Pore Air Pressure
$(u_a - u_w)$	Matric Suction
USCS	Unified Soil Classification System
USDA	United States Department of Agriculture
$\bar{u}_v$	Partial Pressure of Pore Water Vapor
$\bar{u}_{v0}$	Saturation Pressure of Water Vapor
u_w	Pore Water Pressure
V	Volts
V_T	Total Volume
V_w	Volume of Water
v_{w0}	Specific Volume of Water
VWC	Volumetric Water Content
r	Radius of Curvature
R	Universal Gas Constant

S	Degree of Saturation
T	Temperature
w	Gravimetric Water Content
ω_v	Molecular Mass of Water Vapor
ΔV_0	Initial Overall Volume
ΔV_a	Change in Volume of Air
ΔV_v	Change in Volume of Voids
ΔV_w	Change in Volume of Water
θ	Volumetric Water Content
π	Osmotic Suction
ρ_d	Dry Density
ρ_w	Density of Water
σ	Total Normal Stress
σ'	Effective Normal Stress
σ_{mean}	Average Normal Stress
$(\sigma - u_a)$	Net Normal Stress
ψ	Total Suction

CHAPTER 1: INTRODUCTION

1.1 Background

Expansive clays are prevalent in much of the United States and around the world (Nelson and Miller 1992). These soils undergo drastic volume changes due to changes in moisture content. This can lead to damage to pavements and lightly loaded foundations that are underlain by expansive soils. Estimates place the economic losses caused by expansive soils at $9 billion annually, unadjusted for inflation (Jones 1981).

Alabama Highway 5 (AL-5) is a farm-to-market road with large sections constructed directly on expansive clay. AL-5 is a major route between Birmingham, AL and Mobile, AL and carries a lot of truck traffic. Because of the shrinking and swelling of the subgrade with seasonal moisture variations, the pavement is in very poor condition. Large patches, rutting, and very long longitudinal cracks are prevalent on AL-5 as seen in Figure 1 and Figure 2. Resurfacing is necessary every several years in order to maintain a safe riding surface.

Figure 1: Pavement Distress at AL-5 (Herman 2015)

Figure 2: Longitudinal Cracking at AL-5 (Herman 2015)

The Alabama Department of Transportation (ALDOT) sponsored a research project along a section of AL-5 in which several insitu remediation techniques were implemented to attempt to improve the volumetric stability of the subgrade. The goal was to extend the life of the pavement and reduce the resurfacing interval. Long term monitoring of the subgrade and pavement was

included as part of this project to measure the behavior of the subgrade, the impact of the subgrade on the pavement, and the effectiveness of the remediation techniques.

1.2 Objective

The primary objective of this investigation is to measure the shrink-swell behavior of the subgrade at AL-5 and determine the impact of the subgrade on the roadway pavement. Sub-objectives include:

- Measure changes in the moisture content, suction, and pore pressure of the subgrade soil.
- Measure the pavement distress.
- Develop efficient methods of installing instrumentation that can be used to evaluate a soil for expansive potential and depth of active zone.

1.3 Scope

To accomplish the research objectives, instrumentation was installed in the subgrade and pavement of AL-5. This included moisture content sensors, suction sensors, piezometers, and asphalt strain gages. A weather station was also installed at AL-5 to monitor environmental conditions. To facilitate continuous data collection, data acquisition hardware was installed that can be used to remotely monitor the sensors. International roughness index (IRI) data was also collected periodically to evaluate pavement distress. Finally, access tubes for a nuclear moisture probe were installed and readings were taken periodically.

Included in the report below is the background information and a review of the relevant literature. The methodology for selecting the instrumentation and data collection equipment is described along with the installation procedures. Preliminary data collected from AL-5 is also included along with an analysis, summary, and conclusions.

CHAPTER 2: BACKGROUND AND LITERATURE REVIEW

2.1 Overview of Unsaturated Soil Mechanics

Because shrink-swell behavior is a phenomenon occurring primarily in unsaturated soils, it is fitting to review the relevant unsaturated soil mechanics principles. This will provide clarity in later discussions concerning sensor selection and the properties that are to be measured.

2.1.1 Soil as a Four Phase System

Soil is typically thought of as a three phase system composed of soil particles, water, and air. However, for a stress analysis on unsaturated soil, it is appropriate to consider the air-water interface as a fourth phase (Fredlund and Morgenstern 1977). This air-water interface is commonly called the *contractile skin* (Fredlund and Morgenstern 1977). Stress changes in the contractile skin can lead to changes in water content, changes in volume, or changes in shear strength (Fredlund et al. 2012). Figure 3 shows a typical unsaturated soil element with the phases labeled.

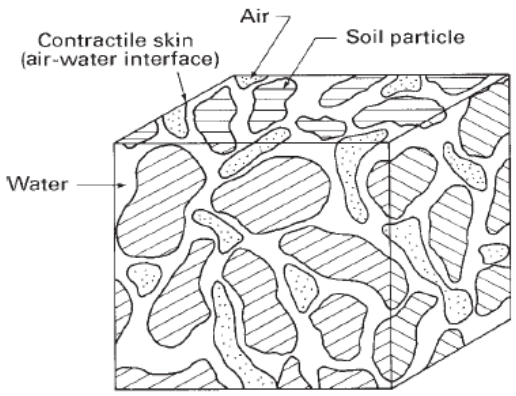

Figure 3: Typical Unsaturated Soil Element with Phases Labeled (Fredlund et al. 2012)

Figure 4 shows the idealized equilibrium condition for the contractile skin. Because the air pressure will be greater than the water pressure in an unsaturated soil, the contractile skin will exhibit a concave curvature toward the air pressure and a tension will be exerted in the contractile skin to maintain equilibrium (Fredlund et al. 2012). The equilibrium condition shown in Figure 4 is given by Equation 1 (Nelson and Miller 1992). Equation 1 is referred to as Kelvin's capillary model (Fredlund and Rahardjo 1993). The surface tension of the contractile skin is a property that varies with temperature (Fredlund and Rahardjo 1993).The pressure difference $u_a - u_w$ in Equation 1 is called the *matric suction*. As can be seen from Equation 1, when matric suction increases, the radius of curvature of the contractile skin decreases.

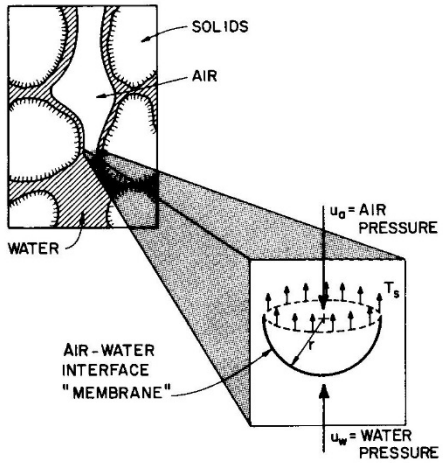

Figure 4: Free Body Diagram of Contractile Skin (Nelson and Miller 1992)

$$\boldsymbol{u_a - u_w = \frac{2T_s}{r}} \qquad \textbf{(1)}$$

Where u_a = air pressure

u_w = water pressure

T_s = surface tension

r = radius of curvature

2.1.2 State Variables for Unsaturated Soils

Fredlund and Rahardjo (1993) define state variables as "non-material variables required for the characterization of a material system." In the context of unsaturated soil mechanics, these state variables can characterize stress equilibrium conditions (*stress state variables*) or can characterize deviations from an initial state (*deformation state variables*). Finally, unique empirical mathematical relationships between state variables can be defined as *constitutive relations* (Fredlund and Rahardjo 1993).

For saturated soils, the stress state and thus the soil behavior is described by the effective stress, given in Equation 2. According to the effective stress concept, soil behavior is governed by the effective stress. Thus, changes in effective stress alter the equilibrium of a saturated soil and are responsible for changes in volume and shear strength (Fredlund et al. 2012).

$$\boldsymbol{\sigma' = \sigma - u_w} \qquad \textbf{(2)}$$

Where σ' = effective normal stress

σ = total normal stress

u_w = pore water pressure

Previously, efforts were made to determine a single effective stress relationship for unsaturated soils (Croney et al. 1958, Bishop 1959, Aitchison 1961, Jennings 1961). However, these relationships incorporated soil properties and thus classify as constitutive relationships rather than stress state descriptions (Fredlund and Rahardjo 1993).

Fredlund and Morgenstern (1977) proposed using two independent stress state variables to describe an unsaturated soil. Their analysis was based on multi-phase continuum mechanics and considered unsaturated soils as a four phase system (Fredlund and Rahardjo 1993). There are

three possible combinations of stress state variables, but the ones typically used are the net normal stress ($\sigma - u_a$) and the matric suction ($u_a - u_w$). These proposed stress variables have been experimentally tested (Fredlund 1973) and have been widely accepted (Fredlund et al. 2012).

The deformation state variables used for unsaturated soils are typically void ratio (e), water content (w), and degree of saturation (S), but other deformation state variables are possible if continuum mechanics notation is used (Fredlund et al. 2012).

2.1.3 Volume Change Behavior and Constitutive Relationships for Unsaturated Soils

Empirical constitutive relationships can be defined for an unsaturated soil that relate changes in stress state variables to changes in deformation state variables. Of particular interest for expansive soils is the volume change relationships. This is analogous to the consolidation equations for a saturated soil in which changes in effective stress are related to changes in void ratio shown in Figure 5.

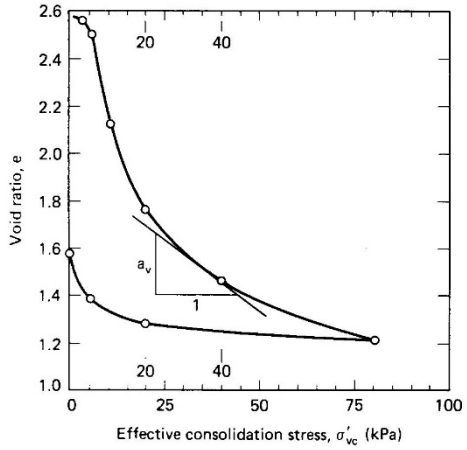

Figure 5: Constitutive Relationship for Saturated Soil Relating Effective Stress and Void Ratio (Holtz and Kovacs 1981)

Because mass is conserved during volume change, for a saturated soil, a change in the volume of voids is equivalent to a change in the volume of water. For an unsaturated soil,

however, continuity is required between the air and water phases as shown by Equation 3 (Fredlund et al. 2012)

It is assumed for Equation 3 that soil particles are incompressible and contractile skin volume change is internal to the soil element.

$$\frac{\Delta V_v}{V_0} = \frac{\Delta V_w}{V_0} + \frac{\Delta V_a}{V_0} \quad \textbf{(3)}$$

Where ΔV_v = change in volume of voids

ΔV_w = change in volume of water

ΔV_a = change in volume of air

V_0 = initial overall volume

Because of this continuity requirement, to completely characterize the volume change behavior of an unsaturated soil, two constitutive relationships are necessary. Typically, the constitutive relationships for the soil structure and the water phase are used. The changes in volume of air can then be solved for by subtraction (Fredlund et al. 2012).

Because volume change is related to two independent stress state variables, the constitutive relationships take the form of a three-dimensional surface (Nelson and Miller 1992). Typical constitutive surfaces and equations are shown below.

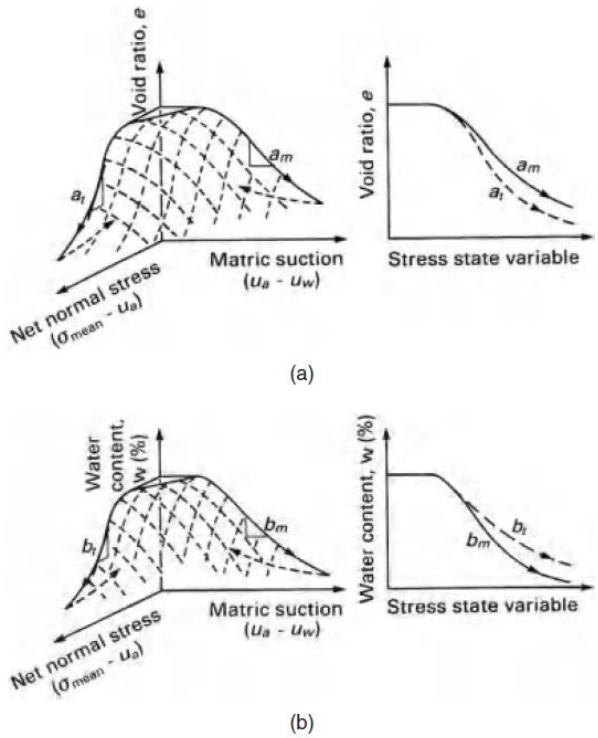

Figure 6: Constitutive Surfaces for an Unsaturated Soil: (a) Void Ratio Constitutive Surface; (b) Water Content Constitutive Surface (Fredlund et al. 2012)

Equations 4 and 5 from Fredlund et al. (2012) describe the constitutive relationships for an unsaturated soil. Because of the nonlinearity of the relationships, an incremental form of the constitutive relationships is used.

$$\boldsymbol{de = a_t d(\sigma_{mean} - u_a) + a_m d(u_a - u_w)} \quad \textbf{(4)}$$

$$\boldsymbol{dw = b_t d(\sigma_{mean} - u_a) + b_m d(u_a - u_m)} \quad \textbf{(5)}$$

Where de = incremental change in void ratio

dw = incremental change in water content (gravimetric)

$d(\sigma_{mean} - u_a)$ = incremental change in net normal stress

$d(u_a - u_w)$ = incremental change in matric suction

a_t = coefficient of compressibility with respect to change in net normal stress

a_m = coefficient of compressibility with respect to change in matric suction

b_t = coefficient of water content change with respect to change in net normal stress

b_m = coefficient of water content change with respect to change in matric suction

$\sigma_{mean} = \frac{\sigma_1+\sigma_2+\sigma_3}{3}$

u_a = pore air pressure

u_w = pore water pressure

It should be noted that because of hysteresis, the constitutive relationship for loading and unloading is independent. The same is likewise true for wetting and drying (Fredlund et al. 2012). This is demonstrated in Figure 7.

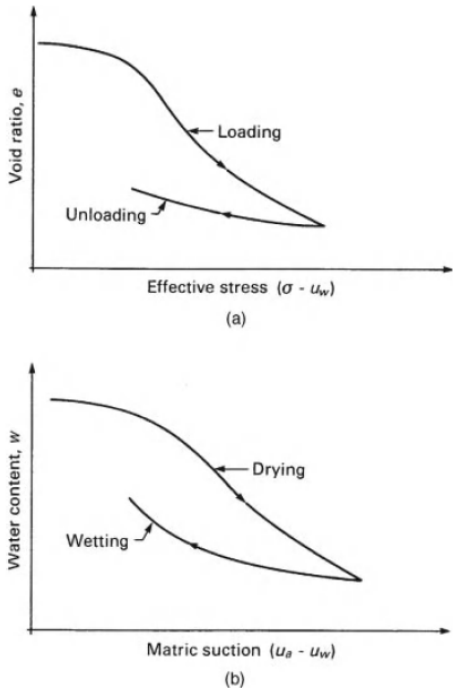

Figure 7: Hysteresis in Constitutive Relationships: (a) Loading and Unloading Curves for Saturated Soil; (b) Drying and Wetting Curves for Incompressible Chalk (Fredlund et al. 2012)

As can be seen in the above figures and equations, when the net normal stress is constant (a good assumption for an existing structure or pavement) volume change is entirely dependent on changes in matric suction.

2.2 Soil Suction

As seen above, a primary component driving volume change in expansive soils is changing matric suction. Because of this, further attention will be given to soil suction.

2.2.1 Components of Soil Suction

In addition to matric suction, *osmotic suction* is present in soils. Osmotic suction is caused by the presence of salts and cations in the soil pore water. Cations held closely to clay particle surfaces will exist in higher concentrations than in the bulk pore water solution. The pressure needed to balance the forces caused by this is called the osmotic pressure or osmotic suction (Nelson and Miller 1992). For most soils, the osmotic suction is fairly constant, meaning changes in total suction are the result of changes in matric suction alone, and matric suction is an appropriate stress-state variable for the soil. However, at very low water contents, the cations in the soil may not be completely hydrated and changes in osmotic suction play a role in changes in total suction. In this case, total suction would be a more appropriate stress-state variable (Nelson and Miller 1992).

Matric suction and osmotic suction as defined above are components of *total suction*. Total suction is typically taken to be the sum of the matric and osmotic components (Fredlund and Rahardjo 1993) as shown in Equation 6. However, Nelson and Miller (1992) note that this relationship has not been demonstrated rigorously to be valid and that this area requires further research.

$$\boldsymbol{\psi = (u_a - u_w) + \pi} \qquad \textbf{(6)}$$

Where ψ = total suction

$u_a - u_w$ = matric suction

π = osmotic suction

Total soil suction, is an intensive variable for soil moisture in an unsaturated soil. Whereas moisture content is an extensive variable and describes the quantity of moisture in the soil, suction describes the state or quality of the soil moisture. Soil suction is essentially the energy state of the soil pore water. In some literature, the term *soil water potential* is used instead of suction. Soil water potential is essentially the negative of soil suction (Decagon Devices, Inc. 2015c).

2.2.2 Thermodynamic Relationship and Equilibrium

The free energy of soil water is typically referenced to that of free, pure water. The term suction is used when the soil water has a free energy less than that of pure water under the ambient air pressure (Mitchell 1993). It can be shown that the suction can be measured in terms of the partial vapor pressure of the pore water (Fredlund and Rahardjo 1993). Equation 7 gives this relationship. The term $\bar{u}_v/\bar{u}_{v0}$ is called the relative humidity. If a soil sample is sealed in a container and allowed to equilibrate, the relative humidity in the container will be related to the soil suction by Equation 7 (Fredlund and Rahardjo 1993), making this relationship important for several methods of measuring total suction.

$$\boldsymbol{\psi = -\frac{RT}{v_{w0}\omega_v} ln\left(\frac{\bar{u}_v}{\bar{u}_{v0}}\right)} \qquad \textbf{(7)}$$

Where ψ = total suction (kPa)

R = universal gas constant [8.31432 J/(mol· K)]

T = absolute temperature (K)

v_{w0} = specific volume of water (inverse of density) (m^3/kg)

ω_v = molecular mass of water vapor (18.016 kg/mol)

$\bar{u}_v$ = partial pressure of pore water vapor (kPa)

$\bar{u}_{v0}$ = saturation pressure of water vapor over a flat surface of pure water at the same

temperature (kPa)

As described by the laws of thermodynamics, two systems in contact with each other will eventually come into thermodynamic equilibrium with each other, with flow occurring along the gradient of the intensive variable (Decagon Devices, Inc. 2015c). This includes not only two soils in contact with each other, but soils in contact with other materials. For example, if a very dry porous object (i.e. high suction, low soil water potential) is in good hydraulic contact with a wet soil (i.e. lower suction, higher soil water potential) water will flow from the soil to the dry object along the gradient of suction (from low suction to high suction) until the soil and the dry object have the same suction. It is important to note that this flow of water does not depend on the moisture content of either object (Fredlund and Rahardjo 1993).

2.2.3 Soil Water Characteristic Curves

A common constitutive relationship between suction and water content is called the soil water characteristic curve (SWCC). A typical SWCC is shown in Figure 8. It should be noted that the SWCC relationship is different for wetting and drying. This hysteresis is shown in Figure 9.

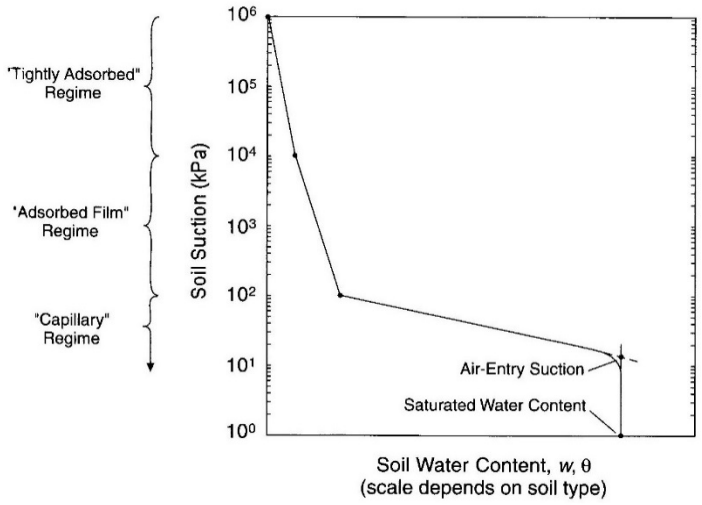

Figure 8: Illustration of McQueen and Miller's (1974) Conceptual Model for General Behavior of the SWCC (Lu and Likos 2004)

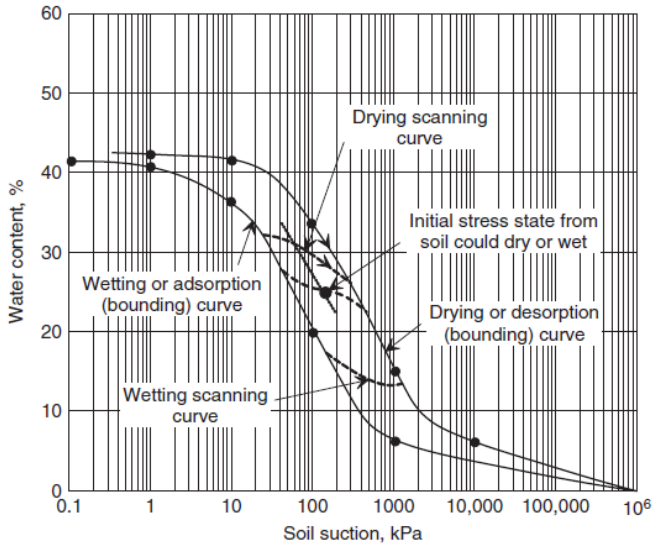

Figure 9: Hysteresis in SWCC (Fredlund et al. 2012)

The three regions shown in Figure 8 come from McQueen and Miller's (1974) model of the SWCC and describe the different mechanisms by which water is held in the soil. In the capillary regime, the water is held in the soil by capillary forces and is controlled mainly by pore size. In the adsorbed film regime, water is held in the soil due to surface forces such as electric field polarization, van der Waals forces, and exchangeable cation hydration. This is a function of the surface area of the soil particles, the surface charge density, and the exchangeable cations. In

the tightly adsorbed regime, water is held by molecular forces, primarily hydrogen bonds (Lu and Likos 2004).

The *air entry suction* (also called air entry value) is the maximum value of suction that can be maintained in a soil prior to the penetration of air. At values of suction below the air entry suction, the soil remains saturated and air cannot enter the soil. The air entry suction is primarily controlled by the largest pore size of the soil (Fredlund and Rahardjo 1993). The air entry suction is given by Kelvin's capillary model equation (Equation 1) with the radius of curvature equal to the maximum pore size (Fredlund and Rahardjo 1993).

The exact shape of the curve will be determined by the soil properties, chiefly the pore-size distribution (Lu and Likos 2004). This is illustrated by Figure 10 which shows SWCCs for sand, silt, and clay. As pore size decreases, the water will be held more tightly to the soil particles, resulting in a larger air-entry suction and capillary regime.

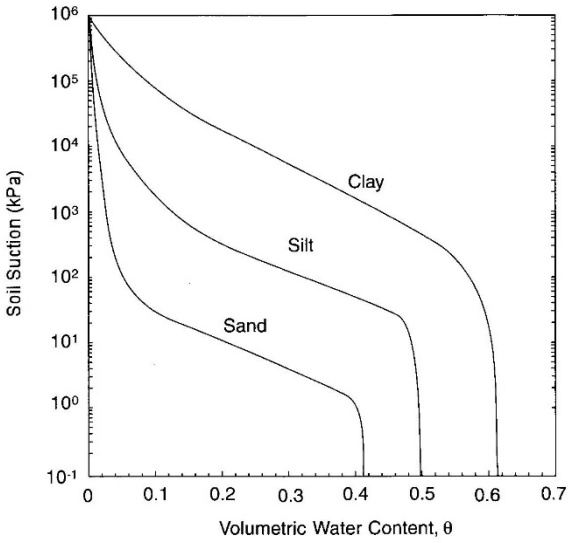

Figure 10: Representative SWCCs for Sand, Silt, and Clay (Lu and Likos 2004)

Porous materials other than soils (e.g. ceramics, filter paper) also have curves that relate suction to water content. These curves are referred to a moisture characteristic curves (Decagon Devices, Inc. 2015c).

2.2.4 Active Zone and Moisture Fluctuations

The water content, and thus soil suction, in the upper few meters of the soil profile is influenced by environmental factors. This upper few meters where the suction changes seasonally is called the *active zone* (Nelson and Miller 1992). Figure 11 shows the active zone along with some environmental factors that influence the soil suction.

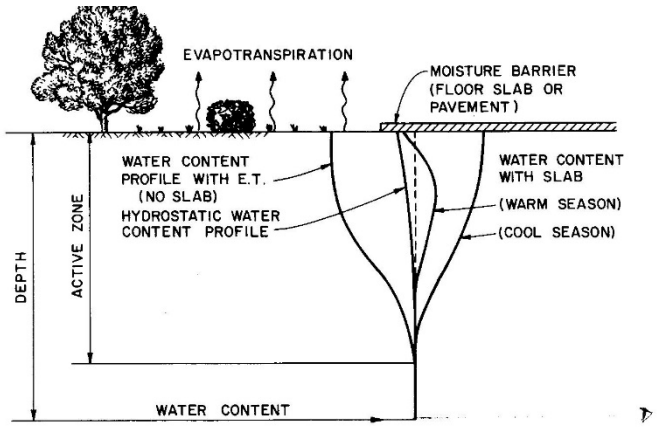

Figure 11: Water Content Profiles in the Active Zone (Nelson and Miller 1992)

2.3 Field Measurement of Soil Suction

A variety of methods are available for measuring soil suction. Each method has benefits and limitations. Methods can be classified as primary or secondary methods. For primary, also called direct, methods suction is measured based on first principles. For secondary, or indirect methods, a property other than suction is measured and this is correlated to suction through the use of a calibration. In the discussion below, focus will be given to field methods for measuring suction.

2.3.1 Primary (Direct) Methods for Measuring Suction

Primary methods for measuring suction rely on first principles. Tensiometers and vapor pressure methods are essentially the only primary methods for measuring suction (Decagon Devices, Inc. 2015c).

2.3.1.1 Tensiometer

The tensiometer is used to measure matric suction. A tensiometer is a tube filled with water with a high air entry ceramic filter and a pressure measuring device. The ceramic filter is placed in contact with the soil and the water in the tensiometer comes to the same matric suction (negative pore water pressure) as the soil water once equilibrium is achieved (Fredlund and Rahardjo 1993). Tensiometers are limited by the fact that the water will cavitate at suctions of approximately one atmosphere or less (Decagon Devices, Inc. 2015c). Because of this, periodic maintenance is required for tensiometers and they cannot be automated. In spite of this limitation, tensiometers can still be very useful in the wet region because they can have very good accuracy (Decagon Devices, Inc. 2015c). Figure 12 shows a conventional tensiometer.

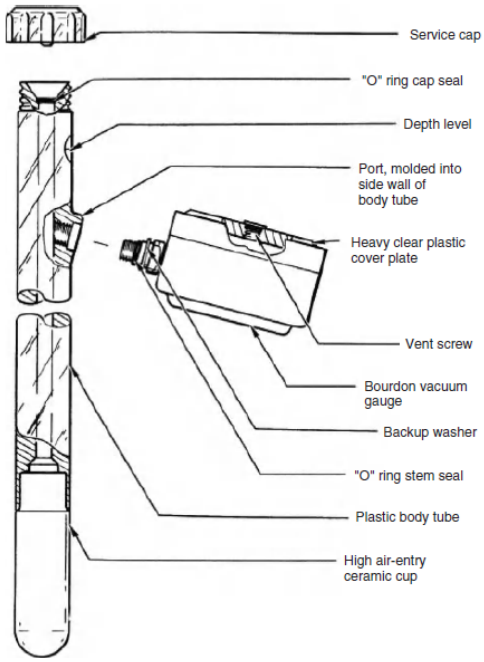

Figure 12: Conventional Tensiometer (Fredlund et al. 2012)

2.3.1.2 Vapor Pressure Methods

Vapor pressure methods rely on the relationship between relative humidity and total suction shown in Equation 7. Thermocouple psychrometers, shown in Figure 13, measures

relative humidity and has been used with success for laboratory suction measurements (Fredlund et al. 2012). However, a constant thermal environment is necessary to accurately measure suction with a psychrometer. Therefore, they are not recommended for field use (Fredlund et al. 2012).

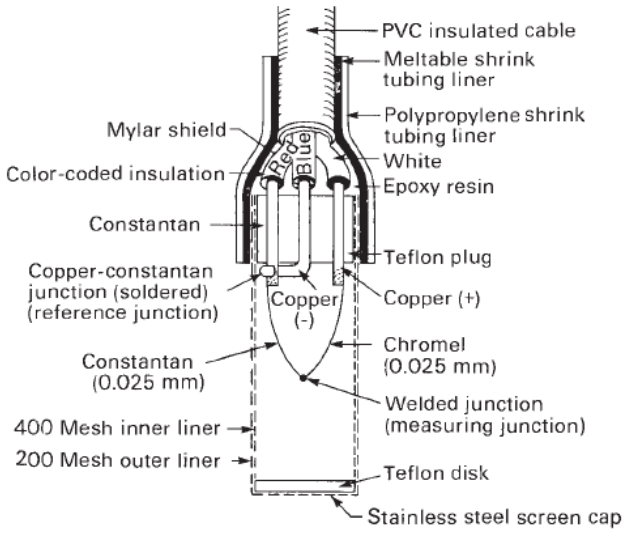

Figure 13: Thermocouple Psychrometer (Fredlund et al. 2012)

2.3.2 Secondary (Indirect) Methods for Measuring Suction

Secondary, or indirect, methods for measuring suction operate by measuring a property other than suction and using a calibration to correlate that property to suction. This is often done by letting a porous material come to equilibrium with the surrounding soil and then measuring the moisture content of the porous material. The moisture characteristic curve for the porous material can then be used to determine the suction.

2.3.2.1 Filter Paper Method

A common laboratory method for measuring suction is the filter paper method. This method can measure either total or matric suction depending on how the test is set up, but the method has demonstrated greater success with measuring total suction (Fredlund et al. 2012). The method is described in ASTM D5298-10. The typical procedure to measure total suction is

to suspend a filter paper above a soil sample and let it come to equilibrium with the soil suction. Deka et al. (1995) report that at least six days are required to reach equilibrium. The gravimetric moisture content of the filter paper is then determined and related to the suction by a calibration. Calibration curves vary for each type of filter paper and can even vary from batch to batch of a single type of filter paper (Likos and Lu 2002). Fredlund et al. (2012) report that total suction as measured by the filter paper method agree fairly closely with psychrometer results.

The filter paper method has not been widely used for insitu measurements (Fredlund and Rahardjo 1993), and not much literature is available. Fredlund and Rahardjo (1993) do provide a possible scheme for using the filter paper technique in situ. This is shown in Figure 14. An insitu filter paper technique was used at an expansive clay test site in Australia, but Fityus et al. (2004) report that this method failed due to the ingress of free water.

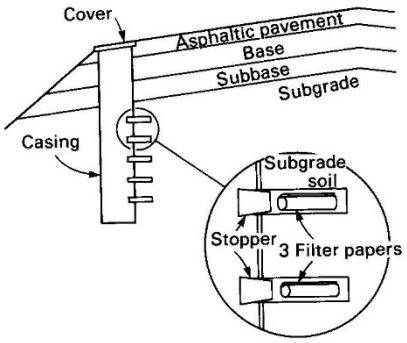

Figure 14: Proposed Scheme for Measuring Total Suction Insitu Using Filter Papers (Fredlund and Rahardjo 1993)

2.3.2.2 Electrical Resistance Sensors

Electrical resistance sensors are the simplest type of suction sensors. They operate based on the principle that a porous material in contact with a soil will equalize and come to the same suction as the soil. The electrical resistance of the porous material will change based on this change in water content (Fredlund et al. 2012). Because they are in contact with the soil, the

matric suction is measured. The porous material used in electrical resistance sensors is typically gypsum granular quartz, but other materials are possible (Fredlund et al. 2012).

Electrical resistance sensors were used by Steinberg (1980) to monitor the moisture of an expansive clay subgrade. This site was a pavement test section on expansive clay that had been remediated with vertical moisture barriers. Initial readings indicated that the sensors responded appropriately to changes in moisture (Steinberg 1981). However, the moisture sensors were later abandoned due to many of the sensors giving irregular readings or being unresponsive (Steinberg 1985). Gypsum block resistance sensors were used by Fityus et al. (2004) at an expansive clay test site, but these sensors failed in very wet and very dry conditions. Furthermore, the results of functioning sensors provided inconsistent results (Fityus et al. 2004).

These sensor failures are not unexpected as it has been noted that resistance sensors do not have the accuracy or long term stability necessary for most geotechnical applications (Fredlund et al. 2012). Additionally, Fredlund et al. (2012) note that this type of sensor provide an indication of wetness, but cannot provide a reliable value of the matric suction, and are thus unsuitable for most engineering applications.

2.3.2.3 Thermal Conductivity Sensors

Thermal conductivity sensors operate on a similar principle to resistance sensors, except that the thermal response of the porous material is measured and correlated to soil suction. Typically a ceramic is used as the porous material. Because this is a contact method, the matric suction is measured. Because the pores in the ceramic of each sensor vary somewhat in size and distribution, each sensor has a unique moisture characteristic curve (Decagon Devices, Inc. 2015c). Additionally, the thermal properties of each sensor vary slightly. Because of this

variation, to obtain accurate readings, individual calibrations are necessary (Flint et al. 2002). Figure 15 shows a typical thermal conductivity sensor.

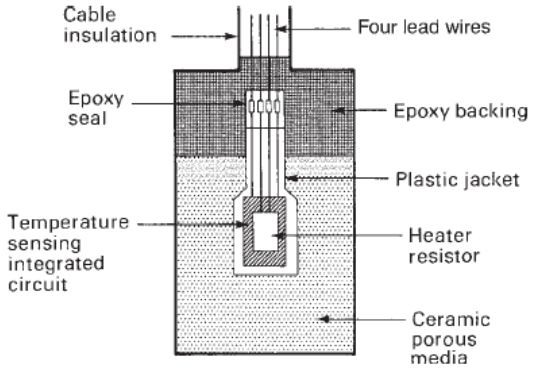

Figure 15: Cross section of AGWA-II thermal conductivity suction sensor (Fredlund et al. 2012)

Thermal conductivity sensors have been widely used to monitor suction in geotechnical engineering applications. Puppala et al. (2010) successfully used thermal conductivity sensors to measure the suction in an expansive clay subgrade. These sensors were installed at a relatively shallow depth (<0.5 m) and were able to detect changes in suction in an attempt to predict shrinkage cracking in the pavement.

Thermal conductivity sensors were used by Nichol et al. (2003) to monitor the moisture movement through coarse mine waste rock. It was reported that several sensors experienced long term drift, possibly from constantly being exposed to suctions less than 20 kPa. No long term drift was reported in other studies (O'Kane et al. 1998, Marjerison et al. 2001) although Nichol et al. (2003) note that the range of matric suction in these studies was generally higher.

2.3.2.4 Dielectric Permittivity Sensors

Dielectric permittivity sensors are similar to thermal conductivity sensors, but the charge storing capacity of the ceramic is measured and correlated to matric suction (Decagon Devices, Inc. 2015b). Also similar to the thermal conductivity sensors, a custom calibration is required to accurately measure suction. A procedure has been developed by Decagon to factory calibrate

these sensors (Decagon Devices, Inc. 2015b). Figure 16 shows a dielectric permittivity suction sensor.

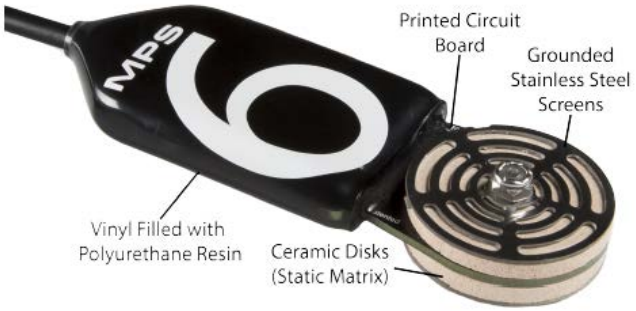

Figure 16: Decagon MPS-6 Dielectric Permittivity Suction Sensor (Decagon Devices, Inc. 2015b)

Dielectric permittivity suction sensors are more common in agricultural use than in geotechnical applications. However, dielectric permittivity suction sensors have been used successfully to measure the depth of the active zone of an expansive clay (Hossain et al. 2016). Malazian et al. (2011) evaluated a dielectric permittivity suction sensor and found it to give consistent results with reasonable accuracy after it had been calibrated.

It should be noted that for contact methods (electrical resistance, thermal conductivity, and dielectric methods), measurements of suction on the wet end are limited by the air entry value of the ceramic or surrounding soil, whichever is greater (Decagon Devices, Inc. 2015b).

2.3 Field Measurement of Soil Moisture Content

As stated by Fredlund et al. (2012), “The void ratio and the water content of a saturated soil bear a fixed relationship by the specific gravity of the soil. However, water content and void ratio become independent variables for unsaturated soils.” Because of this, it is often important to measure the moisture content of unsaturated soils as well as the suction. A review of methods for measuring moisture content in situ is included below.

Most in situ methods measure volumetric moisture content rather than gravimetric moisture content. Volumetric moisture content is referenced to the volume of a representative sample as given by Equation 8. The volumetric and gravimetric moisture contents are related by the dry density as shown by Equation 9.

$$\boldsymbol{\theta = \frac{V_w}{V_T}} \qquad \textbf{(8)}$$

Where θ = volumetric moisture content, expressed as a decimal

V_w = volume of water in a representative sample

V_T = total volume of a representative sample

$$\boldsymbol{\theta = \frac{w}{100} \cdot \frac{\rho_d}{\rho_w}} \qquad \textbf{(9)}$$

Where θ = volumetric moisture content, expressed as a decimal

w = gravimetric moisture content, expressed as a percent

ρ_d = dry density of soil

ρ_w = density of water

A number of methods are available for measuring volumetric water content in the field. These methods are indirect methods, meaning some property other than volumetric moisture content is measured and then correlated to volumetric moisture content by a calibration.

2.3.1 Neutron Moisture Probe

Neutron moisture probes have been in use since the 1950's to measure volumetric moisture content (IAEA 1970). Figure 17 shows a neutron moisture probe. In this method, a source emits "fast" neutrons. The fast neutrons are then slowed down as they come into contact with hydrogen atoms. A detector then measures the number of "slow" neutrons. Because the

primary source of hydrogen in soils is water, the ratio of slow neutrons to fast neutrons can be correlated with the amount of water in a soil (IAEA 1970, Li et al. 2003).

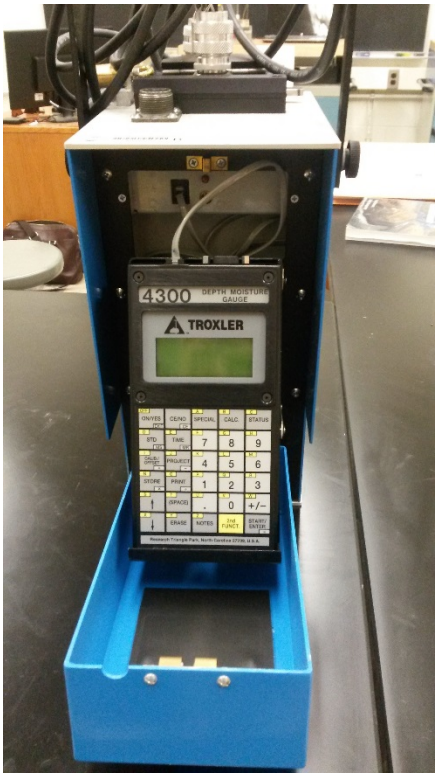

Figure 17: Neutron Moisture Probe

It should be noted that other atoms present in soils slow down the fast neutrons to some degree. To fully account for this, numerical models that incorporate soil chemical composition have been employed for calibrations (Li et al. 2003). While the results of the numerical model compared very well to experimental results, significant disadvantages exist, namely the complexity of the model and the fact that a complete elemental analysis of the soil is required.

Neutron moisture probe measurements were taken at an expansive soil test site near Newcastle, Australia and are recorded by Fityus et al. (2004). It was found that the neutron probe was effective for monitoring relative changes in moisture content. However, they note that

correlation of the neutron moisture probe to absolute moisture content is a very difficult task (Fityus et al. 2004).

2.3.2 TDR Sensors

Time domain reflectometry (TDR) sensors have been widely used in both agriculture and geotechnical engineering to measure soil moisture content. In this method, a voltage pulse is propagated along wave guides that are inserted in the soil. The travel time and attenuation of the wave can be measured to determine the dielectric permittivity of the soil (Topp and Reynolds 1998). Because water has a much higher dielectric permittivity than air or soil solids, this can be correlated to volumetric moisture content through empirical relationships (Topps and Reynolds 1998). A typical TDR Probe is shown in Figure 18.

TDR sensors are typically durable and accurate and have been used in many engineering applications (Fityus et al. 2004, Ng et al. 2003, Freeman et al. 2001, Burrage 2016). With standard factory calibrations, capacitance sensors have an accuracy of ±3% volumetric moisture content (Campbell Scientific, Inc. 2016).

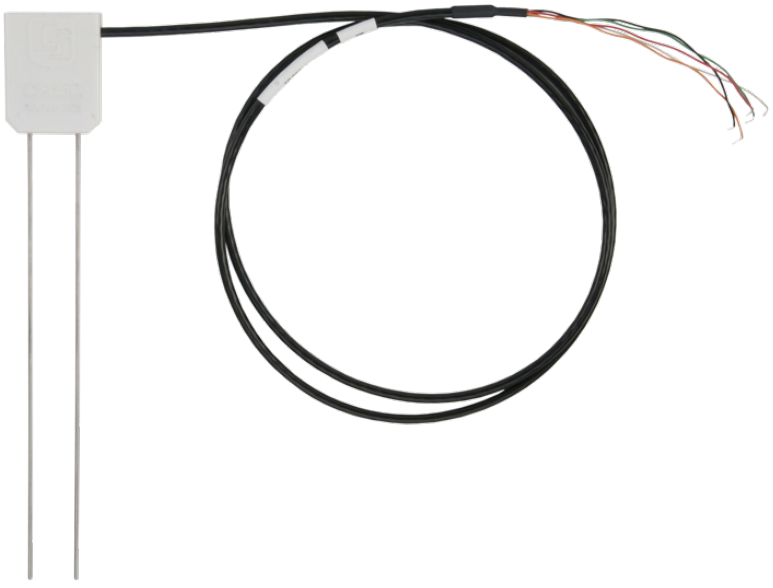

Figure 18: Campbell CS650 TDR Sensor (Campbell Sci. Inc. 2016)

2.3.2 Capacitance Sensors (ECH_2O Sensors)

Similar to TDR sensors, capacitance sensors (ECH_2O sensors) measure dielectric permittivity and correlate it to volumetric moisture content. Rather than measuring the propagation and reflection of a voltage wave pulse, the capacitance of the soil is measured. The dielectric permittivity is then calculated from the capacitance (Decagon Devices, Inc. 2009). A typical capacitance sensor is shown in Figure 19.

Capacitance sensors have not seen as widespread use in civil engineering as TDR sensors, but they have been used extensively in agriculture (Dursun and Ozden 2011, Pardossi 2009,van Iersel et al. 2009). With standard factory calibrations, capacitance sensors have an accuracy of ±3% volumetric moisture content (Decagon Devices, Inc. 2015a).

Figure 19: Decagon 10HS Capacitance Sensor (Decagon Devices, Inc. 2014)

2.4 Pavement Distress Measurement

2.4.1 International Roughness Index

The international roughness index (IRI) is a summary statistic from a pavement profile that describes the roughness qualities that impact vehicle response (Sayers and Karamihas 1998). The IRI is essentially a filtered profile that is accumulated and divided by the length of the profile. The IRI is therefore measured in units of slope, typically inches/mile or meters/kilometer (Sayers and Karamihas 1998). The IRI is a good general pavement condition indicator. Figure 20 shows the typical IRI values for various classes of roads. The FHWA defines IRI values less than 95 as “good”, IRI values between 95 and 170 as “fair”, and IRI values greater than 170 as “poor” (NCHRP 20-24(37) G).

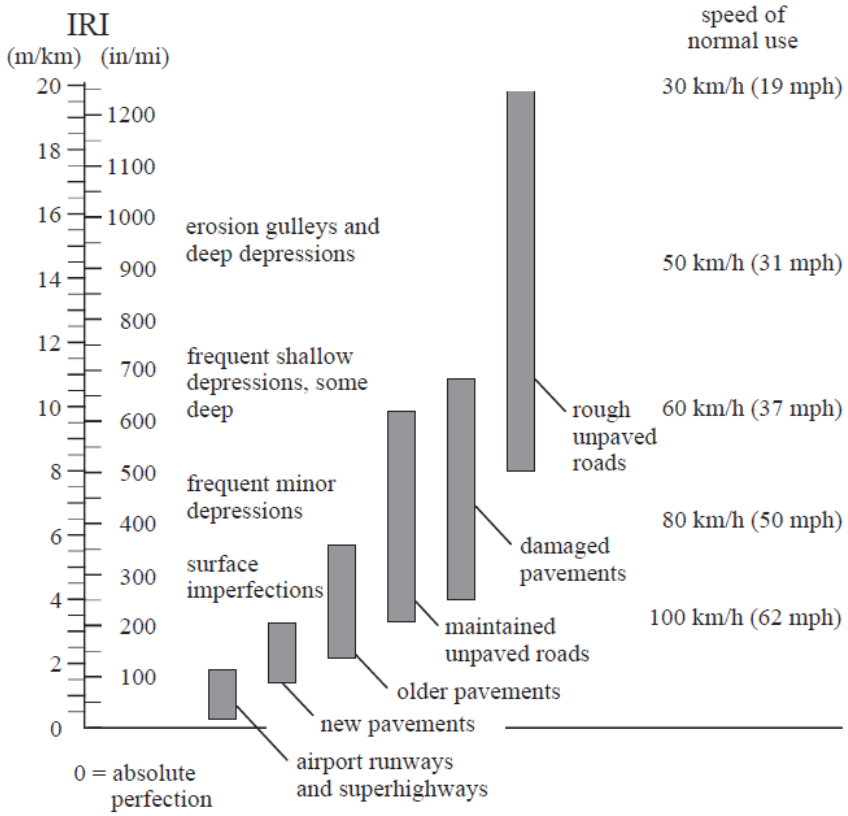

Figure 20: Ranges of IRI for Different Classes of Roads (Sayers and Karamihas 1998)

2.4.2Asphalt Strain Gages

Asphalt strain gages are typically used to monitor dynamic strain in asphalt pavements during loading events (Timm et al. 2004). They have been successfully used in a variety of studies for this purpose (Baker et al. 1994, Timm et al. 2004, Hornyak et al. 2007).

A study at the Korean Highway Corporation Test Road (KHCTR) monitored the long term performance of asphalt strain gages (Seo and Lee 2012). In this study, the condition of the strain gages was monitored and strain gage malfunctions were correlated to pavement condition. Figure 21 shows the performance of the strain gages over time along with the pavement condition index (PCI), rut depth, and fatigue cracking. PCI is a method of rating pavements on a 0 to 5 scale with 0 being the worst condition and 5 being the best (Seo and Lee 2012). It was concluded from this study that the long-term functionality of embedded asphalt strain gages is closely related to the pavement condition (Seo and Lee 2012).

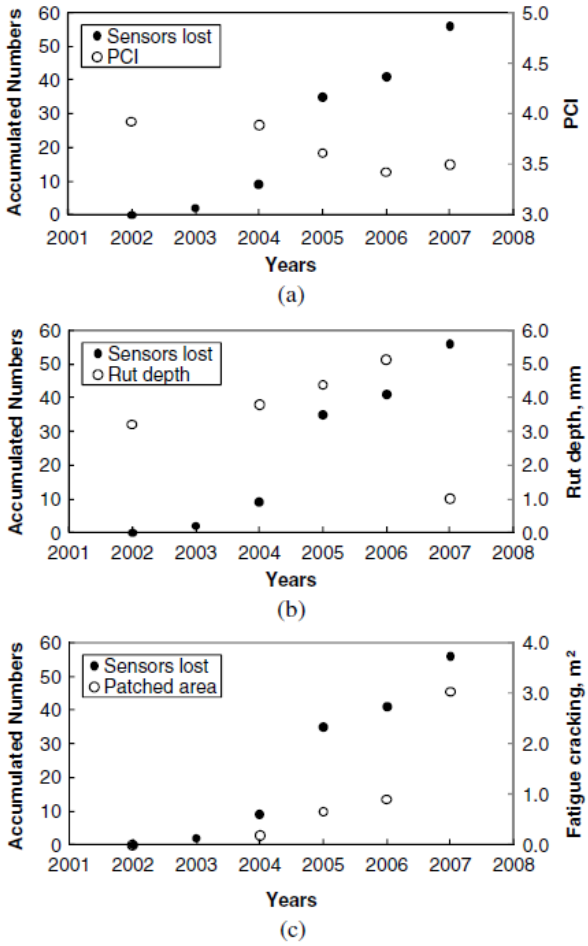

Figure 21: Malfunction of Strain Gages Compared to: (a) Pavement Condition Index (PCI); (b) Rut Depth; and (c) Patched Area (Seo and Lee 2012)

CHAPTER 3: RESEARCH SETTING

3.1 Site Description, Layout, and Nomenclature

The research site consists of a four mile stretch of Alabama Highway 5 in Perry County. The site extends from mile post 50.85 to mile post 54.85. The terrain is generally flat. Much of the surrounding land is wooded area, but significant sections consist of farm land. There is a catfish pond just east of the road near mile point 51.5. There is one bridge in the study area where AL-5 crosses over Washington Creek near mile post 53.7

The study area is divided into eight half-mile test sections, shown in Figure 22 and Table 1. It was intended that each test section receive a different remediation technique. However, initial site exploration indicated that the clay layer in Test Section 8 was thinner than was typical for the rest of the project. Because of this no remediation was done in Test Section 8 and it served as an additional control section. Furthermore, Test Section 7 was also canceled due to the impracticality of the construction technique. Thus, Test Section 6, 7, and 8 all served as control sections. Due to constructability requirements and traffic control requirements, the sand blanket was only constructed in the center of Test Section 1, while the first and last 500 feet in this section received no remediation. These sections served as additional control sections. Construction and resurfacing of the test sections was completed in August 2016.

Table 1: Test Sections

Test Section	Remediation Technique	Milepost
1	Sand Blanket	50.85 - 51.35
2	Vertical Moisture Barriers	51.35 - 51.85
3	Lime Columns	51.85 - 52.35
4	6' Paved Shoulders	52.35 - 52.85
5	Edge Drains	52.85 - 53.35
6	Control	53.35 - 53.85
7	Deep Mixing - Canceled	53.85 - 54.35
8	Control	54.35 - 54.85

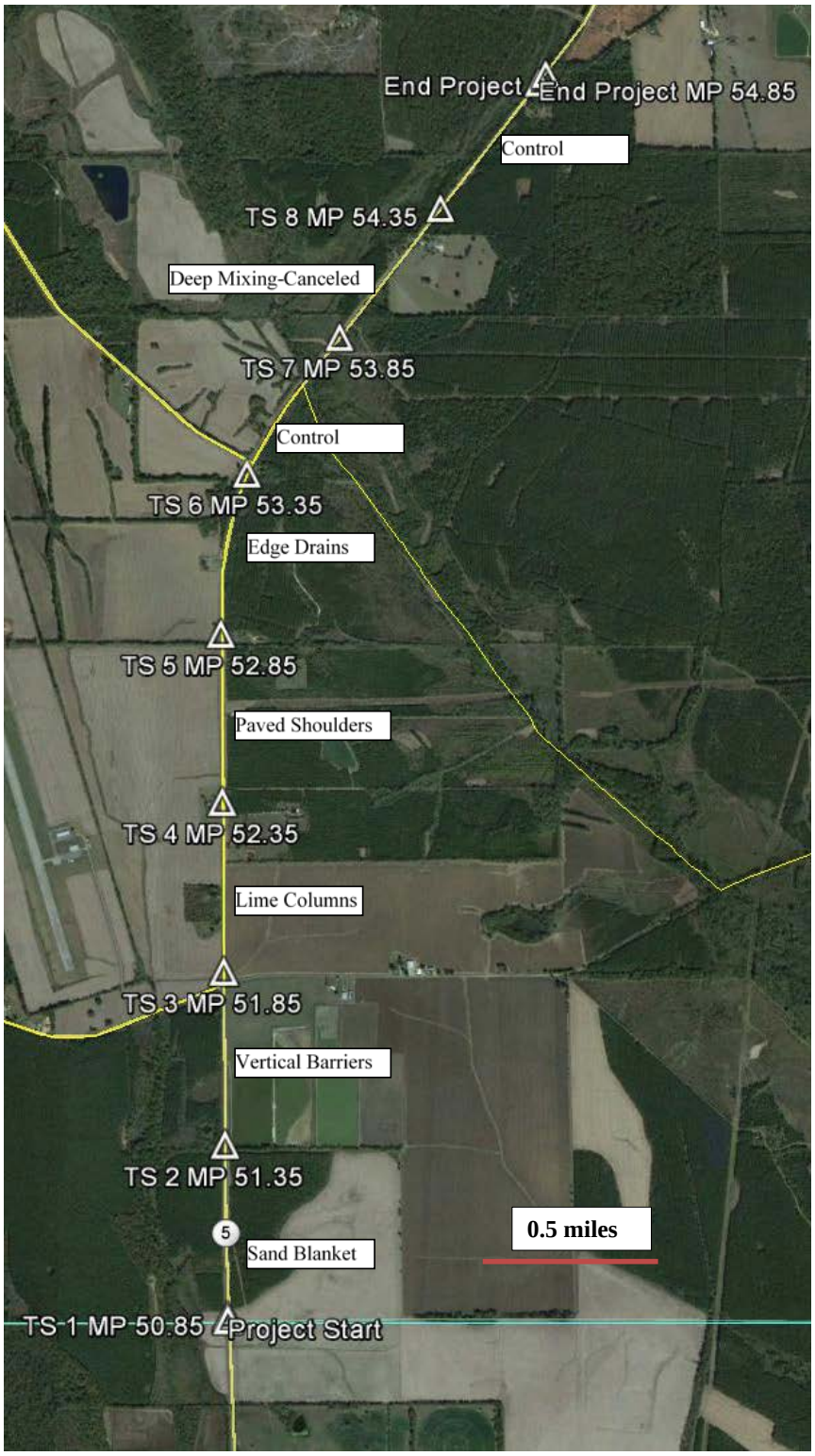

Figure 22: Layout of Research Site (After Google Earth)

3.2 Site Geology

The site lies in the coastal plain physiographic providence in the Black Prairie belt (Monroe 1941). A geologic map of the area is shown in Figure 23. As seen in the figure, most of the study area lies in the Mooreville Chalk formation. Sections near Washington Creek consist of alluvial deposits of Quaternary age. The majority of the Mooreville Chalk is described as "yellowish-gray to olive-gray compact fossiliferous clayey chalk and chalky marl." (Osbourne et al. 1989). The upper and lower portions of the Mooreville Chalk vary from this with the upper 10 feet containing interbedded clay and limestone and the lower few feet containing calcareous sand (Raymond et al. 1988), but these members were not encountered in the study area.

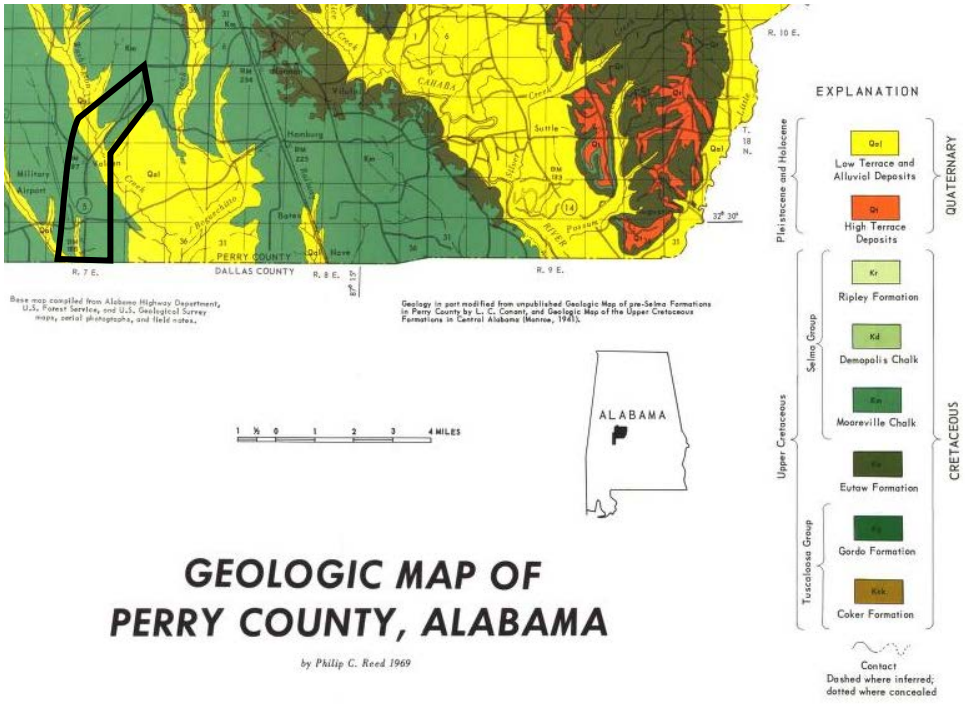

Figure 23: Geologic Map of Perry County, AL. Study Area Outlined (Reed 1969)

3.3 USDA Soil Survey

The United States Department of Agriculture (USDA) conducted a soil survey for Perry County in 1998 that included the research site. The general soil map from the survey is shown in Figure 24. A box is shown around the study area. As seen in Figure 24, the general soil type for the study area is Vaiden-Okolona-Sucarnoochee. These soils are described as somewhat poorly drained brown to olive to gray clays. The parent material of these soils is typically the underlying chalk, although some areas contain clayey alluvium (Harris 1998).

Detailed soil maps were also provided with the soil survey. According to these maps, the predominate soil types were Okolona Silty Clay Loam and Vaiden Clay with smaller sections of Kipling Clay Loam and Sucarnoochee Clay toward the northern end of the project (Test Sections 6-7). These soils are all fairly similar and exhibit moderate to very high swell potential (Harris 1998). Relevant soil properties are shown in Table 2.

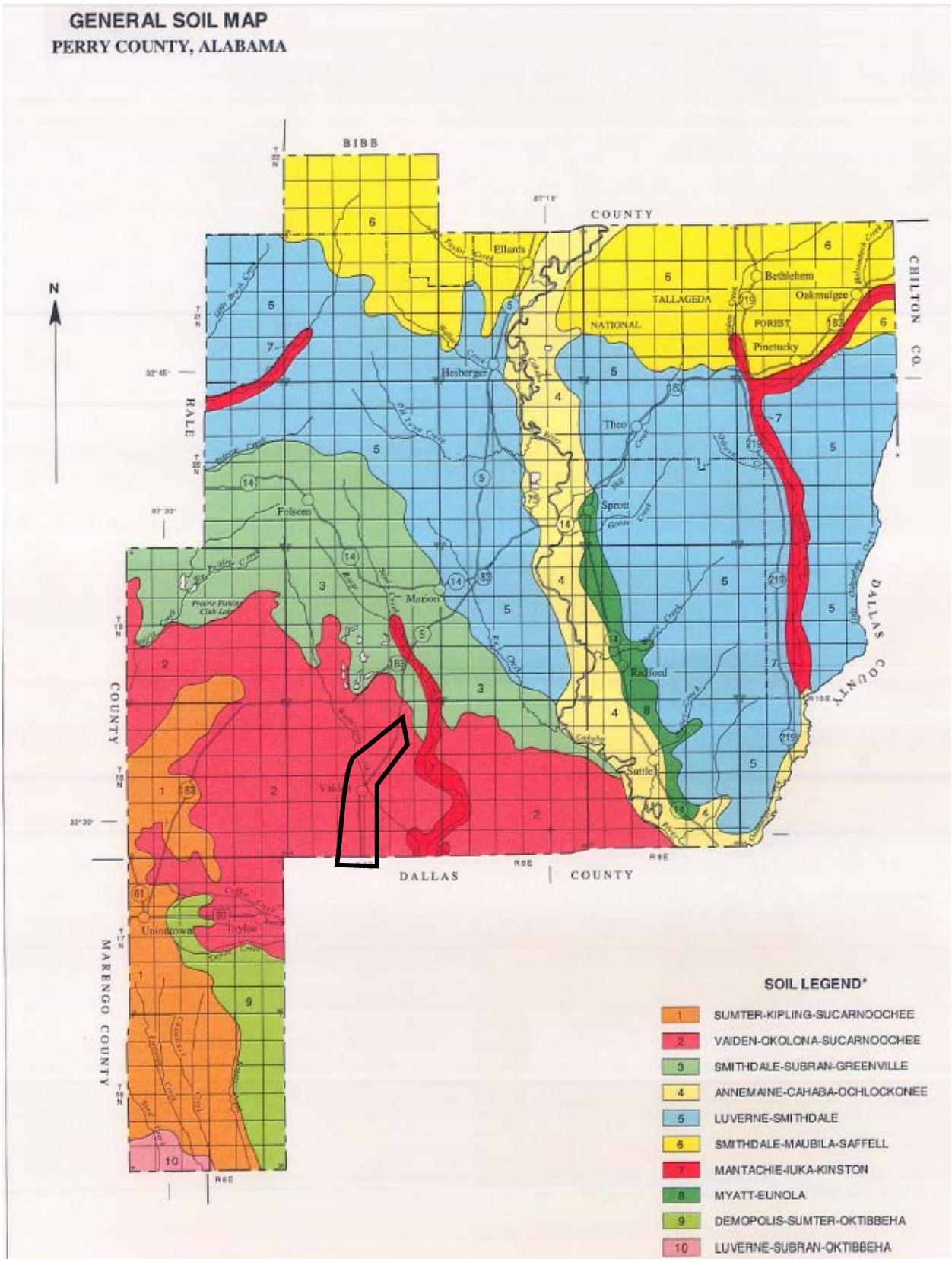

Figure 24: USDA Soil Survey General Soil Map (Harris 1998)

Table 2: Soil Properties from USDA Soil Survey (after Harris 1998)

Type	Depth (in)	USCS Classification	% Passing 200	LL	PI	Permeability (in/hr)	Shrink-Swell potential
Okolona Silty Clay Loam	0-6	CL, CH	85-98	46-55	25-32	<0.06	High
	6-60	CH, MH	90-98	60-90	29-65	<0.06	Very High
Vaiden Clay	0-5	MH, CH	90-100	50-60	20-30	0.06-0.2	High
	5-21	CH, MH	85-100	50-90	30-50	<0.06	Very High
	21-60	CH	85-100	50-90	30-52	<0.06	Very High
Kipling Clay Loam	0-5	CL	85-95	30-45	15-25	0.06-0.2	Moderate
	5-65	CH, CL	85-95	38-70	22-45	0.06-0.2	High
	65-80	CH, CL	75-95	48-80	26-50	<0.06	Very High
Sucarnoochee Clay	0-16	CL, CH, MH	85-95	40-65	15-35	0.06-0.2	High
	16-54	MH, CH, CL	85-98	45-70	20-40	<0.06	High
	54-60	CH, MH	85-98	50-80	25-45	<0.06	High

3.4 Climate

The climate of Perry County, Alabama is primarily influenced by moist tropical air that moves north from the Gulf of Mexico and covers the area. Perry County typically has long, hot summers and cool, short winters. The average summer temperature is 79 degrees with an average daily maximum of 90 degrees. The average winter temperature is 46 degrees with an average daily minimum of 34 degrees (Harris 1998). Thunderstorms are common during the summer and the majority of the annual precipitation falls during the summer months (April – October). Perry County experiences about 54 inches of total annual precipitation (Harris 1998). Every several years the remnants of a hurricane or tropical storm will move inland causing heavy rain for several days (Harris 1998).

3.5 Traffic Data

Traffic data was obtained from ALDOT's traffic database. For a traffic count station located within the bounds of the project at milepoint 51.21, the average annual daily traffic

(AADT) for 2014 was 1120 vehicles. Forty percent of this was truck traffic (class 5 vehicles and above) meaning the average annual daily truck traffic was 448 trucks for 2014 (ALDOT 2016).

3.6 Previous Research

Site investigation and laboratory testing has previously been performed on the subgrade soils and is described in detail elsewhere (Herman 2015, Stallings 2016). Field observations and the soil samples obtained from the site investigation were consistent with the description of the Mooreville Chalk and the soil types in the USDA soil survey (Herman 2015). Stallings (2016) completed a comprehensive laboratory analysis of the soil samples taken from AL-5. This testing included soil classification tests such as grain size analysis and Atterberg limits. One-dimensional swell tests were also performed and soil-water characteristic curves were created for the soils. A summary of the laboratory data collected is shown below. From this laboratory data, it was concluded that the subgrade at AL-5 is expansive and that is the most likely a primary cause of the pavement distress (Stallings 2016).

Table 3: AL-5 Laboratory Data Summary (Stallings 2016)

Borehole	Depth (ft)	LL	PI	%<#200 Sieve	Water Content (%)	Dry Density (pcf)	Specific Gravity	Swell Pressure (psf)
B-1A	1.5	70	46					
B-1A	3.5	88	58					
B-1A	5.5	110	83					
B-1A	7.5	79	50					
B-1A	9.5	103	74					
B-1.5A	1.5	97	68					
B-1.5A	3.5	66	42	98	37.0	84.0	2.75	736.0
B-1.5A	7.5	91	66					
B-1.5A	9.5	85	61	98	32.9	87.5	2.62	1301.0
B-2A	3.0	83	52					
B-2A	5.0	73	48					
B-2A	7.0	86	59					
B-2A	9.0	95	68					
B-2.5A	1.5	70	46					
B-2.5A	3.5	84	58	93	31.9	90.1	2.75	927.0

Borehole	Depth (ft)	LL	PI	%<#200 Sieve	Water Content (%)	Dry Density (pcf)	Specific Gravity	Swell Pressure (psf)
B-2.5A	5.5	79	47					
B-2.5A	7.5			98	29.2	92.4	2.72	1560.0
B-3A	1.5	93	67					
B-3A	3.5	65	41					
B-3A	7.5	74	49					
B-3.5A	1.3	68	40	99	38.6	82.5	2.70	1035.0
B-3.5A	3.3	87	59					
B-3.5A	5.3	84	57					
B-3.5A	7.3			97	41.5	77.7	2.74	1073.0
B-4A	1.8	72	47					
B-4A	5.8	93	70					
B-4.5A	1.2	68	40	97	38.8	81.5	2.72	1082.0
B-4.5A	5.2	97	69					
B-4.5A	7.2			96	33.3	84.4	2.73	
B-5A	1.5	50	26					
B-5A	7.5	91	68					
B-5.5A	1.0	86	60	96	39.6	81.0	2.75	871.0
B-5.5A	7.0	88	61	96	33.3	87.7	2.70	1393.0
B-Tree C	3.0			94	39.6	79.3		622.0
B-Tree C	7.0			94	32.2	89.8		1374.0
B-6A	1.5	97	73					
B-6A	7.5	80	50					
B-6.5A	1.5						2.69	
B-6.5A	3.5	71	47	60	28.2	90.2		509.0
B-6.5A	5.5	57	39					
B-6.5A	7.5	50	35					
B-6.5A	8.8			45				
B-7A	3.5	57	40					
B-7A	5.5	58	38					
B-7A	7.5	63	42					
B-7.5A	5.0	67	49	81	29.2	93.9	2.72	608.0
B-7.5A	7.0	60	42	78	27.8	95.4	2.81	709.0
B-8A	5.0	64	48					
B-8A	7.0	50	34					
B-8.5A	1.0			90				
B-8.5A	3.0			78				

International roughness index (IRI) data was also collected prior to construction to determine a baseline condition for the road. It was found that IRI values higher than the failure

threshold of 170 inches/mile defined by the FHWA were present at AL-5 (Herman 2015, Stallings 2016). The IRI data is shown in Figure 25 through Figure 28. These figures show a measure of the pavement distress for the different wheel paths in each lane.

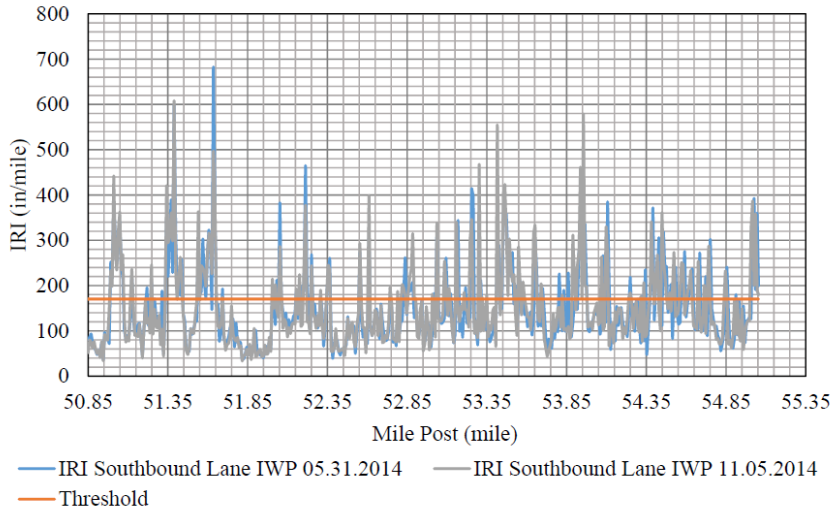

Figure 25: Southbound, Inside Wheel Path IRI Results for May and November 2014 (Stallings 2016)

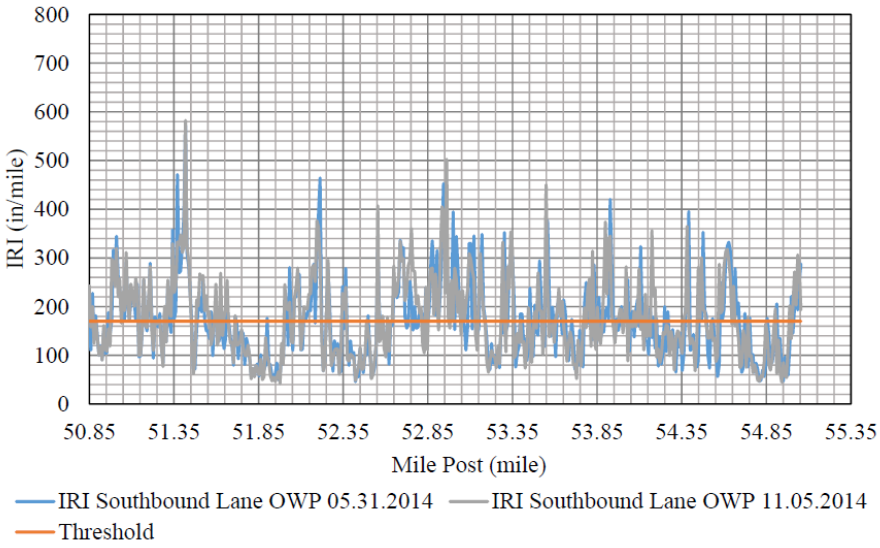

Figure 26: Southbound, Outside Wheel Path IRI Results for May and November 2014 (Stallings 2016)

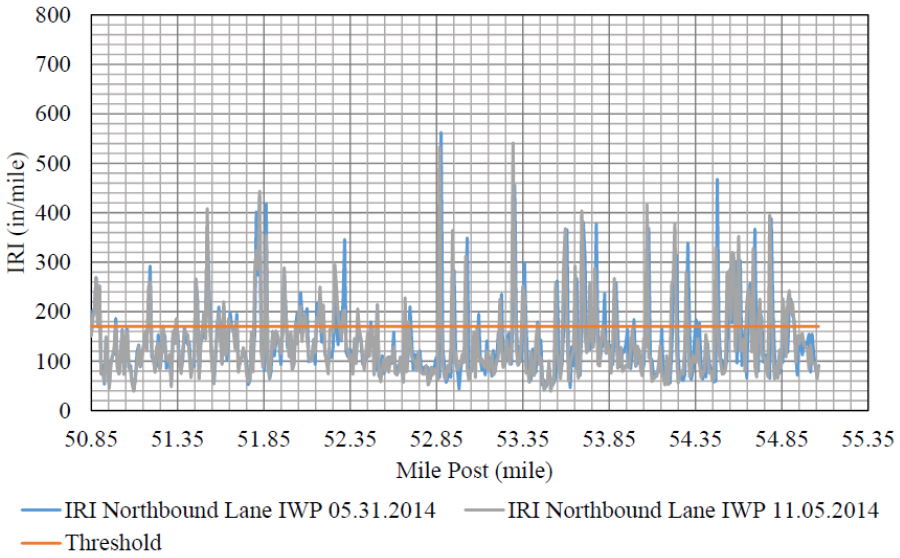

Figure 27: Northbound, Inside Wheel Path IRI Results for May and November 2014 (Stallings 2016)

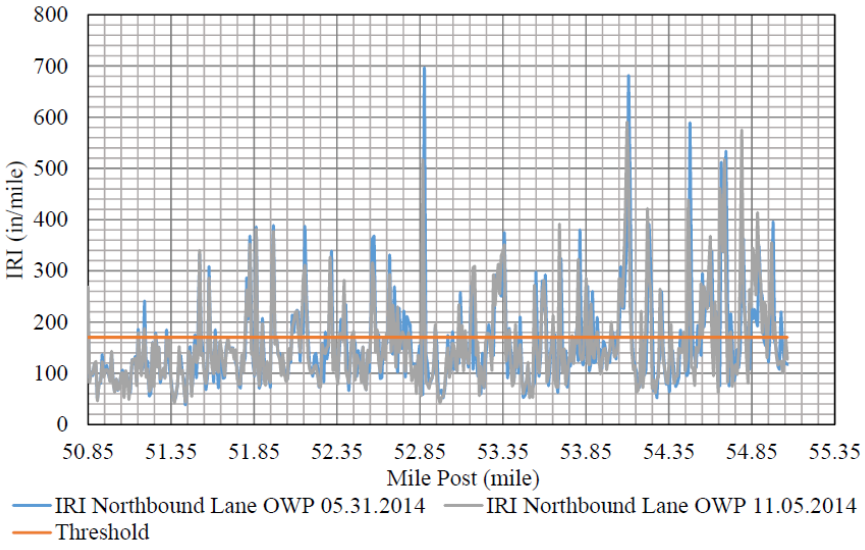

Figure 28: Northbound, Outside Wheel Path IRI Results for May and November 2014 (Stallings 2016)

An electrical conductivity survey was performed in the study area by Herman (2015) to detect any sulfates in the soil. The presence of sulfates combined with lime can cause the formation of an expansive material called ettringite (Little 1995). Herman (2015) found that the

majority of points surveyed fell short of the threshold of 100 mS/m that indicates the presence of sulfates. The electrical conductivity survey results are shown in Figure 29.

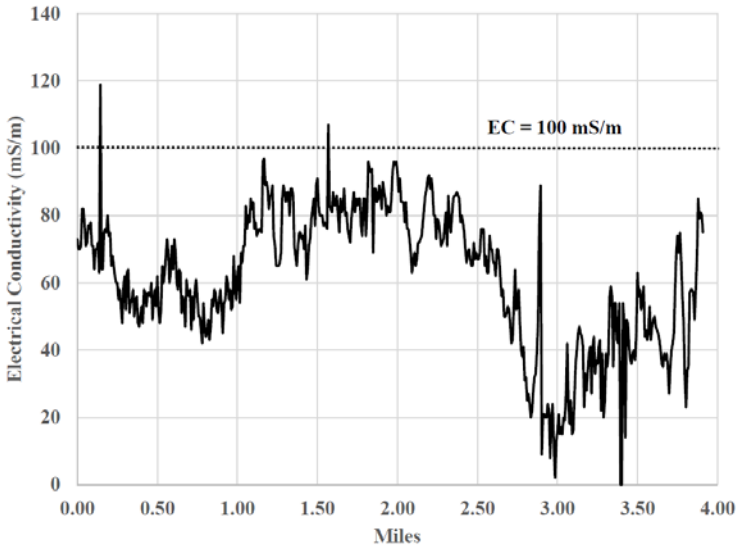

Figure 29: Longitudinal Electrical Conductivity Profile for AL-5 (Herman 2015)

3.7 Remediation Techniques Implemented at AL-5

The remediation techniques mentioned above were selected by ALDOT and Auburn University based on a review of the current literature and state of practice, combined with local experience. They are described briefly below. Full descriptions and documentation of the construction procedures used will be described in a future publication.

3.7.1 Sand Blanket

A drainage layer termed a “sand blanket” was used in Test Section 1. This is essentially an underdrain that is supposed to keep that subgrade at a more constant moisture content. Construction required complete removal of the existing pavement structure. Figure 30 shows the cross-section of the sand blanket test section.

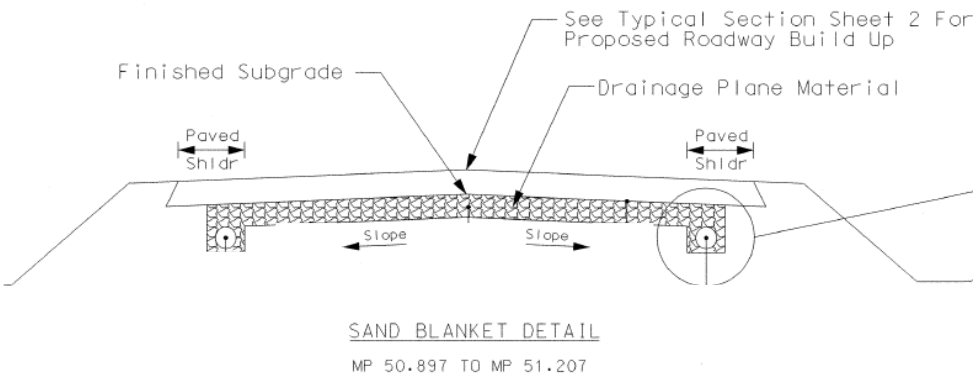

Figure 30: Sand Blanket Cross-Section (ALDOT 2015)

3.7.2 Vertical Moisture Barriers

Vertical moisture barriers are sheets of impervious geosynthetic material that are installed in trenches at the edge of a pavement. Figure 31 shows a typical cross-section for a pavement with vertical moisture barriers. They seek to limit the lateral flow of water into and out of the subgrade. As Nelson and Miller (1992) note, it is generally not practical to install vertical moisture barriers the entire depth of the active zone, but instead they recommend a depth of one-half to two-thirds of the active zone. Vertical moisture barriers have previously been used with some success in other areas of the country (Steinberg 1992).

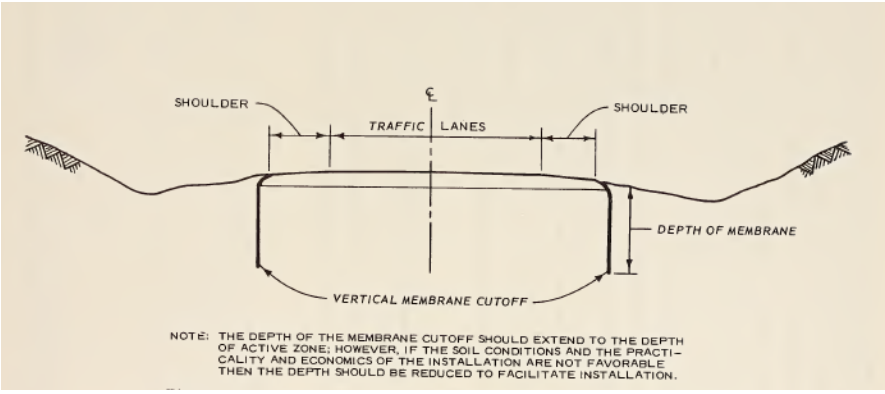

Figure 31: Typical Vertical Moisture Barrier Cross-Section (Snethen 1979)

Part of Test Section 2 was supposed to include barriers that extended ten feet deep, while the remaining part was to have six foot barriers. However, due to cave-ins during construction,

none of the ten foot barriers were able to be installed. Instead, the entire section was constructed with six foot barriers.

3.7.3 Lime Columns

Lime columns seek to chemically stabilize the subgrade. Lime is often mixed into subgrade soils during new construction to stabilize clayey soils. Lime treatment causes fine grained soils to exhibit less plasticity and improved workability (Nelson and Miller 1992). At Test Section 3 of AL-5, Lime was packed into drill-holes in the pavement surface and the shoulder. Figure 32 and Figure 33 show the layout and cross-section of the lime columns. It should be noted that prior to the placement of the final wearing surface, the lime columns reflected through the binder course as shown in Figure 34. This is most likely due to poor compaction during installation. At the time of publication, the lime columns had not reflected through the final wearing surface.

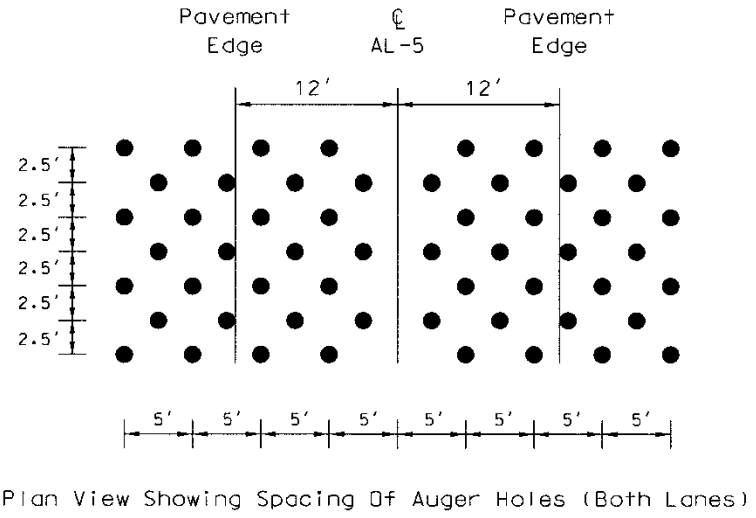

Figure 32: Layout of Lime Columns at AL-5 (ALDOT 2015)

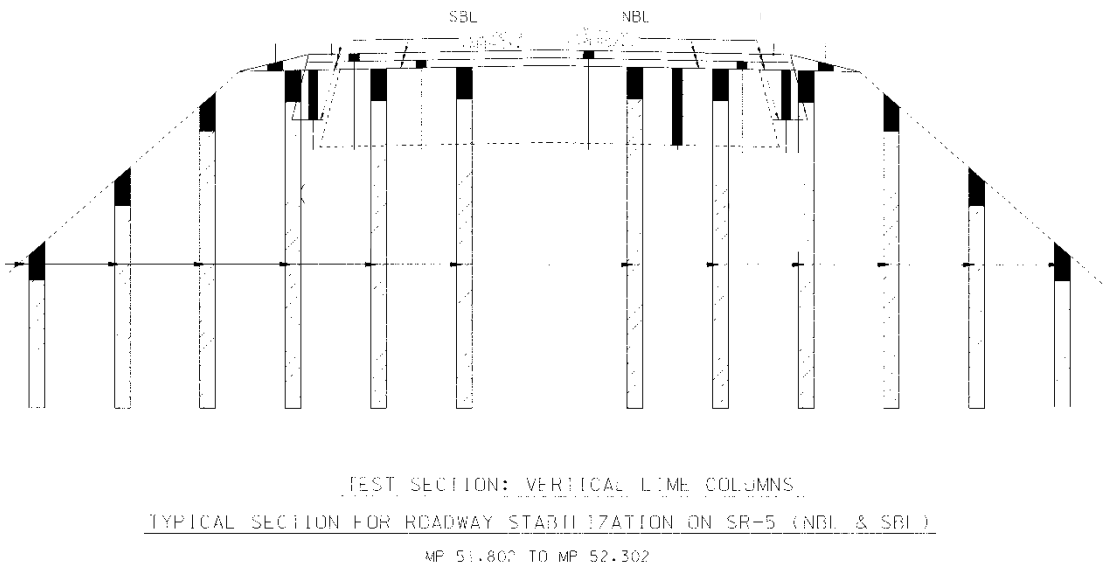

Figure 33: Typical Cross-Section of Lime Columns (ALDOT 2015)

Figure 34: Lime Columns Reflected Through Binder Course and Holding Water

3.7.4 Six Foot Paved Shoulders

It was noted during initial field reconnaissance that large longitudinal cracks were present near the edge of the pavement. Examples of this are shown in Figure 35and Figure 36. This could be due to the fact that moisture fluctuation is greatest near the edge of the pavement and diminishes towards the center, causing differential movement. This is illustrated in Figure 37. Test Section 4 employs six foot wide paved shoulders to try to shift these cracks out of the travel lane. This has the added benefit of providing lateral support to the pavement structure.

Figure 35: Longitudinal Crack in Travel Lane at AL-5

Figure 36: Longitudinal Edge Crack at AL-5

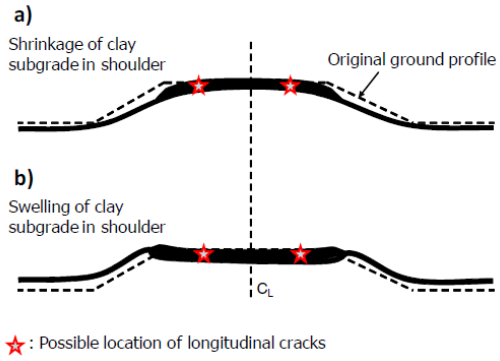

Figure 37: Longitudinal Crack Formation (Zornberg and Gupta 2009)

3.7.5 Edge Drains

Edge drains have been used with some success to mitigate the effects of expansive soils (Chen et al. 2012). They provide drainage at the edge of the pavement to attempt to stabilize the

moisture content of the subgrade, thus preventing heave damage. Edge drains were installed in Test Section 5 at AL-5. Figure 38 shows the typical edge drain cross-section at AL-5.

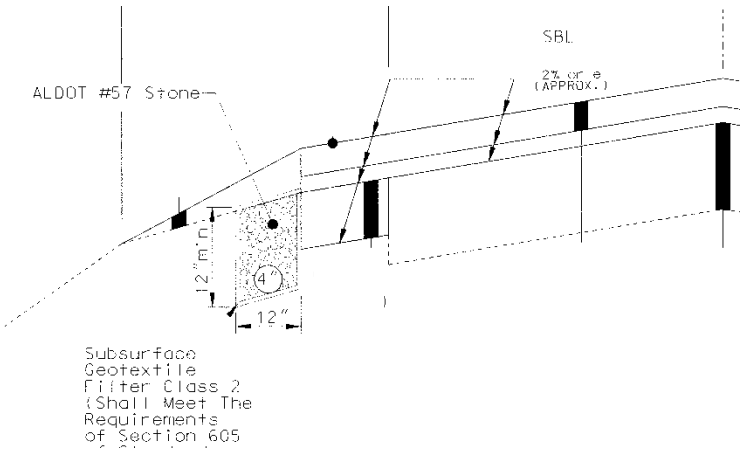

Figure 38: Typical Edge Drain Cross-Section at AL-5 (ALDOT 2015)

3.7.6 Deep Mixing

Madhyannapu et al. (2007, 2009, 2010) evaluated the use of deep soil mixing to stabilize expansive soils. On two test sections in Texas, it was found that movement around the columns was negligible after two years. It was proposed that deep soil mixing be used in Test Section 7 at AL-5. The proposed layout and cross-section for the deep mix columns are shown in Figure 39 and Figure 40. During the installation of test deep mix columns, it was found that they were not practical from a constructability standpoint. Therefore, this remediation technique was canceled and Test Section 7 became an additional control section.

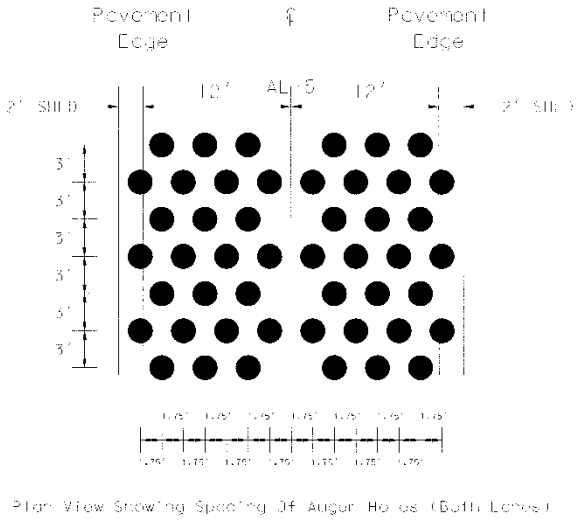

Figure 39: Deep Mix Column Layout (ALDOT 2015)

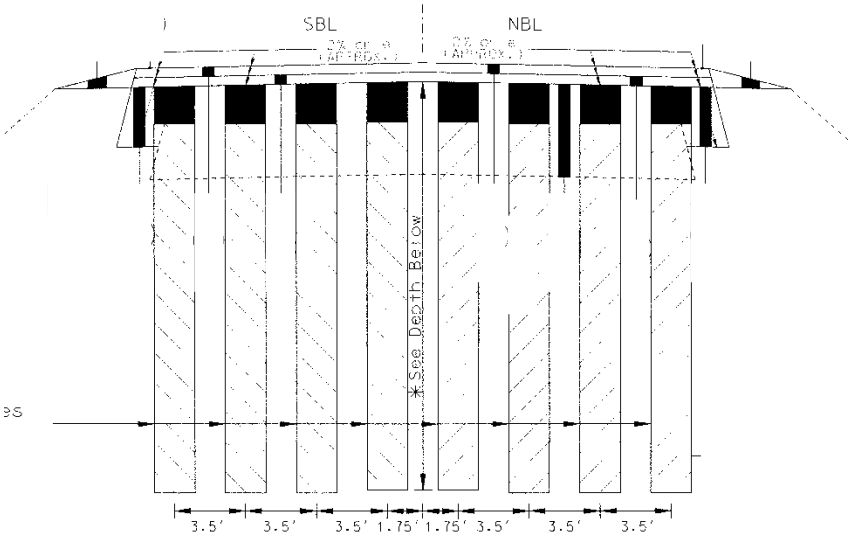

Figure 40: Deep Mix Columns Cross-Section (ALDOT 2015)

CHAPTER 4: INSTRUMENTATION SELECTION

In order to monitor the subgrade behavior and evaluate the test sections at AL-5, instrumentation was installed to collect data on the soil moisture and pavement conditions. Six monitoring locations were selected along AL-5 where sensors would be placed in the pavement and subgrade as well as in the shoulder. These locations corresponded to five remediation techniques and a control section. Additional sensors were placed at a seventh location to monitor the effects of vegetation on matric suction and moisture content. Sensors were selected to measure the soil moisture content, matric suction, pore water pressure, and asphalt strain. A weather station was also installed to monitor environmental conditions at AL-5. Sensors were chosen based on cost, functionality, accuracy, durability, and the ease of which they could be installed.

4.1 Moisture Sensors

The volumetric water content (VWC) of the soil was monitored using Decagon Devices GS1, shown in Figure 41. The GS1 is a capacitive sensor that measures the dielectric permittivity of a soil and correlates that to volumetric water content.

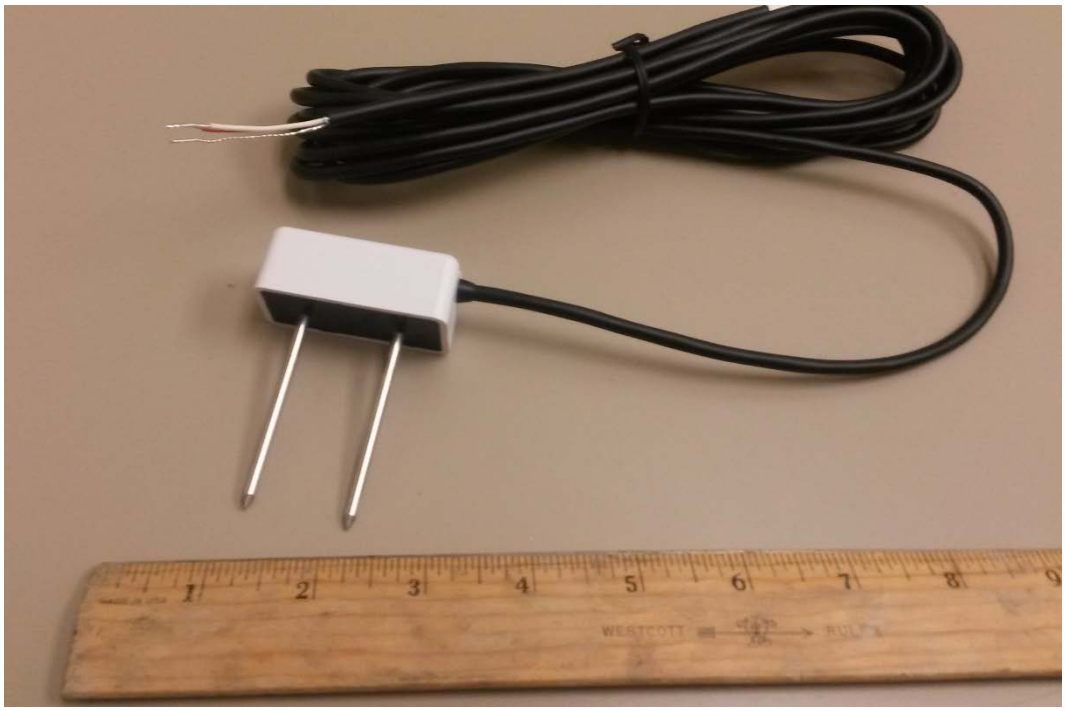

Figure 41: Decagon GS1

The GS1 functions in principle as a parallel plate capacitor with the sensor prongs being the plates and the soil being the dielectric material. The sensor measures the charging time of this capacitor formed by the sensor and soil. The charging time is proportional to the dielectric permittivity of the surrounding medium which is dependent on the amount of water present. The sensor outputs an analog voltage that strongly correlates to volumetric moisture content (Decagon Devices, Inc. 2015a).

Measurements taken by the GS1 are largely independent of soil properties and thus a single calibration, shown in Equation 10, can be used for almost all mineral soils. Decagon (2015a) states that the accuracy provided by this calibration is ±3% VWC. Higher accuracy can be obtained using a soil specific calibration. Because there is little sensor-to-sensor variability, a sensor specific calibration is not necessary for the GS1.

$$\boldsymbol{VWC = 0.000494 * mV - 0.554} \qquad \textbf{(10)}$$

Where VWC = volumetric water content expressed as a decimal

mV = raw GS1 output in millivolts

The GS1 is very compact, giving it an advantage over TDR sensors. Most TDR sensors have long wave guides that must be inserted into the soil. Figure 42 shows a Campbell Scientific CS616, a TDR sensor with 11.75” wave guides and a total length of 15 inches. Even more compact TDR sensors such as the Campbell Scientific CS655 still has a total length of approximately 8 inches (Campbell Scientific, Inc. 2016). Because of this, TDR sensors are impractical for installation in the sidewall of a borehole. The prongs of the GS1 are approximately 2.25 inches long and the sensor body is approximately 2”x1”x0.75”. The total length of the GS1 is only 3 inches, making it ideal to be installed in a borehole.

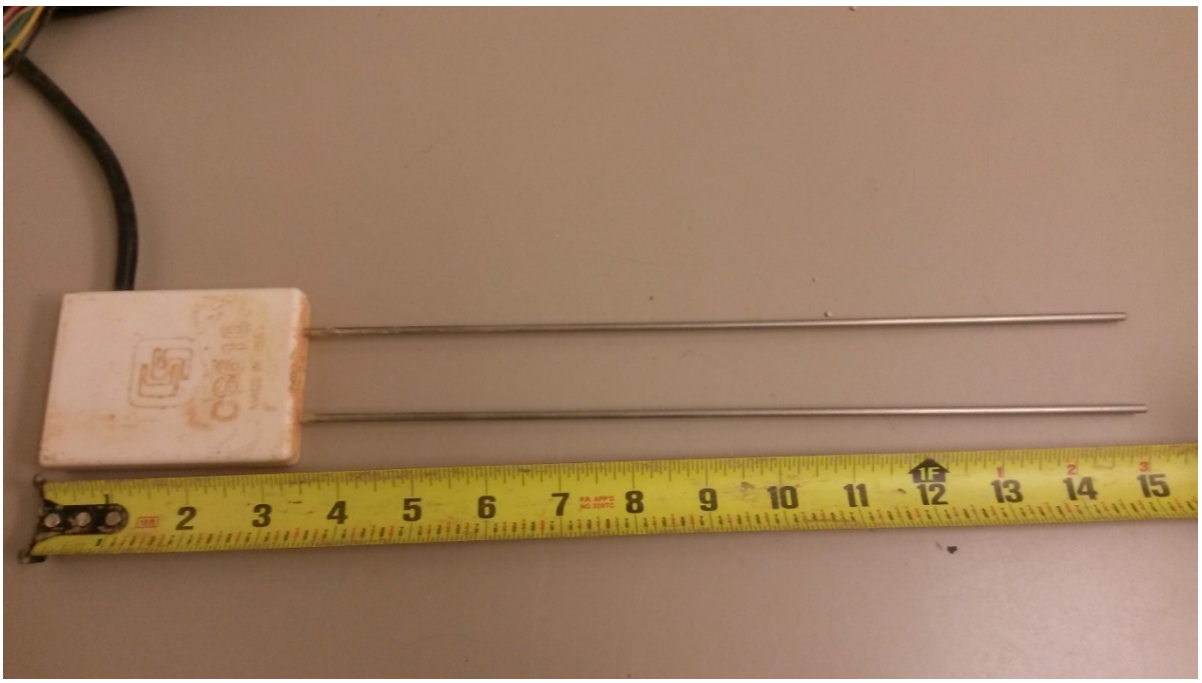

Figure 42: Campbell Scientific CS616 TDR Sensor

4.2 Suction Sensors

The MPS6 from Decagon Devices, shown in Figure 43, was selected to measure matric suction at AL-5. The MPS6 has a ceramic disk that is placed in hydraulic contact with the soil. The suction in the disk equalizes with the soil suction although the disk may have a different moisture content than the soil. The water content of the ceramic is measured using a dielectric technique similar to that described for the Decagon GS1. The moisture characteristic curve of the ceramic can then be used to determine the matric suction. These calculations are performed by the MPS6 and a digital output reports the matric suction and temperature.

Figure 43: Decagon MPS6

Watermark electrical resistance sensors had been successfully used in a previous study at Auburn University (Burrage 2015). However, a review of the relevant literature indicated that these sensors do not possess a high accuracy. Most suction sensors, such as thermal conductivity sensors, require calibration by the user to provide a high degree of accuracy. The equipment needed to calibrate matric suction sensors was not available at Auburn University. The MPS6 offers the advantage of being factory calibrated and was selected because of this.

Because the MPS6 was originally intended for agricultural use, the calibration focused on lower suctions that are of greater interest in agricultural applications. Each MPS6 is individually calibrated at a vacuum saturated state, an air dry state (suctions of 0 kPa and 100,000 kPa, respectively), and at four suction values between 9 kPa and 100 kPa. This leads to an accuracy of ±(10% of the reading + 2 kPa) over the range of 9 kPa to 100 kPa (Decagon Devices, Inc. 2015b). Decagon (2015b) reports that the MPS6 shows good accuracy to suctions of up to 1500 kPa based on Laboratory evaluations. Decagon also reports low sensor-to-sensor variability to suctions of up to 4500 kPa.

The lower limit of the MPS6 is the higher of either the air entry value of the ceramic (9 kPa) or the surrounding soil. At suctions below this the ceramic will be fully saturated and the suction will not be able to be determined.

4.3 Piezometers

In order to measure positive pore pressures if the soil ever became saturated, piezometers were installed in each test section. Vibrating wire piezometers from Geokon were selected for this study. These piezometers are robust and have been used in other research at Auburn University (Burrage 2015). Each 4500S has an individual calibration provided by Geokon. The Geokon 4500S is shown in Figure 44.

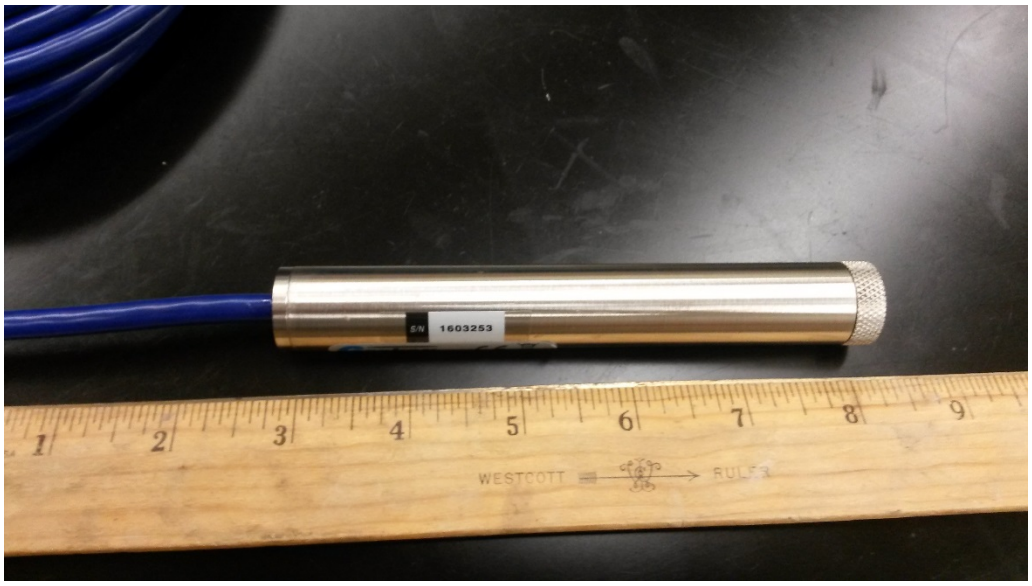

Figure 44: Geokon 4500S

Piezometers must be fully saturated to make measurements, so when used in unsaturated soils, a high air entry (HAE) filter must be used to separate the air and water phase. When an HAE filter is used, piezometers can measure matric suction to values of approximately 100 kPa. At suctions higher than this the water in the piezometer will cavitate and the piezometer will not be able to make measurements. In addition to this, the water compartment behind the HAE filter will dry out over time. Once a piezometer loses its saturation due to cavitation or drying, it will not recover until it is fully saturated again.

Because of these disadvantages and the additional cost and time required to saturate HAE filters, it was decided to order piezometers without HAE filters. The piezometers will mainly be used to monitor positive pore pressures if they develop at AL-5. However, even without the HAE filters, the piezometers will remain saturated in an unsaturated soil until the air entry value of the soil is reached. This means that the piezometers can effectively measure suction up to the air entry value of the soil because the soil functions as an HAE filter.

4.4 Neutron Moisture Probe

In addition to the GS1 moisture sensors, a neutron moisture probe was selected to measure the water content of the subgrade. Unlike the other instruments used at AL-5, the neutron moisture probe is not automated and must be manually read on site. A Troxler Model 4300 Depth Moisture Gauge, shown in Figure 45, was acquired by the Alabama Department of Transportation (ALDOT) for use at AL-5. This model consists of a shield and control unit that attaches to a 1.5 inch diameter probe. The probe contains a neutron source and detector and can be lowered down an access tube to the desired depth to take volumetric moisture readings. The Model 4300 comes with a factory calibration that was performed in sand, but it is recommended that site specific calibrations be performed, especially for soil types other than sand. The methodology and results for the neutron moisture probe will be described in a later publication.

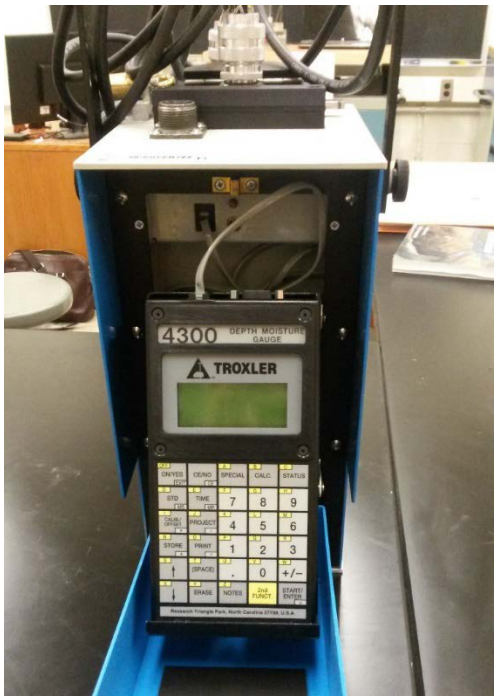

Figure 45: Troxler Model 4300 Depth Moisture Gauge

4.5 Asphalt Strain Gages

Asphalt strain gages were used in this study to try to continuously measure the level of pavement distress. Two types of asphalt strain gages (ASGs) were used at AL-5. The ASG-152 from CTL Group was used in Test Section 1 to monitor the sand blanket. Geocomp asphalt strain gages were used for all other sections. CTL and Geocomp ASGs are shown in Figure 46 and Figure 47, respectively.

Because the sand blanket was fully reconstructed, the ASGs were able to be installed on top of the aggregate base. Because of this, the sand blanket ASGs had to be ordered and installed several months prior to the remaining gages. CTL had the required gages in stock and could deliver them in time for installation. For the remaining gages, which were installed on a milled surface, Geocomp was able to provide a better price and had a shorter delivery time than CTL. Furthermore, CTL gages were installed during the 2015 NCAT Test Track rebuild and had very low survivability. Therefore, the decision was made to use Geocomp gages in the remaining test sections.

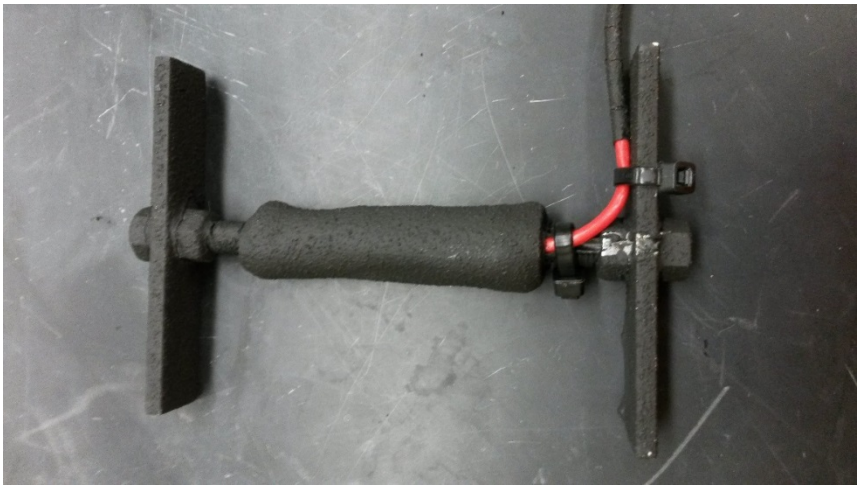

Figure 46: CTL Asphalt Strain Gage

Figure 47: Geocomp Asphalt Strain Gage

The CTL and Geocomp ASGs are almost identical in construction. Each gage consists of a full Wheatstone bridge circuit with four active 350 ohm strain gages mounted on a 6/6 nylon rod. A temperature resistant coating is applied to each gage to ensure it survives paving. Each gage is individually calibrated by the manufacturer.

4.6 Data Acquisition System and Weather Station

A CR6 datalogger from Campbell Scientific was used to monitor the sensors in each location. This datalogger is capable of reading all the sensor types used for this project without additional interfaces. The datalogger is powered by a BP12/CH200 power supply and charging regulator from Campbell Scientific. Each station is also equipped with a solar panel to recharge the batteries. Three AM16/32B multiplexers were used at each station to connect the moisture sensors, piezometers, and asphalt strain gages. Figure 48 shows the CR6, BP12/CH200, and AM16/32B. A Campbell Scientific WTX520 weather sensor was also selected to measure air temperature, barometric pressure, wind speed, wind direction, relative humidity, and precipitation. The WTX520 is shown in Figure 49.

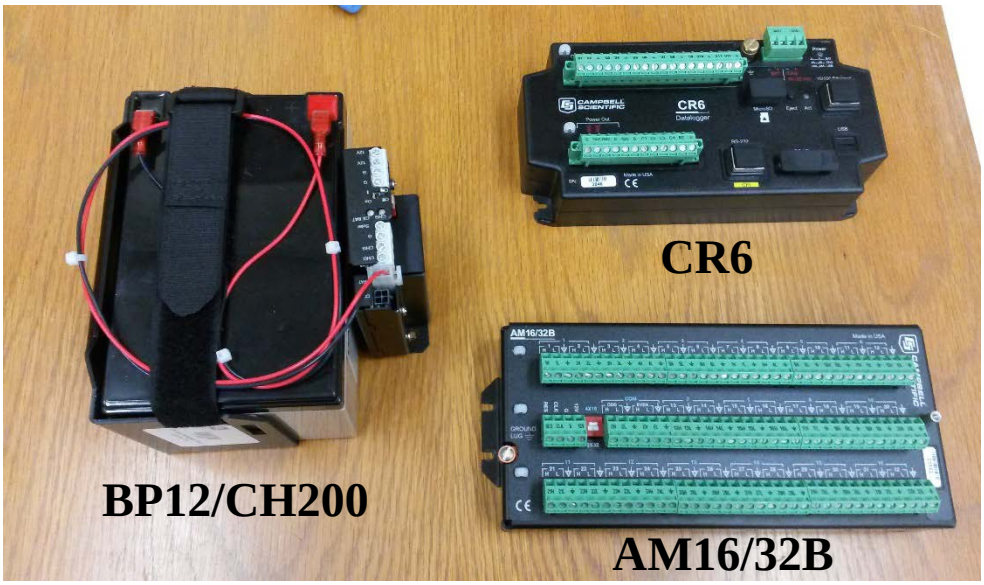

Figure 48: Campbell Scientific CR6, AM16/32B, and BP12/CH200

Figure 49: Campbell Scientific WTX520

Communication equipment was also included in the data acquisition system to allow the data to be collected remotely. This consisted of a spread-spectrum radio for communication between each station and a single cellular modem at a master datalogger that can be accessed remotely. The RavenXTV from Campbell Scientific was selected as the cellular modem. Prior to selecting radios, a test of various radio and antenna combinations was conducted. For this test, a base radio was placed at a datalogger location and a test radio was moved to the next location and communication was attempted. If communication failed, a different radio/antenna combination was tried until a combination worked. Based on the results of the radio test, RF451 radios from Campbell Scientific were selected with 0 dBd omni ¼ wave whip antennas. The RavenXTV and RF451 are shown in Figure 50.

Figure 50: Campbell Scientific RF451 and RavenXTV

CHAPTER 5: INSTRUMENTATION PREPARATION AND LABORATORY TESTING

Prior to installation, all sensors and data acquisition equipment was tested in the laboratory to ensure everything functioned properly. After laboratory testing of the sensors, each sensor was assigned to a location and depth and labeled accordingly. In addition, a calibration was performed on the moisture content sensors.

5.1 GS1 Moisture Content Sensors

Upon receipt of the GS1 moisture sensors, each sensor was tested to ensure it was functioning properly. Using the ProCheck, a readout device supplied by Decagon, each sensor was read in air and submerged in water. There was some noise in the readings when the sensors were submerged, but each sensor responded appropriately. The calibration equation provided by Decagon was used during the lab test, and the sensors read slightly negative volumetric water content (VWC) in air and approximately 60% VWC when submerged. This was consistent with the behavior described by Decagon in the GS1 user manual. The raw readings for all sensors had a coefficient of variation of less than 2% for readings in both air and water. Because of this low sensor-to-sensor variability, a single calibration function was used for all GS1 moisture sensors.

5.1.1 Moisture Sensor Calibration

Decagon reports that a factory calibration is sufficient for most mineral soils. However, grain size and soil and pore water chemistry play a role in the determination of moisture content. To account for these effects, a calibration was performed for the GS1. Because sensor-to-sensor

variability is low, a single calibration was used for all GS1s. To perform the calibration, a bulk sample of soil from Test Section 1 was taken at the time of sensor installation. This sample was oven dried and prepared as described below.

Because the GS1 measures volumetric water content, the sample used for calibration must be at approximately the same dry density as that in the field. A dry density (ρ_d) of 1.345 g/cm^3 was used as determined by Stallings (2016). A specific gravity of solids (G_s) of 2.75 was used in the calculations, also from Stallings (2016). Using Equations 11 and 12, target moisture contents were calculated over a range of saturations. The target moisture contents are shown in Table 4. The amount of water needed to prepare each sample was determined by multiplying the mass of solids by the gravimetric moisture content.

$$\boldsymbol{\theta = S\left(1 - \frac{\rho_d}{\rho_w G_s}\right)} \quad \textbf{(11)}$$

$$\boldsymbol{w = \theta\left(\frac{\rho_w}{\rho_d}\right)} \quad \textbf{(12)}$$

Where θ = volumetric moisture content expressed as a decimal

S = degree of saturation expressed as a decimal

ρ_d = dry density (g/cm^3)

ρ_w = density of water (g/cm^3)

G_s = specific gravity of solids

w = gravimetric moisture content expressed as a decimal

Table 4: Target Moisture Contents for GS1 Calibration

Target Saturation	Target Vol. Moisture Content	Target Grav. Moisture Content
0%	0.0000	0.0000
20%	0.1022	0.0760
40%	0.2044	0.1519
60%	0.3065	0.2279
80%	0.4087	0.3039
100%	0.5109	0.3799

The measurement volume of the GS1 is shown in Figure 51. Care was taken to ensure that the entire measurement volume was full of soil at the correct dry density. A California Bearing Ratio (CBR) mold was used for the calibrations. The mold had a diameter of 6 inches and a height of 7 inches, slightly larger than the measurement volume shown in Figure 51. Figure 52 shows the CBR mold. It was determined that the mold had no effect on the sensor readings by suspending a sensor in open air and moving the sensor slowly down until it was suspended inside the mold. Readings were consistent in free air and inside the mold.

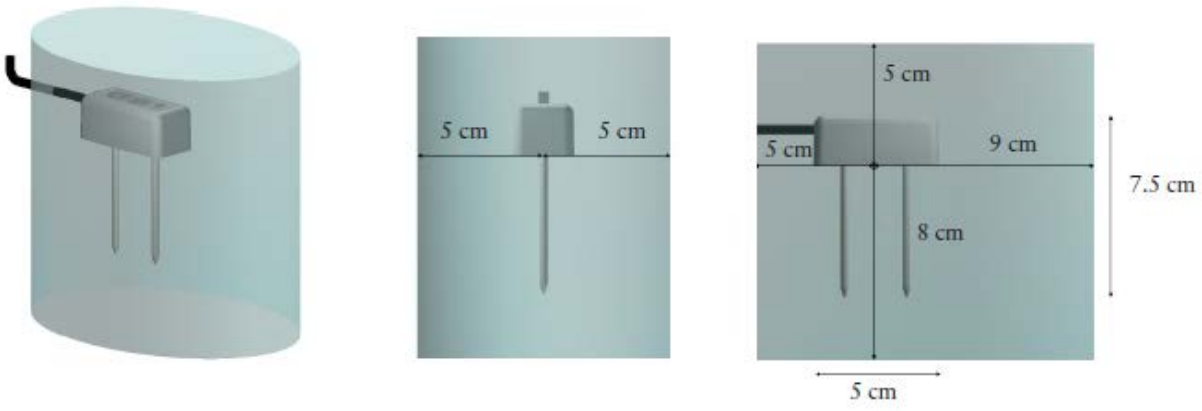

Figure 51: Idealized Measurement Volume of Decagon GS1 Sensor (Cobos 2015)

Figure 52: CBR Mold Used for Moisture Sensor Calibration

To perform the calibration, soil samples were prepared at various moisture contents as described above. The soil was then compacted into the mold to a depth of approximately four inches as shown in Figure 53. The moisture sensor was then installed and soil was compacted above the sensor until the mold was full, shown in Figure 54. A GS1 reading was then taken with a CR6 datalogger. The total mass of soil in the mold was then determined and two gravimetric moisture samples were obtained. This was repeated for all the target moisture contents shown in Table 4.

Figure 53: GS1 Inserted in Soil for Calibration

Figure 54: Full CBR Mold with Sensor Installed

Once the gravimetric moisture content was determined for each sample, the dry density of the sample was determined from the mass of solids in the CBR mold and the volume of the mold. The volumetric moisture content was then calculated using Equation 9. Table 5 shows the GS1 reading, dry density, and moisture content of each sample. The volumetric moisture content was plotted against the GS1 reading and a trendline was fit to the data, shown in Figure 55. It was determined that a third order polynomial closely approximated the data and this was used as the calibration function. The calibration function is given by Equation 13.

Table 5: GS1 Calibration Results

Sample No.	GS1 Reading (mV)	Dry Density (g/cm^3)	Grav. Moisture Content	Vol. Moisture Content
1	1199	1.32	0.0289	0.038
2	1613	1.31	0.1026	0.135
3	1815	1.27	0.1854	0.235
4	1952	1.17	0.2582	0.303
5	2158	1.33	0.3403	0.453
6	2168	1.24	0.4244	0.527

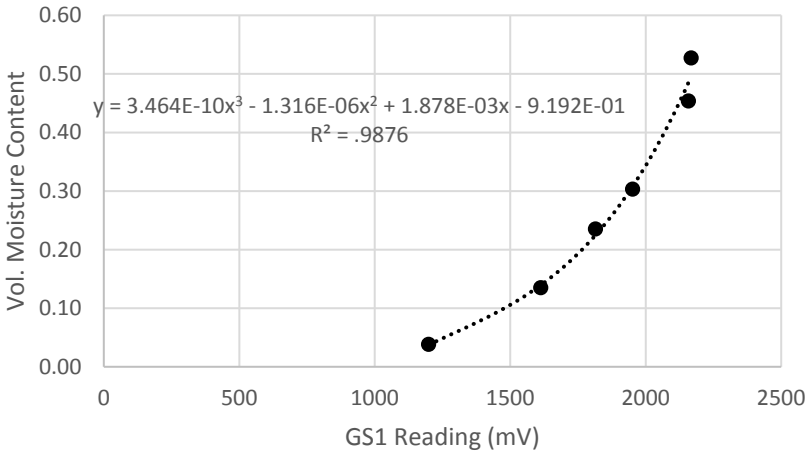

Figure 55: GS1 Calibration Data

$$\boldsymbol{VWC = (3.464 \cdot 10^{-10})mV^3 - (1.316 \cdot 10^{-6})mV^2 + (1.878 \cdot 10^{-3})mV - 0.919} \quad \textbf{(13)}$$

Where VWC = volumetric moisture content expressed as a decimal

mV = raw GS1 output in millivolts

The majority of the field moisture measurements were observed to be on the wetter end of the calibration curve. Because of this, it is recommended that an additional calibration be performed that specifically focuses on points wetter than 40% VWC.

5.2 MPS6 Suction Sensors

Each MPS6 was read in air using the Decagon ProCheck. When checked in air, a lot of noise was present in MPS6 suction readings. This was expected as Decagon (2015b) reports that the sensor readings typically vary from 50,000 kPa to 100,000 kPa when read in air with the noise decreasing when it is installed in soil. Because of this, the sensors were only checked for a suction reading with the proper order of magnitude and a reasonable temperature reading.

The MPS6 outputs processed digital values for suction and temperature using the SDI-12 protocol. For this protocol, all the sensors have an individual address and are read on a single

datalogger channel. Eight MPS6 sensors were to be installed in each test section, so they were assigned SDI-12 addresses of one through eight.

5.3 Geokon 4500S Piezometers

Upon receipt of the 4500S piezometers, each was checked to ensure it was functioning properly and the zero values did not vary significantly from the factory zero values provided by Geokon. The zero values will vary slightly due to differences in barometric pressure and temperature. Even with these variations, however, all the piezometer zero readings had a percent difference of less than 0.3% from the factory zeros and all thermistors provided reasonable temperature readings. Factory calibrations provided by Geokon were used for the piezometers.

5.4 Asphalt Strain Gages

All asphalt strain gages were checked using the procedure described by Timm (2009). Because the CR6 dataloggers used in this study were not available yet, a CR1000 datalogger was used. Each gage was checked to ensure it produced a stable output signal and it responded as expected to applied strain. Additionally, the baseline (unloaded) output voltage was checked. The gage output was recorded in millivolts per volt excitation. Figure 56 shows an example of a typical gage output. This gage has a stable baseline voltage of approximately -1.55 mV/V. When the gage was pushed on (compression), it gave a negative response and when it was pulled (tension) it gave a positive response. Ideally, the baseline output should be close to zero, as an offset baseline can cause gages to go out of range when strain is applied. All gages had stable baseline readings and responded appropriately to tension and compression. The gages with the worst baseline voltage (farthest from zero) were distributed evenly among the test sections.

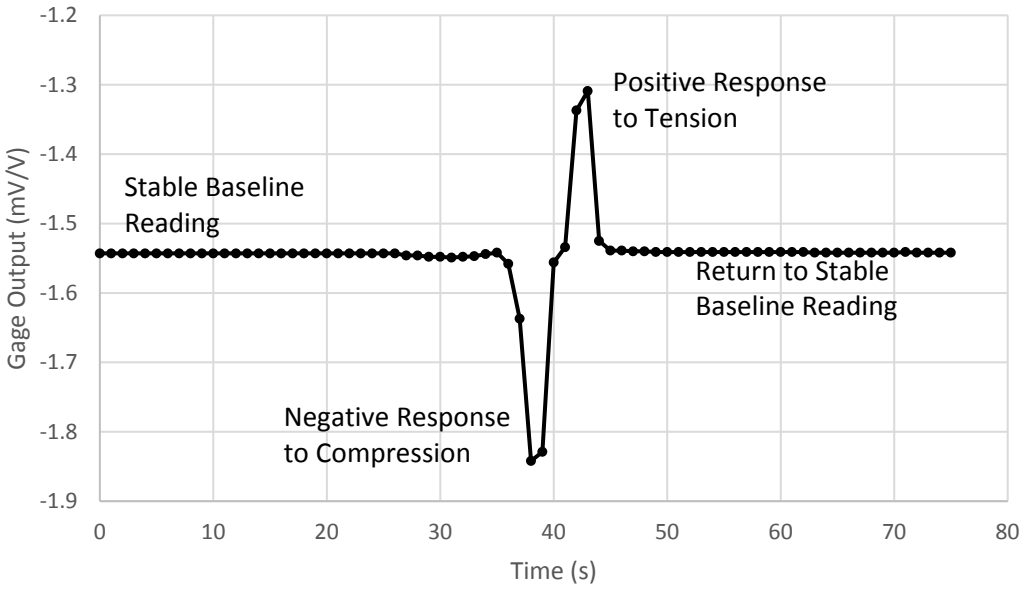

Figure 56: ASG Output during Laboratory Test

Calibration coefficients provided by the sensor manufacturer were used for the asphalt strain gages. This has been the typical practice at the NCAT Test Track (Timm 2009). ASG calibrations were performed by Hornyak et al. (2007) and reasonable agreement was found with the manufacturer calibrations.

5.5 Data Acquisition Equipment

Upon receipt of the data acquisition equipment, it was assembled and wired in enclosures. Figure 57 shows an assembled data acquisition station. Programs for the dataloggers were written by Campbell Scientific and modified to suit the needs of this project. Each datalogger is programed to read all sensors at 30 minute intervals. Once a day the maximum, minimum, and average values for each sensor are recorded to a data table. Raw values and calibrated data are recorded. Datalogger wiring diagrams are shown in Appendix B and datalogger programs are in Appendix C.

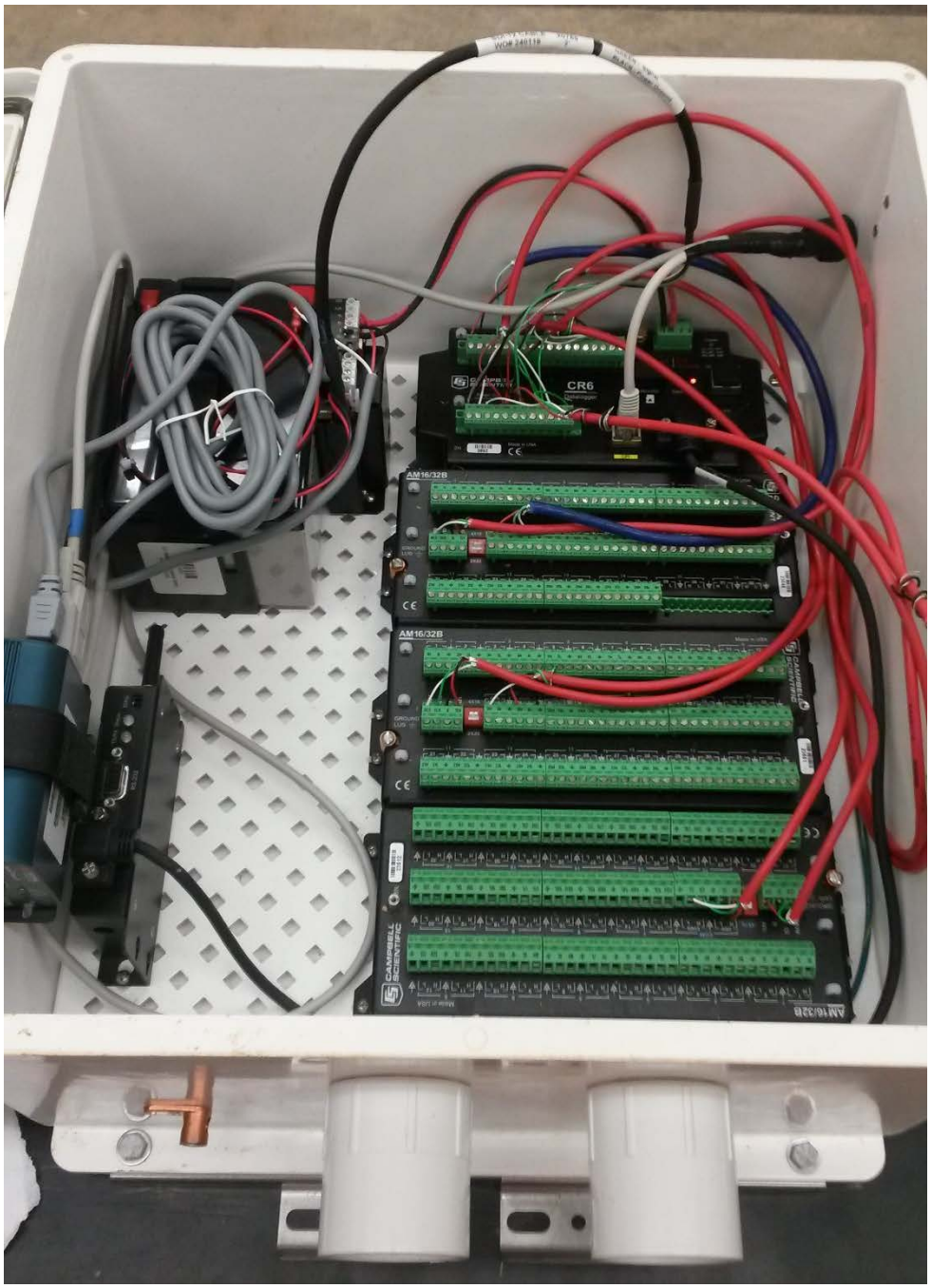

Figure 57: Assembled Data Acquisition Station

CHAPTER 6: SENSOR INSTALLATION

6.1 Instrumentation Locations

To measure the subgrade behavior and evaluate the remediation techniques, each test section that received remediation was instrumented with moisture, suction, pore pressure, and asphalt strain sensors. Neutron moisture probe monitoring wells were also installed near all instrument locations. The decision was made to use the first portion of Test Section 1 as the instrumented control section. This was because the soils in the remaining control sections (Test Section 6 – 8) were slightly different from the rest of the soils on the project (Stallings 2016). In addition to the remediated test sections, the shoulder near a large tree was instrumented with moisture and suction sensors and neutron moisture probe monitoring wells. Figure 58 and Table 6 show the locations of each set of instruments.

Table 6: Instrument Locations

Section	Mile Point
Control	50.900
Sand Blanket	51.066
Vertical Barriers	51.549
Lime Columns	52.140
Paved Shoulders	52.772
Edge Drains	53.102
Tree	53.287

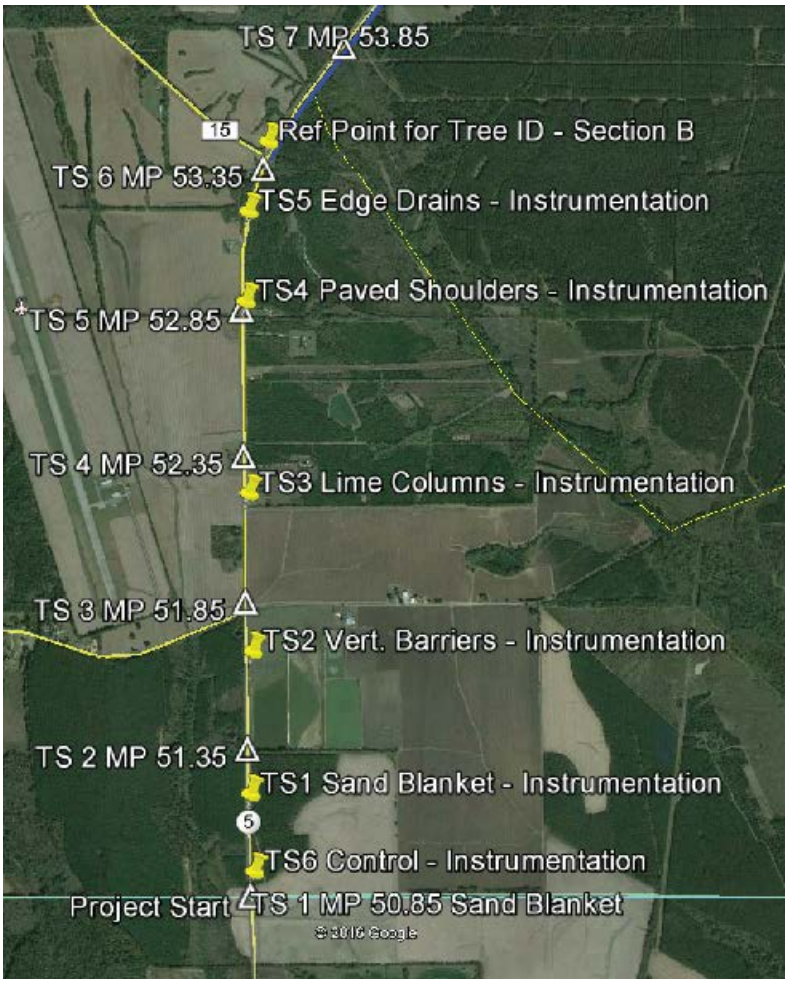

Figure 58: Instrumentation Locations

To monitor moisture content, suction, and pore pressure with depth, these sensors were installed in boreholes in the pavement and shoulder. Neutron moisture probe monitoring wells were installed near each instrumented borehole. The asphalt strain gages were installed in the pavement adjacent to the borehole sensors. Data acquisition equipment was installed at each instrument location as shown in Figure 59. An effort was made to locate the instruments far enough from the test section boundaries to avoid end effects.

Figure 59: Data Acquisition Installation

6.2 Downhole Sensors

To install the downhole sensors, a 6 inch diameter borehole was drilled to a depth total depth of 12 feet. The sensors were then installed from the bottom up. Four moisture sensors, four suction sensors, and two piezometers were installed in each borehole. Target depths were 2.5 ft, 5.0 ft, 7.5 ft, and 10.0 ft for the moisture and suction sensors. Target piezometer depths were 12.0 ft and 7.5 ft. The borehole was backfilled to each installation depth with native material and compacted using an inclinometer tube. The backfill procedure was monitored with a downhole camera to ensure the sensors and wires were not damaged. Because measurement volume of the moisture sensors included a portion of the borehole, it was necessary that the borehole be filled

with the native material. The clay at AL-5 is also a low permeability material which will minimize preferential flow if it is compacted adequately.

6.2.1 Moisture Sensor Installation

The prongs from the moisture sensors had to be inserted into undisturbed soil with no air gaps. In order to insert the sensors horizontally at depths of up to 10 feet, an installation tool was fabricated at Auburn University. The tool consists of a scissor jack mounted to a half of a six inch diameter steel pipe, shown in Figure 60. The moisture sensor was seated on the scissor jack as shown in Figure 61. As the jack extended the sensor prongs were pushed into the soil. A small piece of electrical tape was used to hold the moisture sensor to the tool while it was lowered down the borehole. Extendable rods were used to lower the tool down the borehole and operate the scissor jack. The tool was designed to rest on the bottom of the borehole and install the sensor 12 inches above the bottom of the hole. A six inch diameter borehole was required to install the moisture sensors using the installation tool.

Figure 60: Moisture Sensor Installation Tool

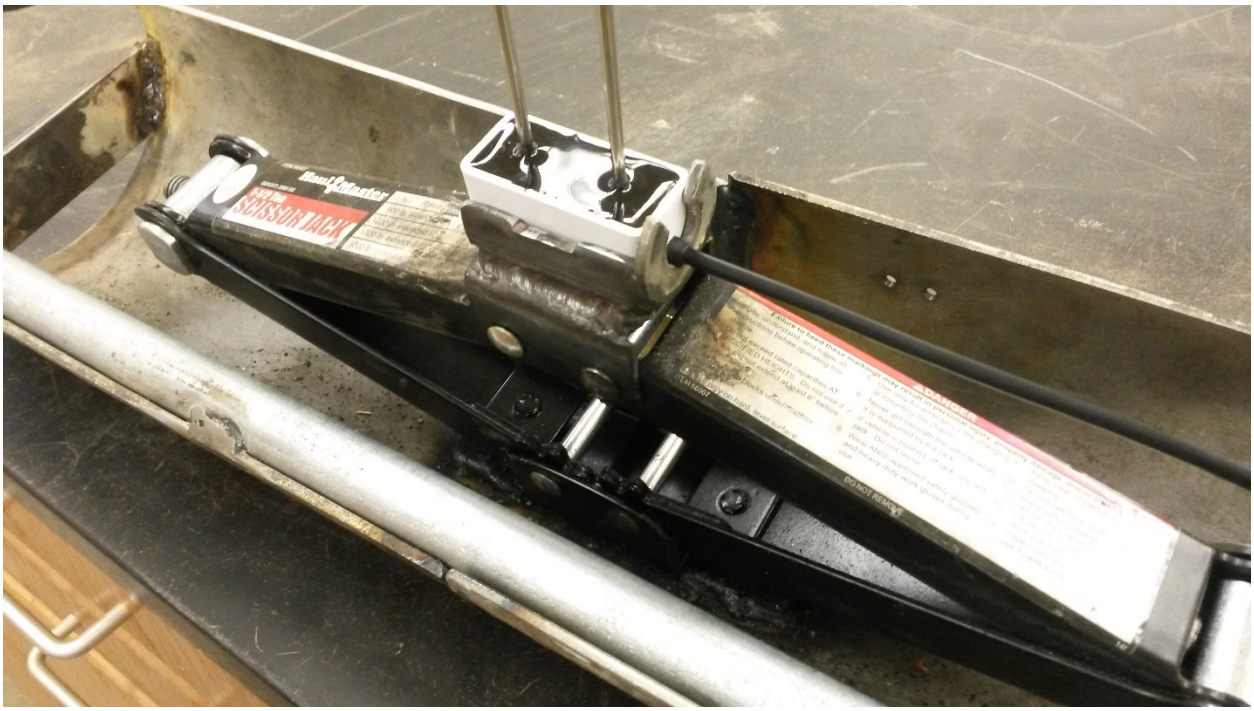

Figure 61: GS1 Seated on Installation Tool

A trial sensor was installed in Montgomery, AL to ensure the installation tool would work properly. The soil it was installed in was a fat clay similar to the subgrade at AL-5. The soil was very stiff and was in a dry condition. A six inch diameter hollow stem auger was used to drill a borehole for sensor installation. The sensor was installed at a depth of approximately two feet so that it could be retrieved. However, because the soil was very stiff and the sensor was not seated properly on the installation tool, the prongs of the sensor bent when it was pushed into the soil, shown in Figure 62. It was decided that a downhole camera should be used at AL-5 to ensure that the sensors remained seated on the installation tool and the prongs did not bend as the sensor was inserted.

Figure 62: Bent Prongs on Trial Sensor

Moisture sensor installation at AL-5 proceeded as planned for the most part. The borehole was backfilled and compacted to 12 inches below the target installation depth to facilitate the installation tool. Due to the backfill procedure used, the actual installation depths typically varied by ±0.1 ft from the target depths. Sensor installation depths are shown in Appendix A. A downhole camera was used to verify the moisture sensor was seated on the installation tool properly and that it was fully inserted into the sidewall of the borehole without the prongs bending. Figure 63 shows a sensor being lowered down the borehole on the installation tool. Figure 64 and Figure 65 show downhole photographs of the moisture sensor installation. Care was taken to ensure other sensors and wires were outside the measurement volume of the moisture sensors, shown in Figure 51.

Figure 63: Moisture Sensor and Installation Tool being Lowered down Borehole

Figure 64: Moisture Sensor Installation

Figure 65: Fully Installed Moisture Sensor

All moisture sensors were installed as described above with the exception of the 7.5 ft sensor in the shoulder borehole of the control section. Due to a malfunction of the installation tool, this sensor could not be installed in the sidewall. Instead, the prongs were inserted into some drill shavings and the sensor was lowered down the hole, shown in Figure 66. Due to possible air gaps near the sensor, the accuracy of readings from this sensor are questionable.

Figure 66: Moisture Sensor Prongs Inserted into Drill Shavings

6.2.2 Suction Sensors

The suction sensors were installed according to the manufacturer's recommendations. Once the appropriate depth was reached, native soil was packed around the ceramic disk. Care was taken not to smear the soil on the disk, but to ensure good hydraulic contact. A prepared suction sensor is shown in Figure 67. This prepared sensor was lowered down the borehole to the correct depth and the hole was backfilled and compacted. A downhole camera was used to monitor the compaction process to ensure the sensor was not damaged.

Figure 67: Suction Sensor Preparation

6.2.3 Piezometers

Two piezometers were installed in each borehole at depths of approximately 12.0 ft and 7.5 ft. The typical procedure for installing piezometers is to place the piezometer in a large volume sand pocket and seal the borehole with bentonite. As noted by Mikkensen and Green (2003), this procedure was developed for stand pipe piezometers and is not necessary for

diaphragm (vibrating wire) piezometers. Therefore, the piezometers were placed in a small bag full of saturated filter sand and lowered down the borehole. The hole was then backfilled and compacted with native material. Because the native material has a very low permeability, it would serve the same function as a bentonite or grout seal. Figure 68 shows the piezometer in the sand-filled bag being lowered down the hole.

Figure 68: Piezometer in Sand-Filled Bag being Lowered Down the Borehole

6.3 Asphalt Strain Gage Installation

Twelve asphalt strain gages (ASGs) were installed in the sand blanket and eight were installed in all other sections. The sand blanket ASGs were ordered and installed several months before the remaining sensors. When the remaining sensors were ordered, it was decided to

decrease the number of ASGs to eight to minimize costs. The layout of the strain gages is shown in Figure 69 and Figure 70. These layouts provide redundancy for both longitudinal and transverse strain. The centerline of the strain gage array was at approximately the center of the travel lane.

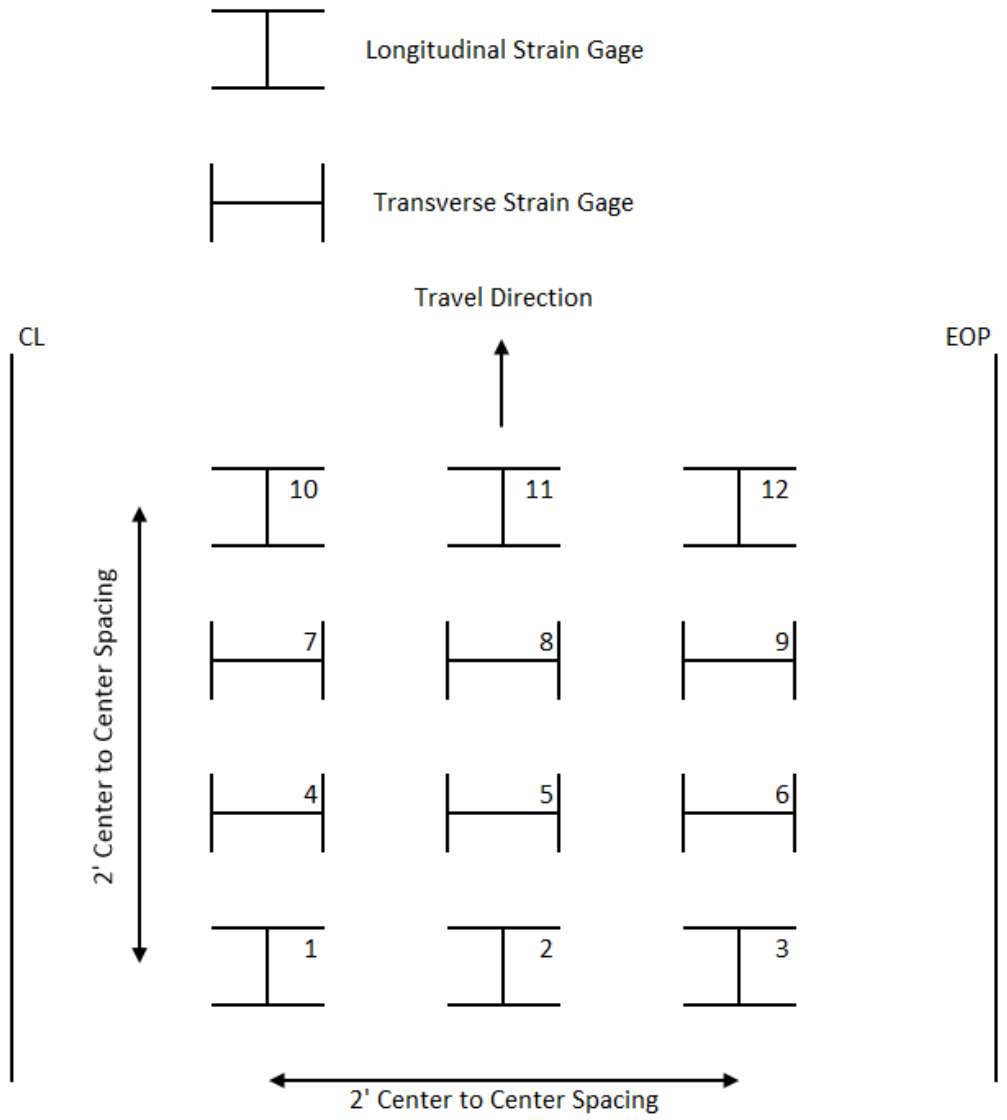

Figure 69: Sand Blanket Strain Gage Layout

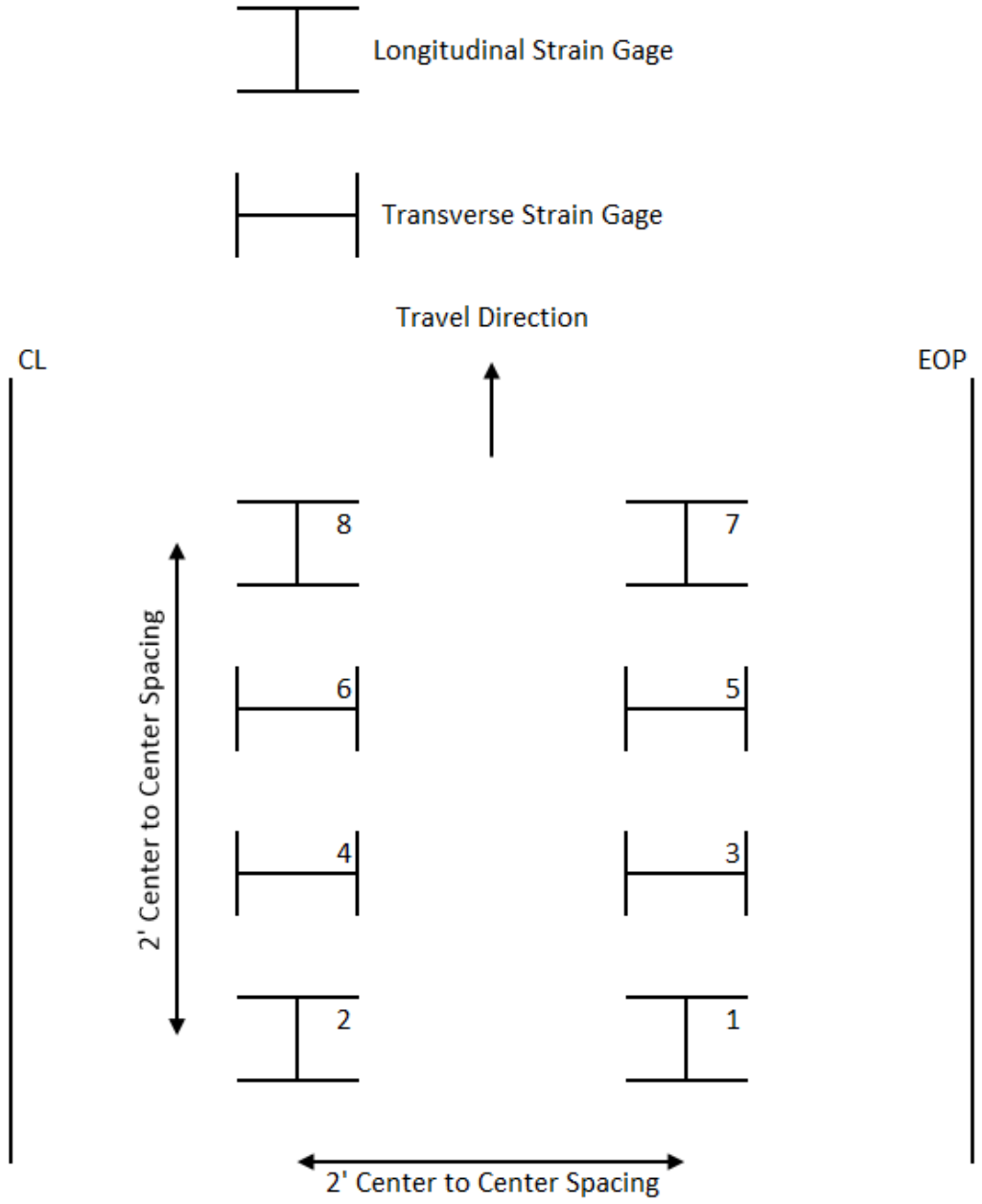

Figure 70: Strain Gage Layout for Sections Other than Sand Blanket

6.3.1 Sand Blanket Asphalt Strain Gages

Because the sand blanket was full depth construction, it was possible to install the asphalt strain gages on top of the aggregate base. This is the procedure that has been used at the NCAT Test Track (Timm 2009).

The gages were first laid out in the correct position and the wires were routed to the edge of the pavement. The wires were then placed in 3/8 inch flexible conduit for added protection. Small trenches were dug in the aggregate base for the wires. Once the wires were in place, the trenches were backfilled and compacted. Immediately prior to paving, the gages were tacked in place using a tack-sand mixture. This is typically done with a binder-sand mixture (Timm 2009), but the paving contractor was unable to provide binder to the site. Tacked gages are shown in Figure 71. Once the gages were tacked in place they were covered with asphalt that was screened through a ¼ inch screen. Static compaction was used to compact the mounds of asphalt over the gages. Figure 72 shows screened asphalt being placed and compacted over the gages. The paving train then passed over the gages. No vibratory compaction was used for the first pass of the roller over the gage array. The gages were monitored during the placement and compaction of the asphalt.

Figure 71: ASGs being Tacked with Tack-Sand Mixture

Figure 72: Screened Asphalt being Placed and Compacted over Gages

6.3.2 All Other Asphalt Strain Gages

Because the test sections other than the sand blanket only received resurfacing and not full depth construction, the strain gages could not be placed in the aggregate base. Instead, sections were milled out for the gage placement, shown in Figure 73. The sections were milled to a depth of three inches to ensure adequate coverage of the ASGs. The gages were then laid out in the proper position. Prior to paving, the gages were tacked to the milled surface using the same tack-sand mixture described above. Once again, the paving contractor was unable to provide binder to the site. After the gages were tacked, the gages and wires were covered with screened

asphalt as described above. Because the wires could not be buried in trenches, they were not placed in conduit, but they were covered with screened asphalt. The wires from the borehole sensors were also covered with screened asphalt. Figure 74 shows the gage array covered with screened asphalt. The gage array was then paved over and compacted without vibration.

Figure 73: Section Milled and Cleaned for placement of ASG Array

Figure 74: Gage Array on Milled Surface Covered with Screened Asphalt

6.4 Sensor Survivability

Sensor survivability was very good at AL-5. All moisture sensors and piezometers survived and are providing reasonable outputs. Five asphalt strain gages did not survive, possibly due to over stressing during construction. A possible future point of failure for the Geocomp asphalt strain gages is the connection of the sensor leads to the datalogger. The leads were very small and tended to break off once they were wired into the datalogger.

All suction sensors initially provided readings, but several stopped functioning shortly after baseline readings were taken. The cause of suction sensor failure in the other sections is currently unknown but is being investigated further. It is also unknown if the suction sensors are

merely temporarily disabled or have permanently failed. Table 7 summarizes the sensor survivability by test section. The overall sensor survivability was 93%.

Table 7: Sensor Survivability

	Moisture			Suction		
Test Section	**Surviving**	**Total**	**Percent Surviving**	**Surviving**	**Total**	**Percent Surviving**
Control	8	8	100%	8	8	100%
Sand Blanket	8	8	100%	8	8	100%
Vertical Barriers	8	8	100%	6	8	75%
Lime Columns	8	8	100%	7	8	88%
Paved Shoulders	8	8	100%	6	8	75%
Edge Drains	8	8	100%	6	8	75%
Trees	4	4	100%	3	4	75%
Total	52	52	100%	44	52	85%
	Piezometer			**ASG**		
Test Section	**Surviving**	**Total**	**Percent Surviving**	**Surviving**	**Total**	**Percent Surviving**
Control	4	4	100%	7	8	88%
Sand Blanket	4	4	100%	11	12	92%
Vertical Barriers	4	4	100%	8	8	100%
Lime Columns	4	4	100%	6	8	75%
Paved Shoulders	4	4	100%	8	8	100%
Edge Drains	4	4	100%	7	8	88%
Trees	NA	NA	NA	NA	NA	NA
Total	24	24	100%	47	52	90%

CHAPTER 7: RESULTS AND DISCUSSION

Baseline moisture, suction, and pore pressure readings are shown below. Because all sensors had been installed for several weeks prior to recording baseline data, it is expected that they have equalized with the surrounding soil. However, it is possible that the sensors are still in the process of equalizing. Data collected over time and sensor responses to environmental changes will indicate if equalization has occurred. Some examples of initial data versus time are shown. As more data is collected, changes in moisture, suction, pore pressure, and asphalt strain will be show with respect to time. Baseline readings for all sensors are tabulated in Appendix A.

7.1 Control

Figure 75 shows the initial water content and suction profiles for the control section. Pore pressure readings and the calculated water table depths are shown in Table 8.

Table 8: Control Piezometer Results

Sensor Location	Sensor Depth (ft)	Pore Pressure (kPa)	Water Table Depth (ft)
Pavement Borehole	7.5	3.6	6.3
Pavement Borehole	12.0	16.8	6.4
Shoulder Borehole	6.2	3.0	5.2
Shoulder Borehole	11.8	19.3	5.3

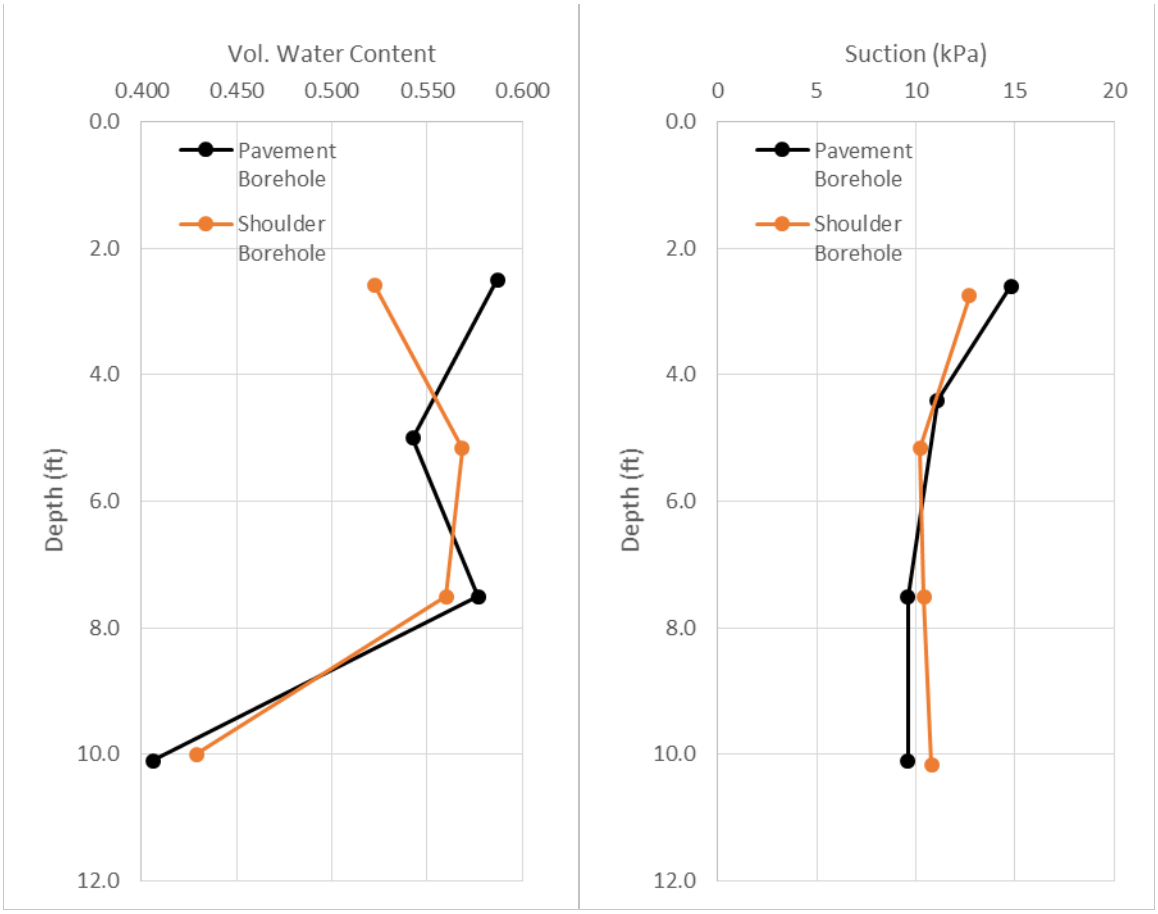

Figure 75: Control, Moisture and Suction vs. Depth

The results from the moisture sensors show that the moisture content does not vary much between the shoulder and pavement subgrade with the exception of the sensors nearest the surface. This is expected because more evapotranspiration can occur in the shoulder than beneath the pavement. Drying in the upper shoulder sensor was also observed over time as shown by the data in Appendix D. This trend was common is several test sections.

As described above, the shoulder moisture sensor at 7.5 feet was installed in disturbed soil. However, the sensor appears to be functioning properly and providing reasonable results. Judgement should be used in evaluation the readings from this sensor in the future.

The moisture content decreases sharply at a depth of ten feet in both the shoulder and pavement borehole. Site exploration performed in 2013 and reported by Stallings (2016) also

showed this drop in moisture content with depth. Samples from a borehole near the control instrumentation indicated a gravimetric moisture content of 37.0% at a depth of 5 feet and a gravimetric moisture content of 32.9% at a depth of 10 feet. This is likely due to a material change to a chalky, clayey marl. This layer change was observed at varying depths across the project, but typically close to ten feet deep (Stallings 2016). There was a question of whether the small sand pocket around the piezometer could have caused this moisture content decrease at the bottom of the borehole. However, the sand was at least one foot below the moisture sensor, well outside the measurement volume. Additionally, there is a small sand pocket around the piezometer at 7.5 feet that does not seem to affect the moisture sensors at that depth. Therefore it was concluded that the most likely explanation is a material change.

The piezometers show a shallower water table in the shoulder than beneath the pavement. However, the shoulder borehole has a lower ground elevation. It is likely that the water table has a relatively constant elevation. The data will be adjusted to account for the elevation difference between the boreholes once the elevation difference is measured. No groundwater was observed during sensor installation or during site exploration (Stallings 2016).

As discussed above, the lower range of the suction sensors is limited by the air entry value of the sensor or the air entry value of the soil, whichever is higher. At suctions below this, the sensor is saturated and reads as if it were at the air entry value of the sensor, which the manufacturer reports is approximately 9 kPa (Decagon Devices, Inc. 2015b). Because the soil at AL-5 is very clayey, it is hypothesized that the air entry value of the soil is higher than that of the suction sensors. Thus sensors reading near 9 kPa indicate that the soil is saturated, either with positive pore pressures or with suctions less than the air entry value of the soil. It appears that all the suction sensors at a depth of five feet and below are in this saturated state. It is expected that

these sensors would be in this saturated state because they are all below the water table or in the capillary fringe.

If the suction increased linearly from the water table (i.e. hydrostatic conditions, no evapotranspiration), the suction sensors at a depth of 2.5 feet would read 7.5 kPa and 11.1 kPa for the shoulder and pavement, respectively. However, the recorded values are greater than this, indicating that the conditions are not hydrostatic and evapotranspiration is occurring.

7.2 Sand Blanket

Figure 76 shows the initial water content and suction profiles for the sand blanket. Pore pressure readings and the calculated water table depths are shown in Table 9.

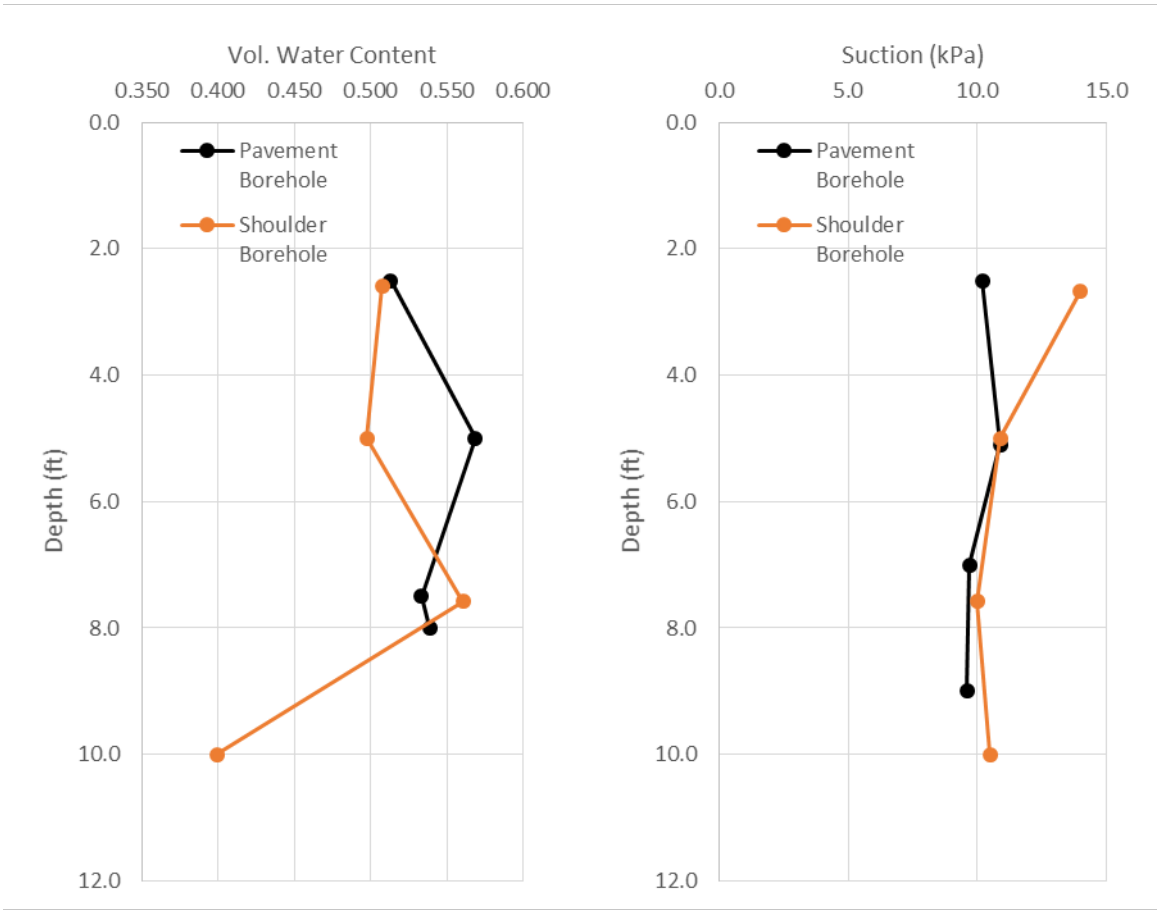

Figure 76: Sand Blanket, Moisture and Suction vs. Depth

Table 9: Sand Blanket Piezometer Results

Sensor Location	Sensor Depth (ft)	Pore Pressure (kPa)	Water Table Depth (ft)
Pavement Borehole	7.0	2.0	6.3
Pavement Borehole	12.2	15.0	7.2
Shoulder Borehole	7.6	3.9	6.3
Shoulder Borehole	11.8	16.2	6.4

As with the control section, the suction values are near the air entry value of the sensor, indicating that the soil is saturated. However, the upper suction sensor in the shoulder does show higher suctions than the hydrostatic condition, indicating that evapotranspiration is occurring in the shoulder. Another trend present in both the sand blanket and control is the moisture content decrease at ten feet, indicating a layer change.

Beneath the pavement, the sand blanket shows lower moisture contents near the surface than the control section, possibly showing that some drainage is occurring in the sand blanket. However, the suction is lower in the sand blanket at this location, indicating it is at or near saturation. This being the case, it is likely the difference in moisture content is the result of material variation.

There is a discrepancy in the piezometer readings beneath the pavement. It is expected that this is an error in the upper sensor. Once borehole elevations are measured these values will be corrected, but it is expected that the water table is at a constant elevation as in the control section, which would correspond to the lower piezometer being correct.

7.3 Vertical Moisture Barriers

Figure 77 shows the initial water content and suction profiles for the vertical moisture barriers. Pore pressure readings and the calculated water table depths are shown in Table 10.

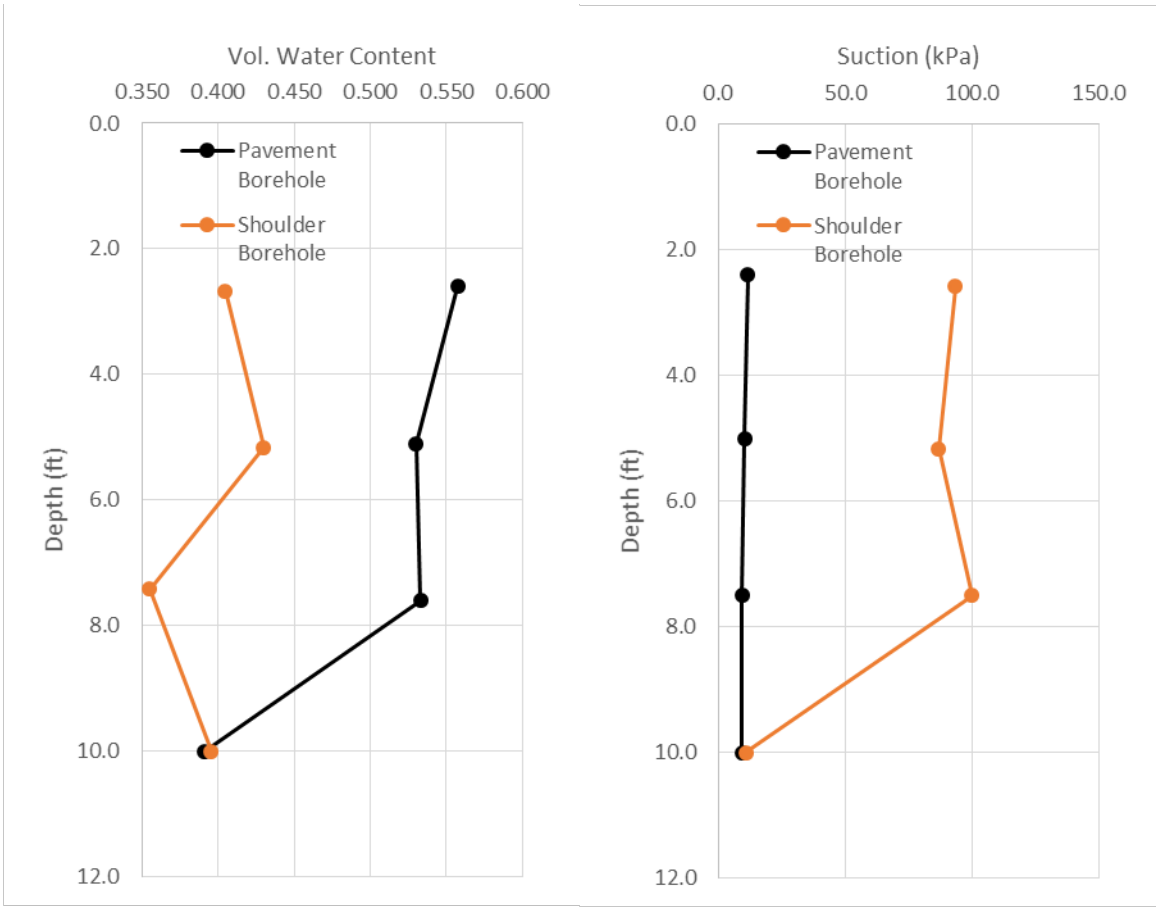

Figure 77: Vertical Moisture Barriers, Moisture and Suction vs. Depth

Table 10: Vertical Moisture Barriers Piezometer Results

Sensor Location	Sensor Depth (ft)	Pore Pressure (kPa)	Water Table Depth (ft)
Pavement Borehole	7.5	1.6	7.0
Pavement Borehole	12.0	14.9	7.0
Shoulder Borehole	7.5	-0.3	7.6
Shoulder Borehole	11.5	3.9	10.5

The pavement suction sensors all read near the air entry value of the sensor, indicating that the pavement subgrade is saturated and have suction values less than the air entry value of the soil. Additionally, the moisture sensors show that the moisture content beneath the pavement is relatively constant with depth with the exception of the sensor at ten feet. This change at ten feet is consistent with the observations in the previous sections, once again indicating a layer change.

Significant suctions and lower moisture contents were observed in the shoulder. This is likely due to several large trees near the edge of the right-of-way. It is important to note that these increases in suction and decreases in moisture content were not observed beneath the pavement, indicating that the vertical moisture barriers are behaving as expected and preventing moisture fluctuations under the pavement.

It is likely that the upper piezometer in the shoulder borehole has lost saturation and is providing erroneous results. The suction values near the depth of the piezometer show that air has entered the soil which would cause this loss of saturation. The lower piezometer in the shoulder appears to be saturated and functioning properly. The piezometer reading show a depressed water table in the shoulder, likely caused by the water uptake of the trees.

7.4 Lime Columns

Figure 78 shows the initial water content and suction profiles for the lime columns. Pore pressure readings and the calculated water table depths are shown in Table 11.

Table 11: Lime Columns Piezometer Results

Sensor Location	Sensor Depth (ft)	Pore Pressure (kPa)	Water Table Depth (ft)
Pavement Borehole	7.4	7.6	4.8
Pavement Borehole	12.1	21.8	4.8
Shoulder Borehole	7.0	9.2	3.9
Shoulder Borehole	12.3	24.7	4.0

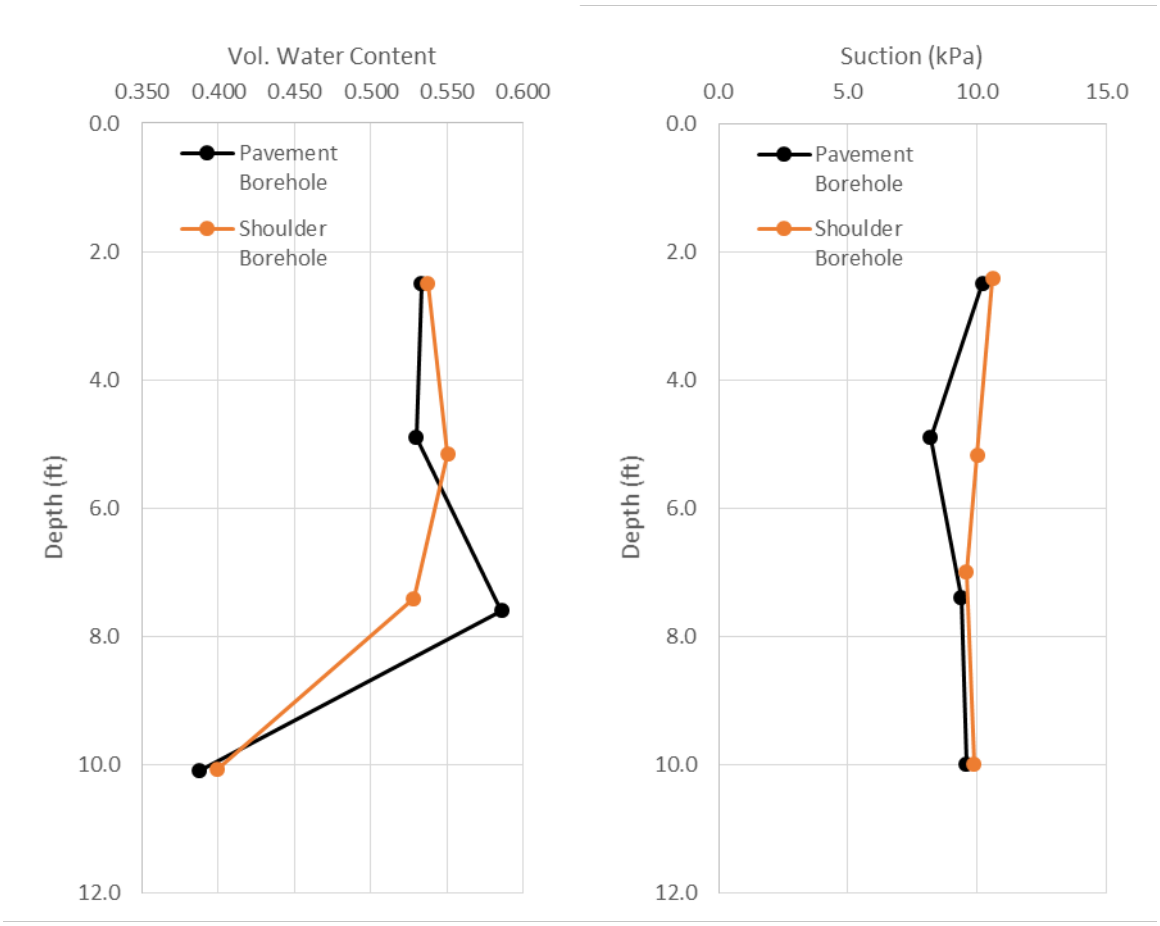

Figure 78: Lime Columns, Moisture and Suction vs. Depth

The water table was higher in the lime columns than in the other sections. The suction sensors all indicated that the soil was saturated confirming the piezometer readings. The moisture content sensors showed similar values for both the pavement and shoulder borehole. No effect from the lime columns is evident in the moisture readings at this time.

7.5 Paved Shoulders

Figure 79 shows the initial water content and suction profiles for the paved shoulders. Pore pressure readings and the calculated water table depths are shown in Table 12.

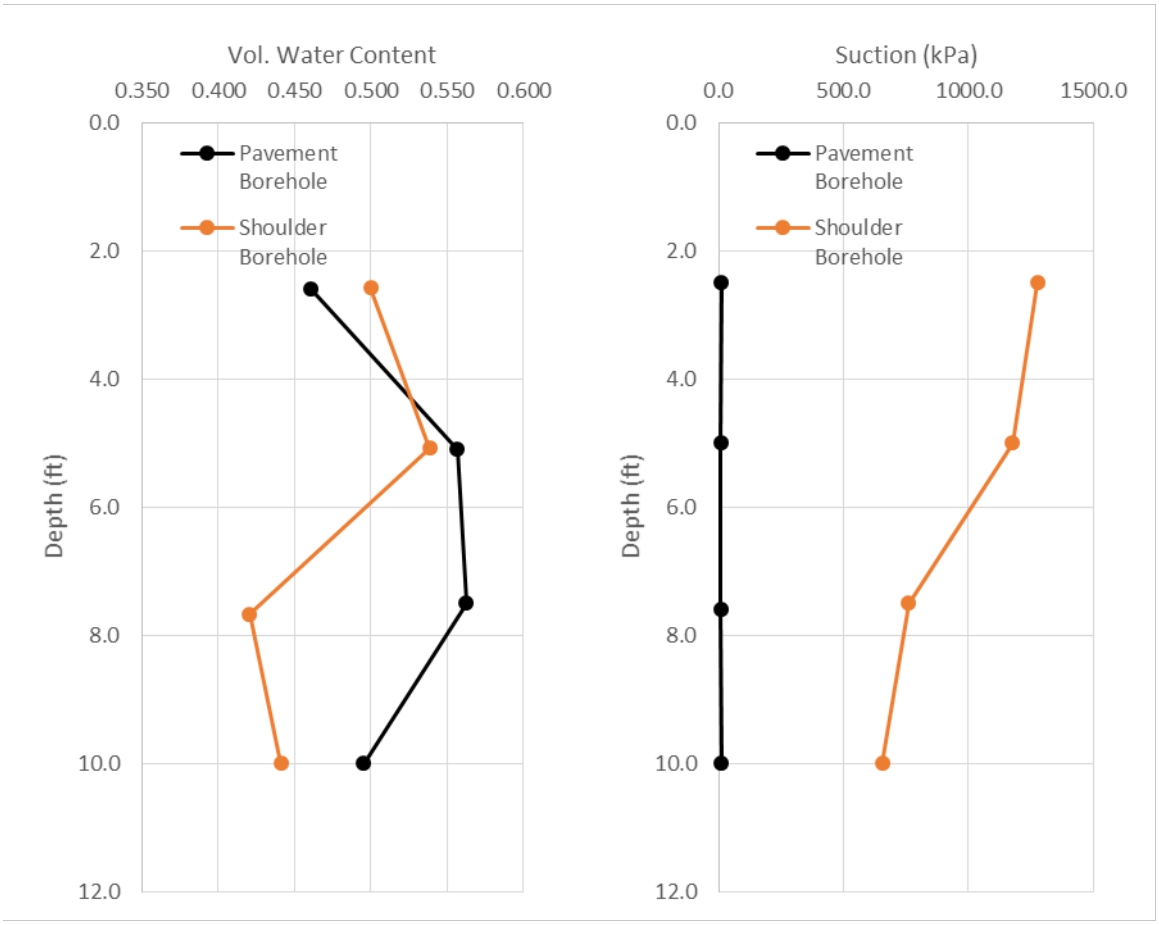

Figure 79: Paved Shoulders, Moisture and Suction vs. Depth

Table 12: Paved Shoulders Piezometer Results

Sensor Location	Sensor Depth (ft)	Pore Pressure (kPa)	Water Table Depth (ft)
Pavement Borehole	7.6	6.6	5.4
Pavement Borehole	11.8	18.8	5.5
Shoulder Borehole	7.5	-0.9	7.8
Shoulder Borehole	11.6	-0.2	11.7

Large trees near the edge of the right-of-way are likely the cause of the high suction values observed in the shoulder of the paved shoulder section. Similar to the vertical barriers, it seems the trees have also caused the piezometers in the shoulder to lose saturation.

The effect of the trees is not seen in the pavement suction sensors which all show the soil to be saturated. This is consistent with hydrostatic conditions which would place all the suction beneath the pavement lower than the air entry value of the sensors.

The lower moisture content in the upper section of pavement borehole is not accompanied by higher suction readings, contrary to what is expected. This could be due to material variability between this upper sensor and the rest of the borehole. This hypothesis is supported by laboratory data from Stallings (2016) which shows the upper portion of this section to be significantly less plastic than the deeper portion. The decrease in moisture content accompanied by a decrease in suction in the shoulder borehole could also be explained by a change in material.

7.6 Edge Drains

Figure 80 shows the initial water content and suction profiles for the edge drains. Pore pressure readings and the calculated water table depths are shown in Table 13.

Table 13: Edge Drains Piezometer Results

Sensor Location	Sensor Depth (ft)	Pore Pressure (kPa)	Water Table Depth (ft)
Pavement Borehole	7.1	1.3	6.7
Pavement Borehole	11.9	14.0	7.2
Shoulder Borehole	7.5	-1.6	8.0
Shoulder Borehole	12.0	3.3	10.9

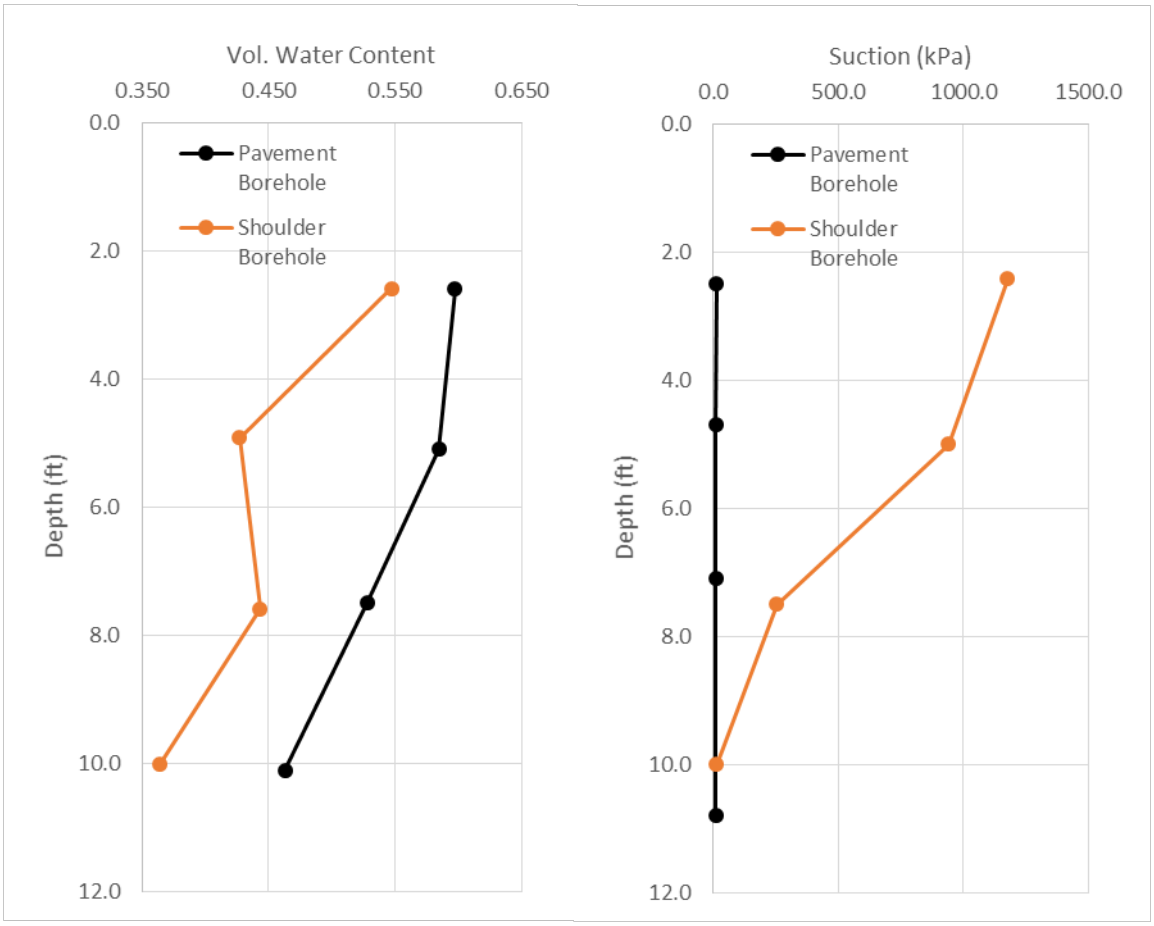

Figure 80: Edge Drains, Moisture and Suction vs. Depth

As with the vertical barriers and paved shoulders, trees near the shoulder hole is likely the cause of the higher suctions and lower moisture contents in the shoulder. The water table is also depressed in the shoulder and the upper piezometer has likely lost saturation as a result of the trees. At the time of baseline readings, desiccation cracks were observed in the surface of the shoulder, consistent with the high suction readings near the surface. In the shoulder, the suction decreases as the moisture content decreases, the opposite of what is expected. It is likely that there is a material change with depth that explains this discrepancy. The soil beneath the pavement does not seem to have felt the effect of the drying in the shoulder, as all the suction sensors are showing saturated conditions. The sharp drop in moisture content at a depth of ten

feet is not observed in the paved shoulders or edge drains. It is likely that the layer change is deeper in this section of the project.

7.7 Trees

Figure 81 shows the initial water content and suction profiles for the tree section. Piezometers were not installed in this section so no pore pressure data is available.

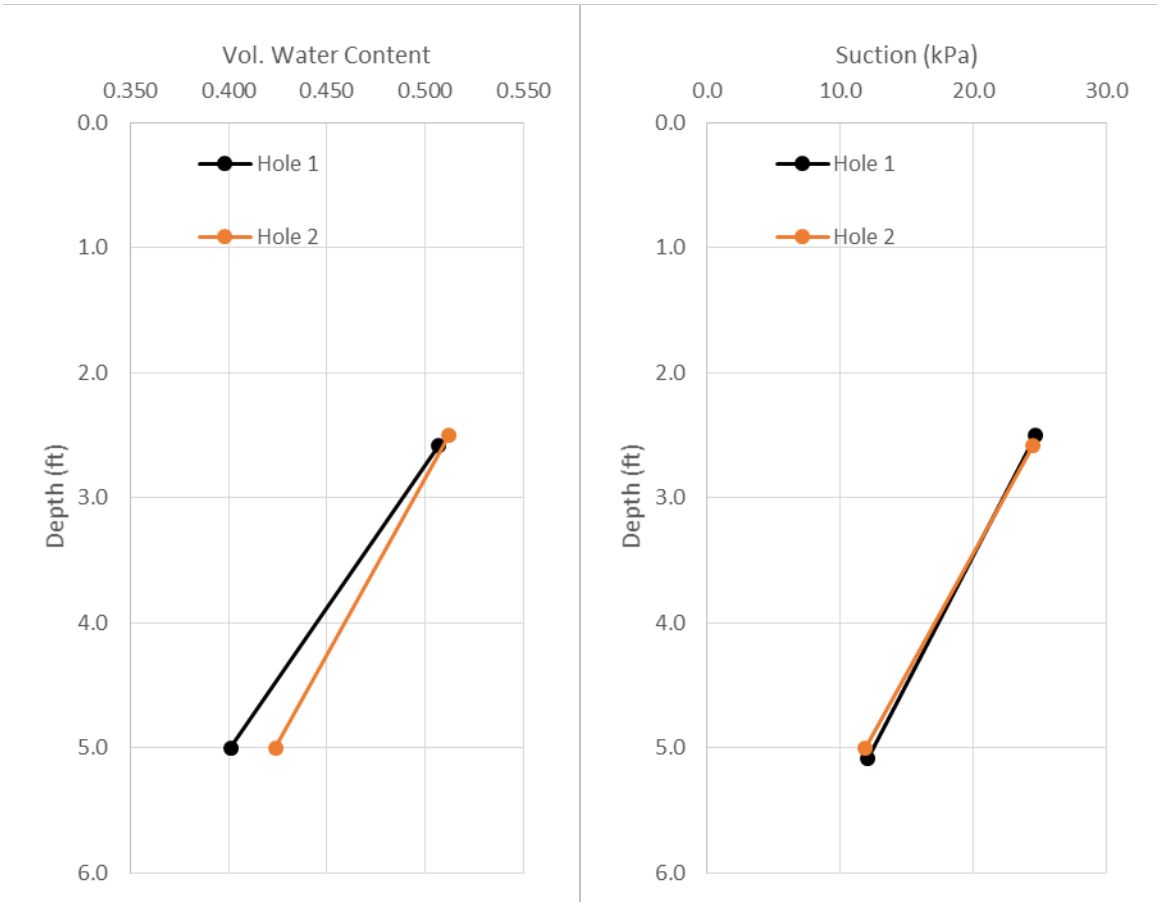

Figure 81: Trees, Moisture and Suction vs. Depth

Two five foot deep instrumentation holes were installed in the shoulder of the edge drain section for the purpose of monitoring the effects of a large tree on the moisture conditions of the soil. Hole 1 is approximately ten feet further away from the large tree than hole 2, yet there is no significant difference in the moisture or suction readings. Furthermore, the low suctions and high moisture contents observed near the large tree are contrary to what is expected based on the

results of the vertical barriers, paved shoulders, and edge drains. In these cases, the trees are farther away from the instrumentation, yet much larger suction values were observed. The cause of these departures from the expected is unknown at this time, but it could possibly be due to effects from the edge drains, material differences, or instrument error.

7.8 Asphalt Strain Gage Discussion

The only data currently available for the asphalt strain gages is the baseline readings. As time progresses, it is expected that the transverse gages will develop tensile strain as longitudinal cracks form. Long wavelength undulations are expected to form in the longitudinal direction as there is differential swelling and shrinking. Therefore, the longitudinal strain gages may read tension or compression depending if the section is swelling or shrinking.

7.9 Comparison to Laboratory Data

The insitu readings of suction and moisture content were compared with laboratory data from Stallings (2016). In spite of the fact that it had been very dry at AL-5 in the months prior to sensor installation, it was observed that the moisture sensors were currently reading higher moisture contents in all places than the insitu moisture contents taken by Stallings. This could be an indication that the response time of the subgrade to environmental stimuli is very long. However, more data is needed to support this hypothesis.

The soil water characteristic curves developed by Stallings (2016) were not extremely useful for predicting the suctions based on the moisture sensor readings. A laboratory SWCC with the typical range of field values is shown in Figure 82. The SWCCs did not capture the wet end of the curve, which is where most of the current moisture contents fall. Because of this, Stallings' curves overestimate the suctions based on the observed moisture contents. Furthermore, Stallings' curves are wetting curves for total suction whereas the suction sensors

measure matric suction and seem to be in a drying cycle. It is recommended that the laboratory SWCCs be extended to include both the very wet values and the drying leg of the curve.

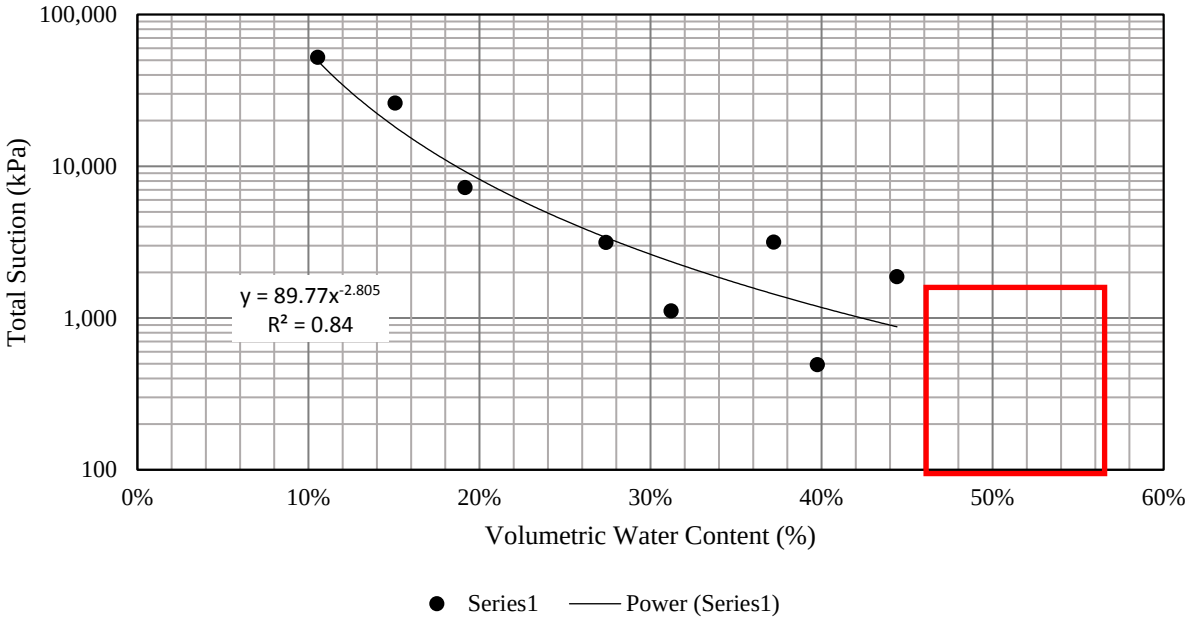

Figure 82: Laboratory SWCC (Edge Drains) with Range of Field Values Shown

7.10 Data versus Time

Some examples of the initial data plotted versus time are shown below. Further results are shown in Appendix D.

7.10.1 Moisture and Suction Sensors

The time results from a moisture sensor are shown in Figure 83. The results from the corresponding suction sensor are shown in Figure 84. Figure 85 shows a partial SWCC that can be created from these sensors. The drying trend shown in Figure 83 and Figure 84 were typical for the majority of the moisture and suction sensors, although the magnitude varied from sensor to sensor. Several of the sensors showed no observable change in moisture and suction, and a small number showed a slight wetting trend. However, no major conclusions can be drawn until more data is collected.

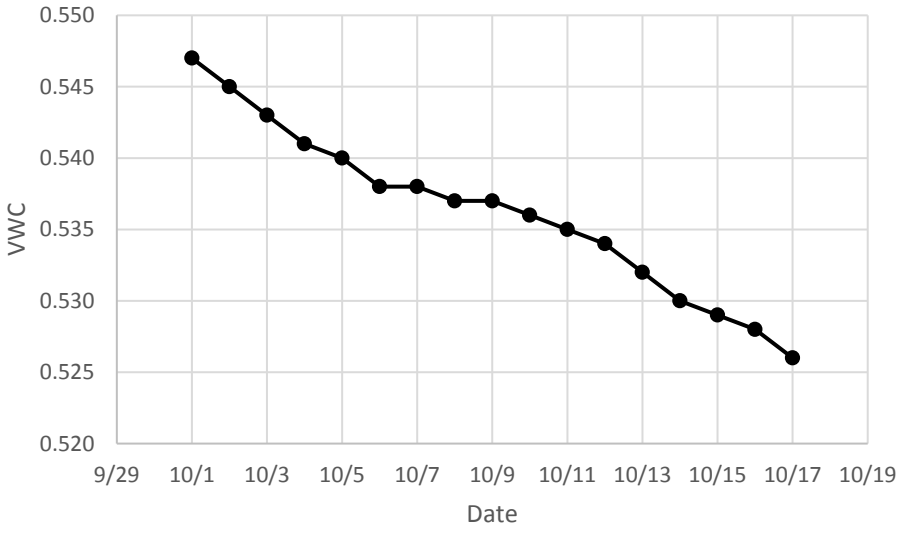

Figure 83: Edge Drains, VWC vs. Time, Shoulder Moisture Sensor, 2.6' Deep

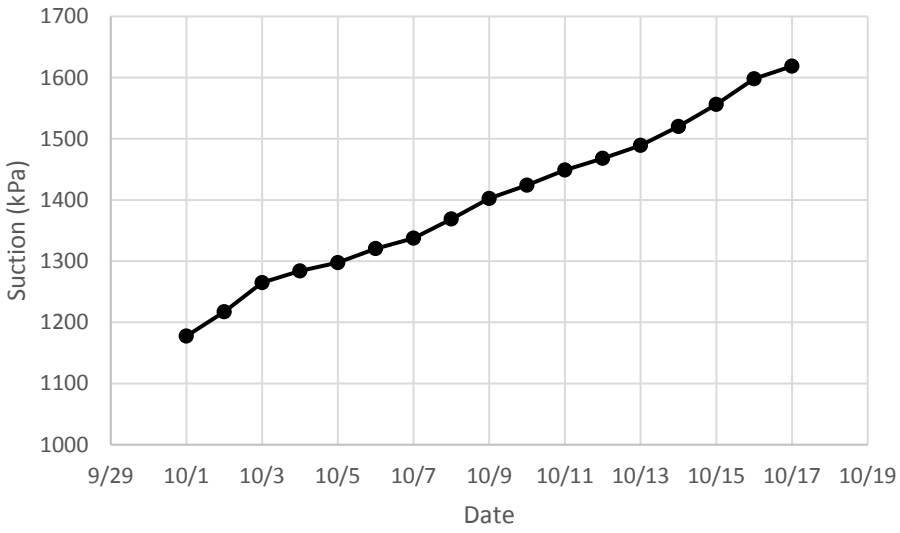

Figure 84: Edge Drains, Suction vs. Time, Shoulder Suction Sensor, 2.4' Deep

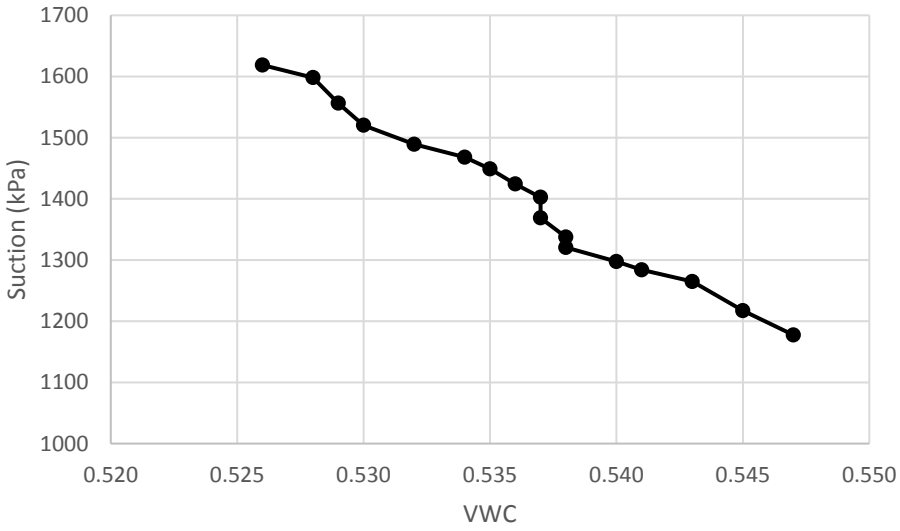

Figure 85: Partial SWCC for Edge Drain Shoulder, Approx. 2.5' Deep

7.10.3 Piezometers

Figure 85 shows the results from the edge drain piezometers. Corresponding to the drying trends seen above, the piezometers showed a slight overall decrease in pore pressure over the time period, with the exception of the shoulder piezometer at a depth of 7.5 feet. As mentioned above, it is suspected that this piezometer has lost saturation and is providing erroneous readings. As stated previously, no major conclusions can be drawn until additional data is collected.

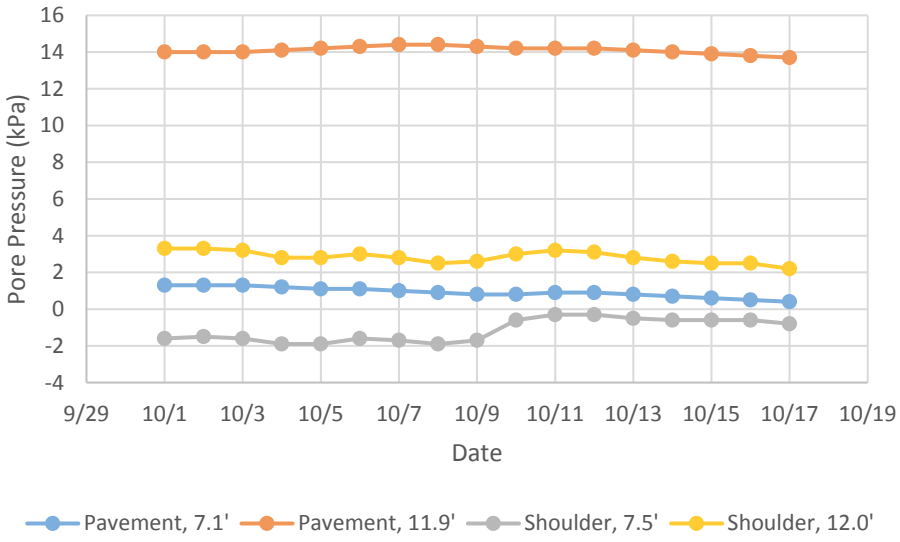

Figure 86: Edge Drain Piezometer Readings vs. Time

7.10.4 Asphalt Strain Gages

Figure 87 shows the response of the longitudinal asphalt strain gages versus time and Figure 88 shows the response of the transverse strain gages. In these figures, the strain that is plotted is the average strain for each day based on 48 readings taken at 30 minute intervals. It was observed that daily temperature fluctuations caused significant changes in the measured asphalt strain. Therefore, the reading schedule was adjusted to record the strain gage readings every 30 minutes. This allows the strain fluctuation due to temperature to be observed. The long-term trend can also be observed by using a low-pass filter to remove the daily changes. Initial data versus time with a 30 minute interval is shown in Figure 89.

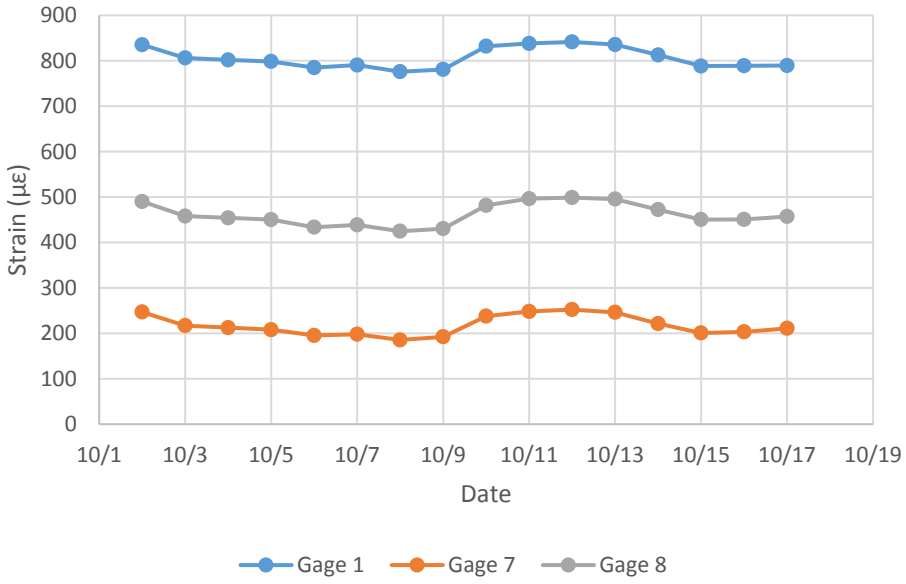

Figure 87: Edge Drain Longitudinal Strain Gages vs. Time

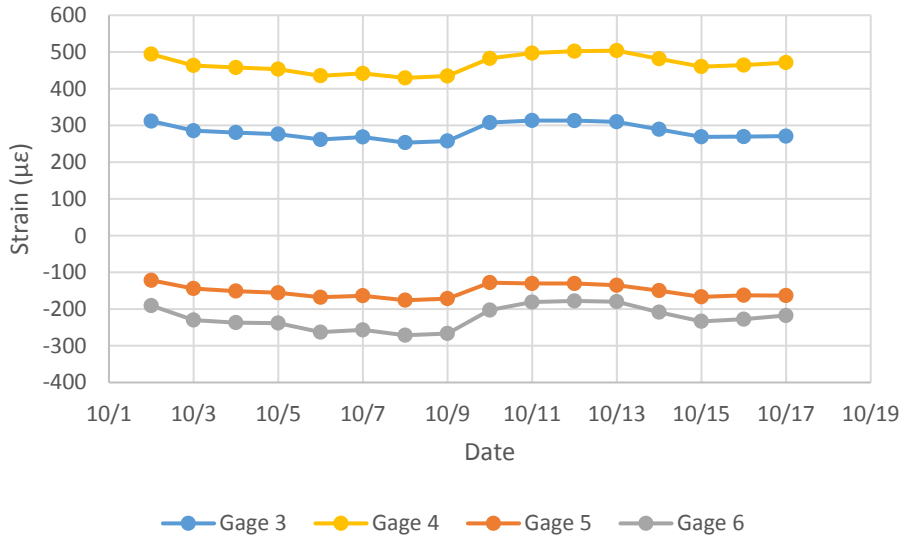

Figure 88: Edge Drain Transverse Strain Gages vs. Time

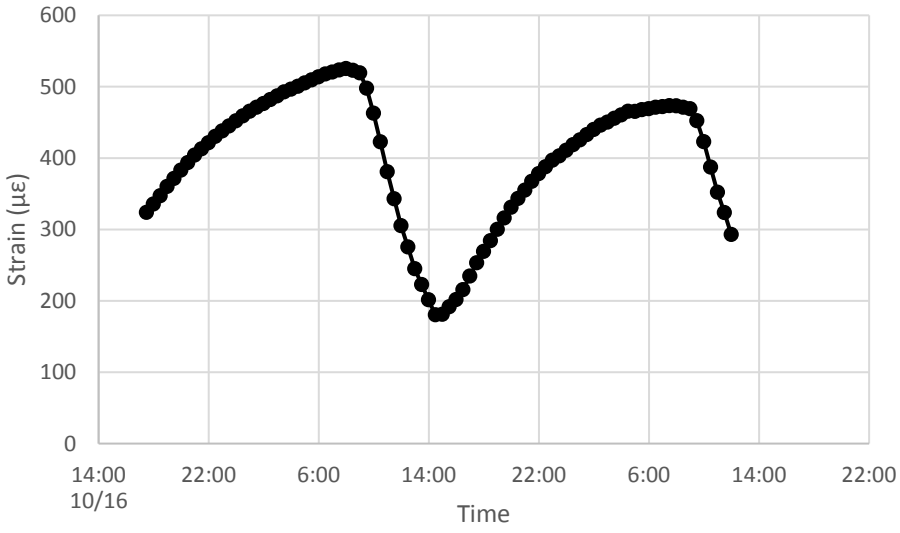

Figure 89: Paved Shoulders ASG 1, Strain vs. Time

CHAPTER 8: SUMMARY, CONCLUSIONS, AND RECOMMENDATIONS

8.1 Summary

AL-5 is a farm-to-market road built on expansive clays that cause significant damage to the pavement. The primary goal of this investigation was to measure properties relating to the shrink-swell behavior at AL-5. The first step to accomplishing this objective was completed by installing instrumentation in the pavement, subgrade, and shoulder of AL-5. Moisture, suction, pore pressure, and asphalt strain sensors were selected, prepared, and installed at AL-5. Baseline readings were taken from all the sensors. These instruments will measure moisture fluctuations in the soil along with asphalt strain and monitoring will continue for several years.

8.2 Conclusions

At the current time, sensors have been installed and baseline readings have been taken. High sensor survivability and properly functioning sensors indicates that the installation methods used were successful. The moisture content, suction, pore pressure, and pavement distress are currently being measured. Changes over time will allow the impact of the subgrade on the pavement to be assessed, the depth of the active zone to be determined, and the effectiveness of each remediation technique to be evaluated. Thus far, the following can be concluded about the subgrade behavior:

- The pavement subgrade is for the most part saturated in all the test sections. However, there are still negative pore pressures (positive suctions) in much of the subgrade.

- High suctions and low moisture contents were observed in the shoulder in the vicinity of large trees, indicating that trees play a significant role in the drying and shrinkage at AL-5.
- Where there were no trees near the sensors, the moisture and suction values from the pavement and shoulder boreholes were very similar.

8.3 Recommendations

It is recommended that monitoring continue over several years in order to observe the seasonal variation in moisture in the subgrade. International roughness index data should be collected periodically so that the pavement distress can be measured over the entire project rather than at discrete locations. These measurements will allow the effectiveness of each test section to be evaluated. The depth of the active zone can also be determined by monitoring the moisture fluctuations. It is also recommended that an additional calibration is performed for the moisture sensor that includes wetter points. Finally, it is recommended that the laboratory soil water characteristic curves be extended.

REFERENCES

Aitchison, G. D. (1961). “Relationship of Moisture and Effective Stress Functions in Unsaturated Soils.” *Pore Pressure and Suction in Soils Conf.* London, England. (47-52). British Nat. Soc. of Int. Soc. Soil Mech. Found Eng.

Alabama Department of Transportation (2015). “Research Project for Soil Stabilization on SR-5 from the Dallas County Line to 0.15 Miles North of E. Goley Road (MP 54.850).” Plans of Proposed Project Number 990305-535-005-401.

Alabama Department of Transportation (2016). “Alabama Traffic Data.” Retrieved Oct. 13, 2016 from https://aldotgis.dot.state.al.us/atd/default.aspx.

ASTM (2010). "D5298-10 Standard Test Method for Measurement of Soil Potential (Suction) Using Filter Paper." ASTM International, West Conshohocken, PA.

Baker, H.B., Buth, M.R. and Van Deusen, D.A., “Minnesota Road Research Project Load Response Instrumentation Installation and Testing Procedures,” Report No. MN/PR-94/01, Minnesota Department of Transportation, St. Paul, MN, 1994.

Bishop, A. W. (1959). “The Principle of Effective Stress.” *Teknisk Ukeblad,* 106(39): 859-863.

Burrage, R. J. (2016). "Full Scale Testing of Two Excavations in an Unsaturated Piedmont Residual Soil." Ph.D. Dissertation, Auburn University.

Campbell Scientific, Inc. (2016). “CS650 and CS655 Water Content Reflectometers.” Instruction Manual. Logan, Utah.

Chen, D. H., Scullion, T., Hong, F., & Lee, J. (2012). Pavement Swelling and Heaving at State Highway 6. *Journal of Performance of Constructed Facilities, 26*(3): 335-344.

Cobos, D. (2015). "Measurement Volume of Decagon Volumetric Water Content Sensors." Application Note. Decagon Devices, Inc. Pullman, Washington.

Croney, D., Coleman, J.D., & Black, W.P.M. (1958). "Movement and Distribution of Water in Soil in Relation to Highway Design and Performance." *Water and Its Conduction in Soils.* Highway Res. Board Special Report no. 40 (226-252). Washington, DC.

Decagon Devices, Inc. (2009). "ECH2O Dielectric Probes vs. Time Domain Reflectometers (TDR)." Application Note. Pullman, WA.

Decagon Devices, Inc. (2014). "10HS Soil Moisture Sensor." Operator's Manual. Pullman, WA.

Decagon Devices, Inc. (2015a). "GS1 Soil Moisture Sensor." Operator's Manual. Pullman, WA.

Decagon Devices, Inc. (2015b). "MPS-2 & MPS-6 Dielectric Water Potential Sensors." Operator's Manual. Pullman, WA.

Decagon Devices, Inc. (2015c). "Water Potential." Accessed Oct. 13, 2016 from www.waterpotential.com.

Deka, R.N., Wairiu, M., Mtakwa, P.W., Mullins, C.E., Veenendaal, E.M., & Townend, J. (1995). "Use and Accuracy of the Filter-Paper Technique for Measurement of Soil Matric Potential." *European Journal of Soil Science,* 46: 233-238.

Dursun, M. and Ozden, S. (2011). "A Wireless Application of Drip Irrigation Automation Supported by Soil Moisture Sensors." *Scientific Research and Essays,* 6(7): 1573-1582.

Fityus, S.G., Smith, D.W., Allman, M.A. (2004). "Expansive Soil Test Site Near Newcastle." *Journal of Geotechnical and Geoenvironmental Engineering,* 130(7): 686-695.

Flint, A.L., Campbell, G.S., Ellett, K.M., Calissendorff, C. (2002). “Calibration and Temperature Correction of Heat Dissipation Matric Potential Sensors.” *Soil Science Society of America Journal*, 66: 1439-1445.

Fredlund, D.G. (1973). “Volume Change Behavior of Unsaturated Soils.” Ph.D. Dissertation, Univ. of Alberta, Edmonton, Alta., Canada.

Fredlund, D. G., and Morgenstern, N. R. (1977). "Stress State Variables for Unsaturated Soils." *ASCE Journal of Geotechnical Engineering Divsion GT5*, 103: 447-466.

Fredlund, D. G., and Rahardjo, H. (1993). *Soil Mechanics for Unsaturated Soils*, John Wiley & Sons, Inc., New York.

Fredlund, D.G., Rahardjo, H., & Fredlund, M.D. (2012). *Unsaturated Soil Mechanics in Engineering Practice.* John Wiley & Sons, Inc., Hoboken, NJ.

Freeman, R.B., Carr, H.T., McEwen, T., Powell, R.B. (2001). “Instrumentation at the National Center for Asphalt Technology Test Track.” U.S. Army Corps of Engineers, Engineer Research and Development Center, Report No. ERDC TR-01-9. Washington, D.C. August 2001.

Google Inc. (2015). Google Earth (Version 7.1.2.2041) [Software]

Harris, M. C. (1998). *Soil Survey of Perry County, Alabama.* Washington, D.C.: United States Department of Agriculture (USDA).

Herman, J.M. (2015). “Damage to Pavements from Expansive Clays: A Review of Behavior and Remediation Techniques.” MCE Research Paper. Auburn University.

Holtz, R. D., and Kovacs, W. D. (1981). *An Introduction to Geotechnical Engineering*, Prentice Hall, Englewood Cliffs, New Jersey.

Hornyak, N.J., J.A. Crovetti, D.E. Newman and J.P. Schabelski, “Perpetual Pavement Instrumentation for the Marquette Interchange Project – Phase 1 Final Report,” WHRP 07-11, Transportation Research Center, Marquette University, 2007.

Hossain, J., Khan, M.S., Hossain, M.S., Ahmed, A. (2016). “Determination of Active Zone in Expansive Clay in North Texas through Field Instrumentation.” Transportation Research Board Annual Meeting 2016. Paper #16-2505.

IAEA (1970). *Neutron Moisture Gages*. International Atomic Energy Agency. Technical Reports Series No. 112. Vienna, Austria.

Jennings, J.E. (1961). “A Revised Effective Stress Law for Use in the Prediction of the Behavior of Unsaturated Soils.” *Pore Pressure and Suction in Soils Conf.* London, England. (26-30). British Nat. Soc. of Int. Soc. Soil Mech. Found Eng.

Jones, D.E. (1981). “Perspectives on Needs for an Availability of Scientific and Technical Information.” Dept. Housing and Urban Development. 1st meeting of Committee on Emergency Management, Commission on Sociotechnical Systems, National Research Council.

Li, J., Smith, D.W., Fityus, S.G., Sheng, D. (2003). “Numerical Analysis of Neutron Moisture Probe Measurements.” *International Journal of Geomechanics*, 3: 11-20.

Likos, W.J. and Lu, N. (2002). “Filter Paper Technique for Measuring Total Suction.” Transportation Research Record 1786. Paper No. 02-2140.

Little, D. N. (1995). *Handbook for Stabilization of Pavement Subgrades and Base Courses with Lime.*

Lu, N., and Likos, W. J. (2004). *Unsaturadted Soil Mechanics*, John Wiley & Sons, Inc., Hoboken, NJ.

Madhyannapu, R. S. (2007). *Deep Mixing Technology for Mitigation of Swell-Shrink Behavior of Expansive Soils of Moderate to Deep Active Depths.* Dissertation, The University of Texas at Arlington.

Madhyannapu, R. S., Puppala, A. J., Bhadriraju, V., & Nazarian, S. (2009). Deep Soil Mixing (DSM) Treatment of Expansive Soils. *2009 US-China Workshop on Ground Improvement Technologies.* ASCE.

Madhyannapu, R. S., Puppala, A. J., Nazarian, S., & Yuan, D. (2010, January 1). Quality Assessment and Quality Control of Deep Soil Mixing Construction for Stabilization Expansive Subsoils. *Journal of Geotechnical and Geoenvironmental Engineering, 136*(1): 119-128.

Malazian, A., Hartsough, P., Kamai, T., Campbell, G.S., Cobos, D.R., Hopmans, J.W. (2011). "Evaluation of MPS-1 Soil Water Potential Sensor." *Journal of Hydrology*, 402: 126-134.

Marjerison, B., Richardson, N., Widger, A., Fredlund D.G., and Berthelot, C. (2001). "Installation of sensors and measurement of soil suction below thin membrane surface pavements in Saskatchewan." Proceedings of the 54th Canadian Geotechnical Conference, Calgary, Alberta: 1328-1334.

McQueen, I. S., and Miller, R. F. (1974). "Approximating Soil Moisture Characteristics from Limited Data: Empirical Evidence and Tentative Model." *Water Resources Research*, 10(3): 521-527.

Mikkensen, P.E., & Green, G.E. (2003). "Piezometers in Fully Grouted Boreholes." *Symposium on Field Measurements in Geomechanics.* Oslo, Norway.

Mitchell, J.K. (1993). *Fundamentals of Soil Behavior*. John Wiley & Sons, Inc., New York, NY.

Monroe, W.H. (1941). *Notes on Deposits of Selma and Ripley Age in Alabama.* Geologic Survey of Alabama, Bulletin No. 48. Tuscaloosa, AL.

NCHRP (2011). “Technical Guidance for Deploying National Level Performance Measurements.” National Cooperative Highway Research Program Report 20-24(37)G.

Nelson, J. D., and Miller, D. J. (1992). *Expansive Soils: Problems and Practice in Foundation and Pavement Engineering*, John Wiley & Sons, Inc., New York.

Ng, C.W.W., Zhan, L.T., Bao, C.G., Fredlund, D.G., & Gong, B.W. (2003). “Performance of an Unsaturated Expansive Soil Slope Subjected to Artificial Rainfall Infiltration.” *Geotechnique,* 53(2): 143-157.

Nichol, C., Smith, L., Beckie, R. (2003). “Long-term Measurement of Matric Suction Using Thermal Conductivity Sensors.” *Can. Geotech. J.,* 40: 587-597.

O’Kane, M., Wilson, G.W., and Barbour, S.L. (1998). “Instrumentation and Monitoring of an Engineered Soil Cover System for Mine Waste Rock.” *Canadian Geotechnical Journal*, 35: 828–846.

Osborne, W.E., Copeland, C.W., & Wheat, D.H. (1989). “Geologic Map of Alabama.” Geological Survey of Alabama, Special Map No. 221. Tuscaloosa, AL.

Pardossi, A., Incrocci, L., Incrocci, G., Malorgio, F., Battista, P., Bacci, L., Rapi, B., Marzialetti, P., Hemming, J., & Balendonck, J. (2009). “Root Zone Sensors for Irrigation Management in Intensive Agriculture.” *Sensors*, 9: 2809-2835.

Puppala, A.J., Manosuthkij, T., Nazarian, S., Hoyos, L.R. (2010). “Threshold Moisture Content and Matric Suction Potentials in Expansive Clays Prior to Initiation of Cracking in Pavements.” *Can. Geotech. J.* 48: 519-531.

Raymond, D.E., Osborne, W.E., Copeland, C.W., & Neathery, T.L. (1988). *Alabama Stratigraphy*. Geologic Survey of Alabama, Circular No. 140. Tuscaloosa, AL.

Reed, P.C. (1969). “Geologic Map of Perry County, Alabama.” Geologic Survey of Alabama, Map No. 118. Tuscaloosa, AL.

Sayers, M. W., & Karamihas, S. M. (1998). *The Little Book of Profiling.* The University of Michigan.

Seo, Y. and Lee, J. (2012). “Short- and Long-Term Evaluation of Asphalt Concrete Strain Gage Installation Methods Applied to the KHCTR.” *Journal of Transportation Engineering,* 138: 690-699.

Snethen, D. R. (1979). *Technical Guidelines for Expansive Soils in Highway Subgrades.* Washington, D.C.: Federal Highway Administration.

Stallings, E.G. (2016). "Investigation of Pavement and Subgrade Distress at Alabama Highway 5." MS Thesis, Auburn University.

Steinberg, M. L. (1980). Deep Vertical Fabric Moisture Seals. *Fourth International Conference on Expansive Soils* (383-400). Denver, CO: ASCE.

Steinberg, M. L. (1981). "Deep Vertical Fabric Moisture Barriers in Swelling Soils." *Transportation Research Record,* 790: 87- 94.

Steinburg, M. L. (1985). "Controlling Expansive Soil Destructiveness by Deep Vertical Geomembranes on Four Highways." *Transportation Research Record*, 1032: 48-53.

Steinberg, M. L. (1992). Vertical Moisture Barrier Update. *Transportation Research Record*, 1362: 111-117.

Timm, D.H., A.L. Priest and T.V. McEwen, "Design and Instrumentation of the Structural Pavement Experiment at the NCAT Test Track," Report No. 04-01, National Center for Asphalt Technology, Auburn University, 2004.

Timm, D.H. (2009). “Design, Construction, and Instrumentation of the 2006 Test Track Structural Study.” Report No. 09-01, National Center for Asphalt Technology, Auburn University, 2009.

Topp, G.C. and Reynolds, W.D. (1998). “Time Domain Reflectometry: A Seminal Technique for Measuring Mass and Energy in Soil.” *Soil and Tillage Research*, 47, 125-132.

Van Iersel, M., Seymour, R.M., Chappell, M., Watson, F., & Dove, S. (2009). “Soil Moisture Sensor-Based Irrigation Reduces Water Use and Nutrient Leaching in a Commercial Nursery.” *SNA Research Conference* 54.

Zornberg, J. G., and Gupta, R. (2009). "Reinforcement of pavements over expansive clay subgrades." *Proc., 17th International Conference on Soil Mechanics and Geotechnical Engineering: The Academia and Practice of Geotechnical Engineering*, 765-768.

APPENDIX A: SENSOR DEPTHS AND BASELINE READINGS

Control

Table 14: Control, Sensor Depths and Baseline Readings

Sensor No.	Sensor Type	Sensor Location	Sensor Depth (ft)	Baseline Reading	
1	Long. ASG	Pavement	NA	NA	με
2	Long. ASG	Pavement	NA	548	με
3	Trans. ASG	Pavement	NA	56	με
4	Trans. ASG	Pavement	NA	-378	με
5	Trans. ASG	Pavement	NA	480	με
6	Trans. ASG	Pavement	NA	102	με
7	Long. ASG	Pavement	NA	12	με
8	Long. ASG	Pavement	NA	13	με
9	Vol. Water Content	Pavement Borehole	2.5	0.587	VWC
10	Vol. Water Content	Pavement Borehole	5.0	0.543	VWC
11	Vol. Water Content	Pavement Borehole	7.5	0.577	VWC
12	Vol. Water Content	Pavement Borehole	10.1	0.406	VWC
13	Matric Suction	Pavement Borehole	2.6	14.8	kPa
14	Matric Suction	Pavement Borehole	4.4	11.1	kPa
15	Matric Suction	Pavement Borehole	7.5	9.6	kPa
16	Matric Suction	Pavement Borehole	10.1	9.6	kPa
17	Pore Pressure	Pavement Borehole	7.5	3.6	kPa
18	Pore Pressure	Pavement Borehole	12.0	16.8	kPa
19	Vol. Water Content	Shoulder Borehole	2.6	0.522	VWC
20	Vol. Water Content	Shoulder Borehole	5.2	0.569	VWC
21	Vol. Water Content	Shoulder Borehole	7.5	0.560	VWC
22	Vol. Water Content	Shoulder Borehole	10.0	0.429	VWC
23	Matric Suction	Shoulder Borehole	2.8	12.7	kPa
24	Matric Suction	Shoulder Borehole	5.2	10.2	kPa
25	Matric Suction	Shoulder Borehole	7.5	10.4	kPa
26	Matric Suction	Shoulder Borehole	10.2	10.8	kPa
27	Pore Pressure	Shoulder Borehole	6.2	3.0	kPa
28	Pore Pressure	Shoulder Borehole	11.8	19.3	kPa

Sand Blanket

Table 15: Sand Blanket, Sensor Depths and Baseline Readings

Sensor No.	Measurement	Sensor Location	Sensor Depth (ft)	Baseline Reading	
1	Long. ASG	Pavement	NA	-561	με
2	Long. ASG	Pavement	NA	-708	με
3	Long. ASG	Pavement	NA	-433	με
4	Trans. ASG	Pavement	NA	-1457	με
5	Trans. ASG	Pavement	NA	-599	με
6	Trans. ASG	Pavement	NA	-777	με
7	Trans. ASG	Pavement	NA	-1497	με
8	Trans. ASG	Pavement	NA	-978	με
9	Trans. ASG	Pavement	NA	-564	με
10	Long. ASG	Pavement	NA	-1962	με
11	Long. ASG	Pavement	NA	NA	με
12	Long. ASG	Pavement	NA	-696	με
13	Vol. Water Content	Pavement Borehole	2.5	0.513	VWC
14	Vol. Water Content	Pavement Borehole	5.0	0.568	VWC
15	Vol. Water Content	Pavement Borehole	7.5	0.533	VWC
16	Vol. Water Content	Pavement Borehole	8.0	0.539	VWC
17	Matric Suction	Pavement Borehole	2.5	10.2	kPa
18	Matric Suction	Pavement Borehole	5.1	10.9	kPa
19	Matric Suction	Pavement Borehole	7.0	9.7	kPa
20	Matric Suction	Pavement Borehole	9.0	9.6	kPa
21	Pore Pressure	Pavement Borehole	7.0	2.0	kPa
22	Pore Pressure	Pavement Borehole	12.2	15.0	kPa
23	Vol. Water Content	Shoulder Borehole	2.6	0.507	VWC
24	Vol. Water Content	Shoulder Borehole	5.0	0.497	VWC
25	Vol. Water Content	Shoulder Borehole	7.6	0.561	VWC
26	Vol. Water Content	Shoulder Borehole	10.0	0.399	VWC
27	Matric Suction	Shoulder Borehole	2.7	14.0	kPa
28	Matric Suction	Shoulder Borehole	5.0	10.9	kPa
29	Matric Suction	Shoulder Borehole	7.6	10.0	kPa
30	Matric Suction	Shoulder Borehole	10.0	10.5	kPa
31	Pore Pressure	Shoulder Borehole	7.6	3.9	kPa
32	Pore Pressure	Shoulder Borehole	11.8	16.2	kPa

Vertical Moisture Barriers

Table 16: Vertical Moisture Barriers, Sensor Depths and Baseline Readings

Sensor No.	Sensor Type	Sensor Location	Sensor Depth (ft)	Baseline Reading	
1	Long. ASG	Pavement	NA	-17	με
2	Long. ASG	Pavement	NA	-175	με
3	Trans. ASG	Pavement	NA	461	με
4	Trans. ASG	Pavement	NA	216	με
5	Trans. ASG	Pavement	NA	35	με
6	Trans. ASG	Pavement	NA	317	με
7	Long. ASG	Pavement	NA	-45	με
8	Long. ASG	Pavement	NA	113	με
9	Vol. Water Content	Pavement Borehole	2.6	0.557	VWC
10	Vol. Water Content	Pavement Borehole	5.1	0.530	VWC
11	Vol. Water Content	Pavement Borehole	7.6	0.533	VWC
12	Vol. Water Content	Pavement Borehole	10.0	0.391	VWC
13	Matric Suction	Pavement Borehole	2.4	11.7	kPa
14	Matric Suction	Pavement Borehole	5.0	10.5	kPa
15	Matric Suction	Pavement Borehole	7.5	9.4	kPa
16	Matric Suction	Pavement Borehole	10.0	9.5	kPa
17	Pore Pressure	Pavement Borehole	7.5	1.6	kPa
18	Pore Pressure	Pavement Borehole	12.0	14.9	kPa
19	Vol. Water Content	Shoulder Borehole	2.7	0.405	VWC
20	Vol. Water Content	Shoulder Borehole	5.2	0.430	VWC
21	Vol. Water Content	Shoulder Borehole	7.4	0.355	VWC
22	Vol. Water Content	Shoulder Borehole	10.0	0.396	VWC
23	Matric Suction	Shoulder Borehole	2.6	93.5	kPa
24	Matric Suction	Shoulder Borehole	5.2	87.0	kPa
25	Matric Suction	Shoulder Borehole	7.5	100.0	kPa
26	Matric Suction	Shoulder Borehole	10.0	10.8	kPa
27	Pore Pressure	Shoulder Borehole	7.5	-0.3	kPa
28	Pore Pressure	Shoulder Borehole	11.8	3.9	kPa

Lime Columns

Table 17: Lime Columns, Sensor Depths and Baseline Readings

Sensor No.	Sensor Type	Sensor Location	Sensor Depth (ft)	Baseline Reading	
1	Long. ASG	Pavement	NA	286.906	με
2	Long. ASG	Pavement	NA	600.3978	με
3	Trans. ASG	Pavement	NA	-337.3015	με
4	Trans. ASG	Pavement	NA	-296.1002	με
5	Trans. ASG	Pavement	NA	159.3457	με
6	Trans. ASG	Pavement	NA	308.7648	με
7	Long. ASG	Pavement	NA	NA	με
8	Long. ASG	Pavement	NA	NA	με
9	Vol. Water Content	Pavement Borehole	2.5	0.533	VWC
10	Vol. Water Content	Pavement Borehole	4.9	0.530	VWC
11	Vol. Water Content	Pavement Borehole	7.6	0.586	VWC
12	Vol. Water Content	Pavement Borehole	10.1	0.387	VWC
13	Matric Suction	Pavement Borehole	2.5	10.2	kPa
14	Matric Suction	Pavement Borehole	4.9	8.2	kPa
15	Matric Suction	Pavement Borehole	7.4	9.4	kPa
16	Matric Suction	Pavement Borehole	10.0	9.6	kPa
17	Pore Pressure	Pavement Borehole	7.4	7.6	kPa
18	Pore Pressure	Pavement Borehole	12.1	21.8	kPa
19	Vol. Water Content	Shoulder Borehole	2.5	0.537	VWC
20	Vol. Water Content	Shoulder Borehole	5.2	0.550	VWC
21	Vol. Water Content	Shoulder Borehole	7.4	0.528	VWC
22	Vol. Water Content	Shoulder Borehole	10.1	0.399	VWC
23	Matric Suction	Shoulder Borehole	2.4	10.6	kPa
24	Matric Suction	Shoulder Borehole	5.2	10.0	kPa
25	Matric Suction	Shoulder Borehole	7.0	9.6	kPa
26	Matric Suction	Shoulder Borehole	10.0	9.9	kPa
27	Pore Pressure	Shoulder Borehole	7.0	9.2	kPa
28	Pore Pressure	Shoulder Borehole	12.3	24.7	kPa

Paved Shoulders

Table 18: Paved Shoulders, Sensor Depths and Baseline Readings

Sensor No.	Sensor Type	Sensor Location	Sensor Depth (ft)	Baseline Reading	
1	Long. ASG	Pavement	NA	189	με
2	Long. ASG	Pavement	NA	99	με
3	Trans. ASG	Pavement	NA	88	με
4	Trans. ASG	Pavement	NA	-401	με
5	Trans. ASG	Pavement	NA	-164	με
6	Trans. ASG	Pavement	NA	7	με
7	Long. ASG	Pavement	NA	626	με
8	Long. ASG	Pavement	NA	315	με
9	Vol. Water Content	Pavement Borehole	2.6	0.461	VWC
10	Vol. Water Content	Pavement Borehole	5.1	0.557	VWC
11	Vol. Water Content	Pavement Borehole	7.5	0.562	VWC
12	Vol. Water Content	Pavement Borehole	10.0	0.495	VWC
13	Matric Suction	Pavement Borehole	2.5	11.1	kPa
14	Matric Suction	Pavement Borehole	5.0	9.5	kPa
15	Matric Suction	Pavement Borehole	7.6	9.5	kPa
16	Matric Suction	Pavement Borehole	10.0	9.9	kPa
17	Pore Pressure	Pavement Borehole	7.6	6.6	kPa
18	Pore Pressure	Pavement Borehole	11.8	18.8	kPa
19	Vol. Water Content	Shoulder Borehole	2.6	0.500	VWC
20	Vol. Water Content	Shoulder Borehole	5.1	0.539	VWC
21	Vol. Water Content	Shoulder Borehole	7.7	0.420	VWC
22	Vol. Water Content	Shoulder Borehole	10.0	0.441	VWC
23	Matric Suction	Shoulder Borehole	2.5	1275.2	kPa
24	Matric Suction	Shoulder Borehole	5.0	1176.9	kPa
25	Matric Suction	Shoulder Borehole	7.5	761.1	kPa
26	Matric Suction	Shoulder Borehole	10.0	654.7	kPa
27	Pore Pressure	Shoulder Borehole	7.5	-0.9	kPa
28	Pore Pressure	Shoulder Borehole	11.6	-0.2	kPa

Edge Drains

Table 19: Edge Drains, Sensor Depths and Baseline Readings

Sensor No.	Sensor Type	Sensor Location	Sensor Depth (ft)	Baseline Reading	
1	Long. ASG	Pavement	NA	752	με
2	Long. ASG	Pavement	NA	NA	με
3	Trans. ASG	Pavement	NA	227	με
4	Trans. ASG	Pavement	NA	399	με
5	Trans. ASG	Pavement	NA	-193	με
6	Trans. ASG	Pavement	NA	-306	με
7	Long. ASG	Pavement	NA	158	με
8	Long. ASG	Pavement	NA	399	με
9	Vol. Water Content	Pavement Borehole	2.6	0.597	VWC
10	Vol. Water Content	Pavement Borehole	5.1	0.585	VWC
11	Vol. Water Content	Pavement Borehole	7.5	0.528	VWC
12	Vol. Water Content	Pavement Borehole	10.1	0.463	VWC
13	Matric Suction	Pavement Borehole	2.5	11.9	kPa
14	Matric Suction	Pavement Borehole	4.7	9.5	kPa
15	Matric Suction	Pavement Borehole	7.1	9.5	kPa
16	Matric Suction	Pavement Borehole	10.8	10.9	kPa
17	Pore Pressure	Pavement Borehole	7.1	1.3	kPa
18	Pore Pressure	Pavement Borehole	11.9	14.0	kPa
19	Vol. Water Content	Shoulder Borehole	2.6	0.547	VWC
20	Vol. Water Content	Shoulder Borehole	4.9	0.427	VWC
21	Vol. Water Content	Shoulder Borehole	7.6	0.443	VWC
22	Vol. Water Content	Shoulder Borehole	10.0	0.364	VWC
23	Matric Suction	Shoulder Borehole	2.4	1177.5	kPa
24	Matric Suction	Shoulder Borehole	5.0	940.6	kPa
25	Matric Suction	Shoulder Borehole	7.5	252.7	kPa
26	Matric Suction	Shoulder Borehole	10.0	11.7	kPa
27	Pore Pressure	Shoulder Borehole	7.5	-1.6	kPa
28	Pore Pressure	Shoulder Borehole	12.0	3.3	kPa

Trees

Table 20: Trees, Sensor Depths and Baseline Readings

Sensor No.	Sensor Type	Sensor Location	Sensor Depth (ft)	Baseline Reading	
1	Vol. Water Content	Hole 1	2.6	0.507	VWC
2	Vol. Water Content	Hole 1	5.0	0.401	VWC
3	Matric Suction	Hole 1	2.5	24.7	kPa
4	Matric Suction	Hole 1	5.1	12.1	kPa
5	Vol. Water Content	Hole 2	2.5	0.512	VWC
6	Vol. Water Content	Hole 2	5.0	0.424	VWC
7	Matric Suction	Hole 2	2.6	24.5	kPa
8	Matric Suction	Hole 2	5.0	11.9	kPa

APPENDIX B: DATALOGGER WIRING DIAGRAMS

Trees Wiring Diagram

Decagon MPS6 to CR6

Decagon MPS6 (1)	
POWER (White)	SW12-2
SIGNAL (Red)	C1
GROUND (Bare)	G

Decagon MPS6 (2)	
POWER (White)	SW12-2
SIGNAL (Red)	C1
GROUND (Bare)	G

*Typical for MPS6 (3-8)

Decagon GS1 to CR6

Decagon GS1 (1)	CR6
POWER (White)	SW12-1
SIGNAL (Red)	U1
GROUND (Bare)	G

Decagon (2)	AM16/32B Multiplexer #3
POWER (White)	SW12-2
SIGNAL (Red)	U2
GROUND (Bare)	G

*Typical for GS1 (3-4)

Campbell PS200 to CR6

Campbell PS200	CR6
SIGNAL (Green)	C1
GROUND (Black)	G
SHIELD (Clear)	G

Lime Columns Wiring Diagram

Multiplexer #1 to Datalogger

(Piezometers)

AM16/32B Multiplexer #1 (4x16 mode)	CR6
COM ODD H	U1
COMM ODD L	U2
COM EVEN H	U3
COM EVEN L	U4
COM Ground	G
12 V	12V
GND	G
RES	C4
CLK	C3

Multiplexer #2 to Datalogger

(Strain Gages)

AM16/32B Multiplexer #2 (4x16 mode)	CR6
COM ODD H	U5
COMM ODD L	G
COM EVEN H	U7
COM EVEN L	U8
COM Ground	G
12 V	12V
GND	G
RES	U12
CLK	C3

Multiplexer #3 to Datalogger

(Strain Gages)

AM16/32B Multiplexer #3 (4x16 mode)	CR6
COM ODD H	SW12-1
COM EVEN H	U9
COM Ground	G
12 V	12V
GND	G
RES	U11
CLK	C3

Decagon MPS6 to CR6

Decagon MPS6 (1)

POWER (White)	SW12-2
SIGNAL (Red)	C1
GROUND (Bare)	G

Decagon MPS6 (2)

POWER (White)	SW12-2
SIGNAL (Red)	C1
GROUND (Bare)	G

*Typical for MPS6 (3-8)

Campbell PS200 to CR6

Campbell PS200	CR6
SIGNAL (Green)	C1
GROUND (Black)	G
SHIELD (Clear)	G

Geokon 4500S to Multiplexer #1

Geokon 4500s (1)	AM16/32B Multiplexer #1
COIL H (Red)	1H
COIL L (Black)	1L
THERM H (Green)	2H
THERM L (White)	2L

Geokon 4500s (2)	AM16/32B Multiplexer #1
COIL H (Red)	3H
COIL L (Black)	3L
THERM H (Green)	4H
THERM L (White)	4L

*Typical for Geokon Sensors (3-4)

Asphalt Strain Gage to Multiplexer #2

ASG (1)	AM16/32B Multiplexer #2
EX H (Red)	1H
EX L (Black)	1L
SIGNAL H (Green)	2H
SIGNAL L (White)	2L

ASG (2)	AM16/32B Multiplexer #1
EX H (Red)	3H
EX L (Black)	3L
SIGNAL H (Green)	4H
SIGNAL L (White)	4L

*Typical for ASG (3-8)

Decagon GS1 to Multiplexer #3

Decagon GS1 (1)	AM16/32B Multiplexer #3
POWER (White)	1H
SIGNAL (Red)	2H
GROUND (Bare)	G

Decagon (2)	AM16/32B Multiplexer #3
POWER (White)	3H
SIGNAL (Red)	4H
GROUND (Bare)	G

*Typical for GS1 (3-8)

Campbell WTX520 to CR6

Campbell WTX520	CR6
12V (Red)	12V
POWER GROUND (Black)	G
SIGNAL (Green)	C1
SIGNAL Ground (White)	C1

RF451 to CR6 via CS I/O Port

RavenXTV to CR6 via RS232 Port

Sand Blanket Wiring Diagram

Multiplexer #1 to Datalogger

(Piezometers)

AM16/32B Multiplexer #1 (4x16 mode)	CR6
COM ODD H	U1
COMM ODD L	U2
COM EVEN H	U3
COM EVEN L	U4
COM Ground	G
12 V	12V
GND	G
RES	C4
CLK	C3

Multiplexer #2 to Datalogger

(Strain Gages)

AM16/32B Multiplexer #2 (4x16 mode)	CR6
COM ODD H	U5
COMM ODD L	G
COM EVEN H	U7
COM EVEN L	U8
COM Ground	G
12 V	12V
GND	G
RES	U12
CLK	C3

Multiplexer #3 to Datalogger

(Strain Gages)

AM16/32B Multiplexer #3 (4x16 mode)	CR6
COM ODD H	SW12-1
COM EVEN H	U9
COM Ground	G
12 V	12V
GND	G
RES	U11
CLK	C3

Decagon MPS6 to CR6

Decagon MPS6 (1)

POWER (White)	SW12-2
SIGNAL (Red)	C1
GROUND (Bare)	G

Decagon MPS6 (2)

POWER (White)	SW12-2
SIGNAL (Red)	C1
GROUND (Bare)	G

*Typical for MPS6 (3-8)

RF451 to CR6 via CS I/O Port

Geokon 4500S to Multiplexer #1

Geokon 4500s (1)	AM16/32B Multiplexer #1
COIL H (Red)	1H
COIL L (Black)	1L
THERM H (Green)	2H
THERM L (White)	2L

Geokon 4500s (2)	AM16/32B Multiplexer #1
COIL H (Red)	3H
COIL L (Black)	3L
THERM H (Green)	4H
THERM L (White)	4L

*Typical for Geokon Sensors (3-4)

Asphalt Strain Gage to Multiplexer #2

ASG (1)	AM16/32B Multiplexer #2
EX H (Red)	1H
EX L (Black)	1L
SIGNAL H (Green)	2H
SIGNAL L (White)	2L

ASG (2)	AM16/32B Multiplexer #1
EX H (Red)	3H
EX L (Black)	3L
SIGNAL H (Green)	4H
SIGNAL L (White)	4L

*Typical for ASG (3-12)

Decagon GS1 to Multiplexer #3

Decagon GS1 (1)	AM16/32B Multiplexer #3
POWER (White)	1H
SIGNAL (Red)	2H
GROUND (Bare)	G

Decagon (2)	AM16/32B Multiplexer #3
POWER (White)	3H
SIGNAL (Red)	4H
GROUND (Bare)	G

*Typical for GS1 (3-8)

Campbell PS200 to CR6

Campbell PS200	CR6
SIGNAL (Green)	C1
GROUND (Black)	G
SHIELD (Clear)	G

Control, Vertical Barrier, Paved Shoulders, Edge Drains Wiring Diagram

Multiplexer #1 to Datalogger

(Piezometers)

AM16/32B Multiplexer #1 (4x16 mode)	CR6
COM ODD H	U1
COMM ODD L	U2
COM EVEN H	U3
COM EVEN L	U4
COM Ground	G
12 V	12V
GND	G
RES	C4
CLK	C3

Multiplexer #2 to Datalogger

(Strain Gages)

AM16/32B Multiplexer #2 (4x16 mode)	CR6
COM ODD H	U5
COMM ODD L	G
COM EVEN H	U7
COM EVEN L	U8
COM Ground	G
12 V	12V
GND	G
RES	U12
CLK	C3

Multiplexer #3 to Datalogger

(Strain Gages)

AM16/32B Multiplexer #3 (4x16 mode)	CR6
COM ODD H	SW12-1
COM EVEN H	U9
COM Ground	G
12 V	12V
GND	G
RES	U11
CLK	C3

Decagon MPS6 to CR6

Decagon MPS6 (1)

POWER (White)	SW12-2
SIGNAL (Red)	C1
GROUND (Bare)	G

Decagon MPS6 (2)

POWER (White)	SW12-2
SIGNAL (Red)	C1
GROUND (Bare)	G

*Typical for MPS6 (3-8)

RF451 to CR6 via CS I/O Port

Geokon 4500S to Multiplexer #1

Geokon 4500s (1)	AM16/32B Multiplexer #1
COIL H (Red)	1H
COIL L (Black)	1L
THERM H (Green)	2H
THERM L (White)	2L

Geokon 4500s (2)	AM16/32B Multiplexer #1
COIL H (Red)	3H
COIL L (Black)	3L
THERM H (Green)	4H
THERM L (White)	4L

*Typical for Geokon Sensors (3-4)

Asphalt Strain Gage to Multiplexer #2

ASG (1)	AM16/32B Multiplexer #2
EX H (Red)	1H
EX L (Black)	1L
SIGNAL H (Green)	2H
SIGNAL L (White)	2L

ASG (2)	AM16/32B Multiplexer #1
EX H (Red)	3H
EX L (Black)	3L
SIGNAL H (Green)	4H
SIGNAL L (White)	4L

*Typical for ASG (3-8)

Decagon GS1 to Multiplexer #3

Decagon GS1 (1)	AM16/32B Multiplexer #3
POWER (White)	1H
SIGNAL (Red)	2H
GROUND (Bare)	G

Decagon (2)	AM16/32B Multiplexer #3
POWER (White)	3H
SIGNAL (Red)	4H
GROUND (Bare)	G

*Typical for GS1 (3-8)

Campbell PS200 to CR6

Campbell PS200	CR6
SIGNAL (Green)	C1
GROUND (Black)	G
SHIELD (Clear)	G

APPENDIX C: DATALOGGER PROGRAMS

Control Datalogger Program

```
'CR6 Series
'Created by Garrett Wheeler
'for Auburn Univesity Selma project
'
'Modified by Dan Jackson
'
'8 full bridge strain gages Geocomp asphalt gages
'8 SE sensors decagon gs1
'8 decagon mps6 sdi-12
'4 VW piezometers geokon 4500
'30 minute measurements
'daily table
'
StationName=Control

'Declare Variables and Units

'dim variables for default voltage and temp measurement
Public BattV
Public PTemp_C

'dim variables for VW Piezometers
'Geokon 4500s Serial #s: 1603641,1603640,1603255,1603256
Dim Count
Public VW(6)
Public Freq(4)
'Public Amp(4)
'Public SNRat(4)
'Public NFreq(4)
'Public DRat(4)
Public TT(4)
Public Digits(4)
Public PorePressure(4)
```

```
Public WTDepth(4)
'depth to each piezometer in feet
Public PiezoDepth(4)={7.5,12.0,6.2,11.8}
'vw gage and temp factors
Public G_Factor(4)={-0.1119,-0.114,-0.1134,-0.1092}
Public T_Factor(4)={-0.05138,-0.05387,-0.06126,-0.09075}
' zero values for digits and temp. Factory zero used for piezo 1 and 2
'(Field zero was not recorded).
'Field zero used for piezo 3 and 4.
Public Digits0(4)={9048,8655,8813.8,8715.4}
Public TT0(4)={20.6,20.4,32.9,31.9}

'Dim variables for ASGs
'Geocomp ASGs: A35,A2,A13,A28,A3,A42,A1,A30
Public LCount
Public Vr1000(8) 'full bridge result in mv/V ex.
Public Strain(8) 'strain result in microstrain
'ASG calibration factors in me/mV @ 2.5V Ex.
Public GFsRaw(8)={223.88,263.02,271.27,252.90,274.19,268.20,259.74,274.41}

'dim variables for GS1 (Moisture)
'Decagon GS1 serial #s: 02-800,02-834,02-837,02-814,02-809,02-847,02-793,02-790
Public MCount
Public RawVWC(8)
Public VWC(8)

'dim variables for MPS6 (suction)
'Decagon MPS6 serial #s: 08-764,08-768,08-790,08-773,08-763,08-767,08-761,08-791
Public NCount
Public MPS6(8,2)

'Dim variables for CH200
Public CH200_M0(9)
'Battery voltage: VDC
Alias CH200_M0(1)=VBatt
Units VBatt = Volts
'Current going into, or out of, the battery: Amps
Alias CH200_M0(2)=IBatt
Units IBatt=Amps
'Current going to the load: Amps
Alias CH200_M0(3)=ILoad
Units ILoad=Amps
'Voltage coming into the charger: VDC
```

```
Alias CH200_M0(4)=V_in_chg
Units V_in_chg = Volts
'Current coming into the charger: Amps
Alias CH200_M0(5)=I_in_chg
Units I_in_chg = amps
'Charger temperature: Celsius
Alias CH200_M0(6)=Chg_TmpC
Units Chg_TmpC = deg C
'Charging state: Cycle, Float, Current Limited, or None
Alias CH200_M0(7)=Chg_State
'Charging source: None, AC, or Solar
Alias CH200_M0(8)=Chg_Source
'Check battery error: 0=normal, 1=check battery
Alias CH200_M0(9)=Ck_Batt

'Arrays to hold the associated words for the charge state, charge source,
'and check battery values.
Dim ChargeStateArr(6) As String
Dim ChargeSourceArr(3) As String
Dim CheckBatteryArr(2) As String

'Variables to hold the words for charge state, charge source, and check
'battery.
Public ChargeState As String
Public ChargeSource As String
Public CheckBattery As String

Alias MPS6(1,1)=Suction1
Alias MPS6(2,1)=Suction2
Alias MPS6(3,1)=Suction3
Alias MPS6(4,1)=Suction4
Alias MPS6(5,1)=Suction5
Alias MPS6(6,1)=Suction6
Alias MPS6(7,1)=Suction7
Alias MPS6(8,1)=Suction8
Alias MPS6(1,2)=Temp1
Alias MPS6(2,2)=Temp2
Alias MPS6(3,2)=Temp3
Alias MPS6(4,2)=Temp4
Alias MPS6(5,2)=Temp5
Alias MPS6(6,2)=Temp6
Alias MPS6(7,2)=Temp7
Alias MPS6(8,2)=Temp8
```

```
Units BattV=Volts
Units PTemp_C=Deg C
Units Freq=Hz
'Units Amp=mV RMS
'Units NFreq=Hz
Units TT=Deg C

Units TT0=Deg C
Units Digits=Digits
Units Digits0=Digits
Units PorePressure=kPa
Units WTDepth=feet

Units Suction1=kPa
Units Suction2=kPa
Units Suction3=kPa
Units Suction4=kPa
Units Suction5=kPa
Units Suction6=kPa
Units Suction7=kPa
Units Suction8=kPa

Units Temp1=Deg C
Units Temp2=Deg C
Units Temp3=Deg C
Units Temp4=Deg C
Units Temp5=Deg C
Units Temp6=Deg C
Units Temp7=Deg C
Units Temp8=Deg C


Units Strain=microstrain
Units Vr1000=mV/V



'Define Data Tables
'Data table for processed data
DataTable(Control_Daily,True,-1)

  DataInterval(0,1,Day,10)
```

```
  Minimum(1,BattV,IEEE4,False,False)
  Average(1,PTemp_C,IEEE4,False)
  Minimum (6,CH200_M0(),IEEE4,False,False)
  Maximum (6,CH200_M0(),IEEE4,False,False)


  'VW Piezometer Data. Record time stamp for max/min temperature
  'pore pressure in kPa, WT depth in feet, temp in celsius
  Average(4,PorePressure(),IEEE4,False)
  Minimum(4,PorePressure(),IEEE4,False,False)
  Maximum(4,PorePressure(),IEEE4,False,False)
  Average(4,WTDepth(),IEEE4,False)
  Minimum(4,WTDepth(),IEEE4,False,False)
  Maximum(4,WTDepth(),IEEE4,False,False)
  Average(4,TT(),IEEE4,False)
  Minimum(4,TT(),IEEE4,False,True)
  Maximum(4,TT(),IEEE4,False,True)

  'ASG Data. Record time stamp for max/min strain
  'ASG strain in microstrain
  Average(8,Strain(),IEEE4,False)
  Minimum(8,Strain(),IEEE4,False,True)
  Maximum(8,Strain(),IEEE4,False,True)

  'GS1 Data
  'VWC as a decimal
  Average(8,VWC(),IEEE4,False)
  Minimum(8,VWC(),IEEE4,False,False)
  Maximum(8,VWC(),IEEE4,False,False)

  'MPS6 data. Record time stamp for max/min temperature.
  'Suction in kPa,Temp in celsius
  Average(16,MPS6(),IEEE4,False)
  Minimum(16,MPS6(),IEEE4,False,True)
  Maximum(16,MPS6(),IEEE4,False,True)
  TableFile("CRD:Control_Daily",8,-1,0,1,day,0,0)
EndTable

'Data table for raw data
DataTable(Control_Raw,true,-1)

  DataInterval(0,1,Day,10)
  'VW Piezometer Raw Data (frequency in Hz)
```

```
  Average(4,Freq(),IEEE4,False)
  Minimum(4,Freq(),IEEE4,False,False)
  Maximum(4,Freq(),IEEE4,False,False)
  'ASG Raw Data (full bridge measurements in mV/V,Exicitation=2.5V)
  Average(8,Vr1000(),IEEE4,False)
  Minimum(8,Vr1000(),IEEE4,False,True)
  Maximum(8,Vr1000(),IEEE4,False,True)
  'GS1 Raw Data (single ended measurements in mV)
  Average(8,RawVWC(),IEEE4,False)
  Minimum(8,RawVWC(),IEEE4,False,False)
  Maximum(8,RawVWC(),IEEE4,False,False)
  TableFile("CRD:Control_Raw",8,-1,0,0,day,0,0)
EndTable


'Main Program
BeginProg
  'Main Scan
  Scan(30,Min,1,0)
    'Default CR6 Datalogger Battery Voltage measurement 'BattV'
    Battery(BattV)
    'Default CR6 Datalogger Wiring Panel Temperature measurement 'PTemp_C'
    PanelTemp(PTemp_C,60)

    ChargeStateArr(1) = "Regulator Fault"
    ChargeStateArr(2) = "No Charge"
    ChargeStateArr(3) = "Current Limited"
    ChargeStateArr(4) = "Cycle Charging"
    ChargeStateArr(5) = "Float Charging"
    ChargeStateArr(6) = "Battery Test"
    ChargeSourceArr(1) = "None"
    ChargeSourceArr(2) = "Solar"
    ChargeSourceArr(3) = "Continuous"
    CheckBatteryArr(1) = "Normal"
    CheckBatteryArr(2) = "Check Battery"

    'Turn first AM16/32 Multiplexer On
    PortSet(C4,1)
    Delay(0,150,mSec)
    Count=1
    SubScan(0,uSec,4)
      'Switch to next AM16/32 Multiplexer channel
      PulsePort(C3,10000)
```

```
    'Geokon 4500 Series Vibrating Wire Piezometer measurement 'Freq()'
    VibratingWire(VW(1),1,U1,1000,4000,1,0.01,"",60,1.4051E-3,2.369E-4,1.019E-7)
    Freq(Count)=VW(1)
    'Amp(Count)=VW(2) 'These measurements are not necessary
    'SNRat(Count)=VW(3)
    'NFreq(Count)=VW(4)
    'DRat(Count)=VW(5)
    TT(Count)=VW(6)
    'Calculate digits 'Digits()'
    Digits(Count)=Freq(Count)^2/1000
    'Calculate PorePressure (kPa)
    PorePressure(Count)=(Digits(Count)-Digits0(Count))*G_Factor(Count)+(TT(Count)-
TT0(Count))*T_Factor(Count)
    'Calculate WT depth in feet
    WTDepth(Count)=PiezoDepth(Count)-((PorePressure(Count)/9.81)*3.281)
    Count=Count+1
  NextSubScan
  'Turn AM16/32 Multiplexer Off
  PortSet(C4,0)
  Delay(0,150,mSec)

  'Full Bridge Strain
  PortSet(U12,1)
  Delay(0,150,mSec)
  LCount=1
  SubScan(0,uSec,8)
   'Switch to next AM16/32 Multiplexer channel
   PulsePort(C3,10000)
   BrFull(Vr1000(LCount),1,mV200,U7,U5,1,2500,True,True,500,60,1,0)
   'calculate microstrain from calibration factors
   Strain(LCount)=Vr1000(LCount)*GFsRaw(LCount)
   LCount=LCount+1
  NextSubScan
  'turn off multiplexer
  PortSet(U12,0)
  Delay(0,150,mSec)

  'turn on 3rd mux for GS1 measurements
  PortSet(U11,1)
  Delay(0,150,mSec)
  MCount=1
  SubScan(0,uSec,8)
   'Switch to next AM16/32 Multiplexer channel
```

```
      PulsePort(C3,10000)
      SW12(1,1)
      Delay(0,150,mSec)
      'GS1 measurements 'VWC()' on the AM16/32 Multiplexer
      VoltSe(RawVWC(MCount),1,mV5000,U9,True,500,60,1,0)
      VWC(MCount)=((3.464*(10^-10))*(RawVWC(MCount)^3))-((1.316*(10^-
6))*(RawVWC(MCount)^2))+((1.878*(10^-3))*RawVWC(MCount))-0.9192
      MCount=MCount+1
      SW12(1,0)
    NextSubScan
    'turn off multiplexer
    PortSet(U11,0)
    Delay(0,150,mSec)

    'read SDI-12 Sensors
    SW12(2,1)
    Delay(0,1,sec)
    For NCount=1 To 8
      SDI12Recorder(MPS6(NCount,1),C1,NCount,"M!",1,0)
      Delay(0,1,sec)
    Next NCount
    SW12(2,0)

    'read CH200
    SDI12Recorder (CH200_M0(),C1,0,"MC!",1.0,0)
    'Array values start with one. Values for charge state start with -1.
    'Have to shift the value by two to line it up with the correct words
    'in the array.
    ChargeState = ChargeStateArr(Chg_State + 2)
    'Values for charge source start with zero. Have to shift the value
    'by one to line it up with the correct words in the array.
    ChargeSource = ChargeSourceArr(Chg_Source + 1)
    'Values for check battery start with zero. Have to shift the value
    'by one to line it up with the correct words in the array.
    CheckBattery = CheckBatteryArr(Ck_Batt + 1)


    'Call Data Tables and Store Data
    CallTable Control_Daily
    CallTable Control_Raw
  NextScan
EndProg
```

Sand Blanket Datalogger Program

```
'CR6 Series
'Created by Garrett Wheeler
'for Auburn Univesity Selma project
'
'Modified by Dan Jackson
'
'12 full bridge strain gages CTL asphalt gages
'8 SE sensors decagon gs1
'8 decagon mps6 sdi-12
'4 VW piezometers geokon 4500
'30 minute measurements
'daily table
'
StationName=SandBlanket

'Declare Variables and Units

'dim variables for default voltage and temp measurement
Public BattV
Public PTemp_C

'dim variables for vw piezometers
'Geokon 4500S serial #s: 1603233,1603234,1603235,1603236
Dim Count
Public VW(6)
Public Freq(4)
'Public Amp(4)
'Public SNRat(4)
'Public NFreq(4)
'Public DRat(4)
Public TT(4)
Public Digits(4)
Public PorePressure(4)
Public WTDepth(4)
'depth to each piezometer in feet
Public PiezoDepth(4)={7.0,12.2,7.6,11.8}
'vw gage and temp factors
Public G_Factor(4)={-0.118,-0.1109,-0.11,-0.1132}
Public T_Factor(4)={-0.04549,-0.1532,-0.1037,-0.04752}
' zero values for digits and temp. Factory zero used for piezo 1 and 2
'(Field zero was not recorded).
```

```
'Field zero used for piezo 3 and 4.
Public Digits0(4)={8795,8821,8864.5,8738.9}
Public TT0(4)={19.8,19.8,29.1,29.6}

'dim variables for ASGs
'CTL ASGs: A78,A81,A74,A68,A79,A76,A45,A66,A77,A80,A67,A75
Public LCount
Public Vr1000(12) 'full bridge result in mv/V ex.
Public Strain(12) 'strain result in microstrain
'ASG calibration factors in me/mV @ 2.5V Ex.
Public
GFsRaw(12)={288,288.63,287.42,280.14,294.92,287.11,287.71,294.3,301.72,299.82,290.1,297.
03}

'dim variables for GS1 (moisture)
'Decagon GS1 serial #s: 02-795,02-842,02-830,02-841,02-821,02-807,02-796,02-823
Public MCount
Public RawVWC(8)
Public VWC(8)

'dim variables for MPS6 (suction)
'Decagon MPS6 serial #s: 08-756,08-757,08-758,08-759,08-755,08-803,08-772,08-782
Public NCount
Public MPS6(8,2)

'Dim variables for CH200
Public CH200_M0(9)
'Battery voltage: VDC
Alias CH200_M0(1)=VBatt
Units VBatt = Volts
'Current going into, or out of, the battery: Amps
Alias CH200_M0(2)=IBatt
Units IBatt=Amps
'Current going to the load: Amps
Alias CH200_M0(3)=ILoad
Units ILoad=Amps
'Voltage coming into the charger: VDC
Alias CH200_M0(4)=V_in_chg
Units V_in_chg = Volts
'Current coming into the charger: Amps
Alias CH200_M0(5)=I_in_chg
Units I_in_chg = amps
'Charger temperature: Celsius
```

```
Alias CH200_M0(6)=Chg_TmpC
Units Chg_TmpC = deg C
'Charging state: Cycle, Float, Current Limited, or None
Alias CH200_M0(7)=Chg_State
'Charging source: None, AC, or Solar
Alias CH200_M0(8)=Chg_Source
'Check battery error: 0=normal, 1=check battery
Alias CH200_M0(9)=Ck_Batt

'Arrays to hold the associated words for the charge state, charge source,
'and check battery values.
Dim ChargeStateArr(6) As String
Dim ChargeSourceArr(3) As String
Dim CheckBatteryArr(2) As String

'Variables to hold the words for charge state, charge source, and check
'battery.
Public ChargeState As String
Public ChargeSource As String
Public CheckBattery As String

Alias MPS6(1,1)=Suction1
Alias MPS6(2,1)=Suction2
Alias MPS6(3,1)=Suction3
Alias MPS6(4,1)=Suction4
Alias MPS6(5,1)=Suction5
Alias MPS6(6,1)=Suction6
Alias MPS6(7,1)=Suction7
Alias MPS6(8,1)=Suction8
Alias MPS6(1,2)=Temp1
Alias MPS6(2,2)=Temp2
Alias MPS6(3,2)=Temp3
Alias MPS6(4,2)=Temp4
Alias MPS6(5,2)=Temp5
Alias MPS6(6,2)=Temp6
Alias MPS6(7,2)=Temp7
Alias MPS6(8,2)=Temp8

Units BattV=Volts
Units PTemp_C=Deg C
Units Freq=Hz
'Units Amp=mV RMS
'Units NFreq=Hz
```

```
Units TT=Deg C

Units TT0=Deg C
Units Digits=Digits
Units Digits0=Digits
Units PorePressure=kPa
Units WTDepth=feet

Units Suction1=kPa
Units Suction2=kPa
Units Suction3=kPa
Units Suction4=kPa
Units Suction5=kPa
Units Suction6=kPa
Units Suction7=kPa
Units Suction8=kPa

Units Temp1=Deg C
Units Temp2=Deg C
Units Temp3=Deg C
Units Temp4=Deg C
Units Temp5=Deg C
Units Temp6=Deg C
Units Temp7=Deg C
Units Temp8=Deg C

Units Strain=microstrain
Units Vr1000=mV/V



'Define Data Tables
'Data table for processed data
DataTable(SandBlanket_Daily,True,-1)

  DataInterval(0,1,Day,10)
  Minimum(1,BattV,IEEE4,False,False)
  Average(1,PTemp_C,IEEE4,False)
  Minimum (6,CH200_M0(),IEEE4,False,False)
  Maximum (6,CH200_M0(),IEEE4,False,False)


  'VW Piezometer Data. Record time stamp for max/min temperature
```

```
  'pore pressure in kPa, WT depth in feet, temp in celsius
  Average(4,PorePressure(),IEEE4,False)
  Minimum(4,PorePressure(),IEEE4,False,False)
  Maximum(4,PorePressure(),IEEE4,False,False)
  Average(4,WTDepth(),IEEE4,False)
  Minimum(4,WTDepth(),IEEE4,False,False)
  Maximum(4,WTDepth(),IEEE4,False,False)
  Average(4,TT(),IEEE4,False)
  Minimum(4,TT(),IEEE4,False,True)
  Maximum(4,TT(),IEEE4,False,True)

  'ASG Data. Record time stamp for max/min strain
  'ASG strain in microstrain
  Average(12,Strain(),IEEE4,False)
  Minimum(12,Strain(),IEEE4,False,True)
  Maximum(12,Strain(),IEEE4,False,True)

  'GS1 Data
  'VWC as a decimal
  Average(8,VWC(),IEEE4,False)
  Minimum(8,VWC(),IEEE4,False,False)
  Maximum(8,VWC(),IEEE4,False,False)

  'MPS6 data. Record time stamp for max/min temperature.
  'Suction in kPa,Temp in celsius
  Average(16,MPS6(),IEEE4,False)
  Minimum(16,MPS6(),IEEE4,False,True)
  Maximum(16,MPS6(),IEEE4,False,True)
  TableFile("CRD:SandBlanket_Daily",8,-1,0,1,day,0,0)
EndTable

'Data table for raw data
DataTable(SandBlanket_Raw,true,-1)

  DataInterval(0,1,Day,10)
  'VW Piezometer Raw Data (frequency in Hz)
  Average(4,Freq(),IEEE4,False)
  Minimum(4,Freq(),IEEE4,False,False)
  Maximum(4,Freq(),IEEE4,False,False)
  'ASG Raw Data (full bridge measurements in mV/V,Exicitation=2.5V)
  Average(12,Vr1000(),IEEE4,False)
  Minimum(12,Vr1000(),IEEE4,False,True)
  Maximum(12,Vr1000(),IEEE4,False,True)
```

```
  'GS1 Raw Data (single ended measurements in mV)
  Average(8,RawVWC(),IEEE4,False)
  Minimum(8,RawVWC(),IEEE4,False,False)
  Maximum(8,RawVWC(),IEEE4,False,False)
  TableFile("CRD:SandBlanket_Raw",8,-1,0,0,day,0,0)
EndTable


'Main Program
BeginProg
  'Main Scan
  Scan(30,Min,1,0)
    'Default CR6 Datalogger Battery Voltage measurement 'BattV'
    Battery(BattV)
    'Default CR6 Datalogger Wiring Panel Temperature measurement 'PTemp_C'
    PanelTemp(PTemp_C,60)

    ChargeStateArr(1) = "Regulator Fault"
    ChargeStateArr(2) = "No Charge"
    ChargeStateArr(3) = "Current Limited"
    ChargeStateArr(4) = "Cycle Charging"
    ChargeStateArr(5) = "Float Charging"
    ChargeStateArr(6) = "Battery Test"
    ChargeSourceArr(1) = "None"
    ChargeSourceArr(2) = "Solar"
    ChargeSourceArr(3) = "Continuous"
    CheckBatteryArr(1) = "Normal"
    CheckBatteryArr(2) = "Check Battery"

    'Turn first AM16/32 Multiplexer On
    PortSet(C4,1)
    Delay(0,150,mSec)
    Count=1
    SubScan(0,uSec,4)
      'Switch to next AM16/32 Multiplexer channel
      PulsePort(C3,10000)
      'Geokon 4500 Series Vibrating Wire Piezometer measurement 'Freq()'
      VibratingWire(VW(1),1,U1,1000,4000,1,0.01,"",60,1.4051E-3,2.369E-4,1.019E-7)
      Freq(Count)=VW(1)
      'Amp(Count)=VW(2) 'These measurements are not necessary
      'SNRat(Count)=VW(3)
      'NFreq(Count)=VW(4)
      'DRat(Count)=VW(5)
```

```
    TT(Count)=VW(6)
    'Calculate digits 'Digits()'
    Digits(Count)=Freq(Count)^2/1000
    'Calculate PorePressure (kPa)
    PorePressure(Count)=(Digits(Count)-Digits0(Count))*G_Factor(Count)+(TT(Count)-
TT0(Count))*T_Factor(Count)
    'Calculate WT depth in feet
    WTDepth(Count)=PiezoDepth(Count)-((PorePressure(Count)/9.81)*3.281)
    Count=Count+1
  NextSubScan
  'Turn AM16/32 Multiplexer Off
  PortSet(C4,0)
  Delay(0,150,mSec)

  'Full Bridge Strain
  PortSet(U12,1)
  Delay(0,150,mSec)
  LCount=1
  SubScan(0,uSec,12)
   'Switch to next AM16/32 Multiplexer channel
   PulsePort(C3,10000)
   BrFull(Vr1000(LCount),1,mV200,U7,U5,1,2500,True,True,500,60,1,0)
   'calculate microstrain from calibration factors
   Strain(LCount)=Vr1000(LCount)*GFsRaw(LCount)
   LCount=LCount+1
  NextSubScan
  'turn off multiplexer
  PortSet(U12,0)
  Delay(0,150,mSec)

  'turn on 3rd mux for GS1 measurements
  PortSet(U11,1)
  Delay(0,150,mSec)
  MCount=1
  SubScan(0,uSec,8)
   'Switch to next AM16/32 Multiplexer channel
   PulsePort(C3,10000)
   SW12(1,1)
   Delay(0,150,mSec)
   'GS1 measurements 'VWC()' on the AM16/32 Multiplexer
   VoltSe(RawVWC(MCount),1,mV5000,U9,True,500,60,1,0)
   VWC(MCount)=((3.464*(10^-10))*(RawVWC(MCount)^3))-((1.316*(10^-
6))*(RawVWC(MCount)^2))+((1.878*(10^-3))*RawVWC(MCount))-0.9192
```

```
    MCount=MCount+1
    SW12(1,0)
  NextSubScan
  'turn off multiplexer
  PortSet(U11,0)
  Delay(0,150,mSec)

  'read SDI-12 Sensors
  SW12(2,1)
  Delay(0,1,sec)
  For NCount=1 To 8
    SDI12Recorder(MPS6(NCount,1),C1,NCount,"M!",1,0)
    Delay(0,1,sec)
  Next NCount
  SW12(2,0)

  'read CH200
  SDI12Recorder (CH200_M0(),C1,0,"MC!",1.0,0)
  'Array values start with one. Values for charge state start with -1.
  'Have to shift the value by two to line it up with the correct words
  'in the array.
  ChargeState = ChargeStateArr(Chg_State + 2)
  'Values for charge source start with zero. Have to shift the value
  'by one to line it up with the correct words in the array.
  ChargeSource = ChargeSourceArr(Chg_Source + 1)
  'Values for check battery start with zero. Have to shift the value
  'by one to line it up with the correct words in the array.
  CheckBattery = CheckBatteryArr(Ck_Batt + 1)


  'Call Data Tables and Store Data
  CallTable SandBlanket_Daily
  CallTable SandBlanket_Raw
 NextScan
EndProg
```

Vertical Barriers Datalogger Program

```
'CR6 Series
'Created by Garrett Wheeler
'for Auburn Univesity Selma project
'
'Modified by Dan Jackson
'
'8 full bridge strain gages Geocomp asphalt gages
'8 SE sensors decagon gs1
'8 decagon mps6 sdi-12
'4 VW piezometers geokon 4500
'30 minute measurements
'daily table
'
StationName=VerticalBarriers

'Declare Variables and Units

'dim variables for default voltage and temp measurement
Public BattV
Public PTemp_C

'dim variables for vw piezometers
'Geokon 4500S serial #s: 1603237,1603238,1603239,1603240
Dim Count
Public VW(6)
Public Freq(4)
'Public Amp(4)
'Public SNRat(4)
'Public NFreq(4)
'Public DRat(4)
Public TT(4)
Public Digits(4)
Public PorePressure(4)
Public WTDepth(4)
'depth to each piezometer in feet
Public PiezoDepth(4)={7.5,12.0,7.5,11.8}
'vw gage and temp factors
Public G_Factor(4)={-0.104,-0.1113,-0.1139,-0.1154}
Public T_Factor(4)={-0.07496,-0.0757,-0.06354,-0.05386}
' zero values for digits and temp.
'Field zero used
```

```
Public Digits0(4)={8870.3,8936.8,8727.2,8811.5}
Public TT0(4)={26.8,23.2,26.9,26.9}

'dim variables for ASGs
'Geocomp ASGs: A34,A12,A20,A4,A16,A14,A44,A21
Public LCount
Public Vr1000(8) 'full bridge result in mv/V ex.
Public Strain(8) 'strain result in microstrain
'ASG calibration factors in me/mV @ 2.5V Ex.
Public GFsRaw(8)={226.37,256.32,275.70,265.63,261.86,266.71,293.65,265.60}

'dim variables for GS1 (moisture)
'Decagon GS1 serial #s: 02-820,02-831,02-798,02-819,02-808,02-829,02-822,02-804
Public MCount
Public RawVWC(8)
Public VWC(8)

'dim variables for MPS6 (suction)
'Decagon MPS6 serial #s: 08-776,08-783,08-800,08-789,08-812,08-816,08-778,08-780
Public NCount
Public MPS6(8,2)

'Dim variables for CH200
Public CH200_M0(9)
'Battery voltage: VDC
Alias CH200_M0(1)=VBatt
Units VBatt = Volts
'Current going into, or out of, the battery: Amps
Alias CH200_M0(2)=IBatt
Units IBatt=Amps
'Current going to the load: Amps
Alias CH200_M0(3)=ILoad
Units ILoad=Amps
'Voltage coming into the charger: VDC
Alias CH200_M0(4)=V_in_chg
Units V_in_chg = Volts
'Current coming into the charger: Amps
Alias CH200_M0(5)=I_in_chg
Units I_in_chg = amps
'Charger temperature: Celsius
Alias CH200_M0(6)=Chg_TmpC
Units Chg_TmpC = deg C
'Charging state: Cycle, Float, Current Limited, or None
```

```
Alias CH200_M0(7)=Chg_State
'Charging source: None, AC, or Solar
Alias CH200_M0(8)=Chg_Source
'Check battery error: 0=normal, 1=check battery
Alias CH200_M0(9)=Ck_Batt

'Arrays to hold the associated words for the charge state, charge source,
'and check battery values.
Dim ChargeStateArr(6) As String
Dim ChargeSourceArr(3) As String
Dim CheckBatteryArr(2) As String

'Variables to hold the words for charge state, charge source, and check
'battery.
Public ChargeState As String
Public ChargeSource As String
Public CheckBattery As String

Alias MPS6(1,1)=Suction1
Alias MPS6(2,1)=Suction2
Alias MPS6(3,1)=Suction3
Alias MPS6(4,1)=Suction4
Alias MPS6(5,1)=Suction5
Alias MPS6(6,1)=Suction6
Alias MPS6(7,1)=Suction7
Alias MPS6(8,1)=Suction8
Alias MPS6(1,2)=Temp1
Alias MPS6(2,2)=Temp2
Alias MPS6(3,2)=Temp3
Alias MPS6(4,2)=Temp4
Alias MPS6(5,2)=Temp5
Alias MPS6(6,2)=Temp6
Alias MPS6(7,2)=Temp7
Alias MPS6(8,2)=Temp8

Units BattV=Volts
Units PTemp_C=Deg C
Units Freq=Hz
'Units Amp=mV RMS
'Units NFreq=Hz
Units TT=Deg C

Units TT0=Deg C
```

```
Units Digits=Digits
Units Digits0=Digits
Units PorePressure=kPa
Units WTDepth=feet

Units Suction1=kPa
Units Suction2=kPa
Units Suction3=kPa
Units Suction4=kPa
Units Suction5=kPa
Units Suction6=kPa
Units Suction7=kPa
Units Suction8=kPa

Units Temp1=Deg C
Units Temp2=Deg C
Units Temp3=Deg C
Units Temp4=Deg C
Units Temp5=Deg C
Units Temp6=Deg C
Units Temp7=Deg C
Units Temp8=Deg C


Units Strain=microstrain
Units Vr1000=mV/V



'Define Data Tables
'Data table for processed data
DataTable(VertBarriers_Daily,True,-1)

  DataInterval(0,1,Day,10)
  Minimum(1,BattV,IEEE4,False,False)
  Average(1,PTemp_C,IEEE4,False)
  Minimum (6,CH200_M0(),IEEE4,False,False)
  Maximum (6,CH200_M0(),IEEE4,False,False)


  'VW Piezometer Data. Record time stamp for max/min temperature
  'pore pressure in kPa, WT depth in feet, temp in celsius
  Average(4,PorePressure(),IEEE4,False)
```

```
  Minimum(4,PorePressure(),IEEE4,False,False)
  Maximum(4,PorePressure(),IEEE4,False,False)
  Average(4,WTDepth(),IEEE4,False)
  Minimum(4,WTDepth(),IEEE4,False,False)
  Maximum(4,WTDepth(),IEEE4,False,False)
  Average(4,TT(),IEEE4,False)
  Minimum(4,TT(),IEEE4,False,True)
  Maximum(4,TT(),IEEE4,False,True)

  'ASG Data. Record time stamp for max/min strain
  'ASG strain in microstrain
  Average(8,Strain(),IEEE4,False)
  Minimum(8,Strain(),IEEE4,False,True)
  Maximum(8,Strain(),IEEE4,False,True)

  'GS1 Data
  'VWC as a decimal
  Average(8,VWC(),IEEE4,False)
  Minimum(8,VWC(),IEEE4,False,False)
  Maximum(8,VWC(),IEEE4,False,False)

  'MPS6 data. Record time stamp for max/min temperature.
  'Suction in kPa,Temp in celsius
  Average(16,MPS6(),IEEE4,False)
  Minimum(16,MPS6(),IEEE4,False,True)
  Maximum(16,MPS6(),IEEE4,False,True)
  TableFile("CRD:VertBarriers_Daily",8,-1,0,1,day,0,0)
EndTable

'Data table for raw data
DataTable(VertBarriers_Raw,true,-1)

  DataInterval(0,1,Day,10)
  'VW Piezometer Raw Data (frequency in Hz)
  Average(4,Freq(),IEEE4,False)
  Minimum(4,Freq(),IEEE4,False,False)
  Maximum(4,Freq(),IEEE4,False,False)
  'ASG Raw Data (full bridge measurements in mV/V,Exicitation=2.5V)
  Average(8,Vr1000(),IEEE4,False)
  Minimum(8,Vr1000(),IEEE4,False,True)
  Maximum(8,Vr1000(),IEEE4,False,True)
  'GS1 Raw Data (single ended measurements in mV)
  Average(8,RawVWC(),IEEE4,False)
```

```
  Minimum(8,RawVWC(),IEEE4,False,False)
  Maximum(8,RawVWC(),IEEE4,False,False)
  TableFile("CRD:VertBarriers_Raw",8,-1,0,0,day,0,0)
EndTable


'Main Program
BeginProg
  'Main Scan
  Scan(30,Min,1,0)
    'Default CR6 Datalogger Battery Voltage measurement 'BattV'
    Battery(BattV)
    'Default CR6 Datalogger Wiring Panel Temperature measurement 'PTemp_C'
    PanelTemp(PTemp_C,60)

    ChargeStateArr(1) = "Regulator Fault"
    ChargeStateArr(2) = "No Charge"
    ChargeStateArr(3) = "Current Limited"
    ChargeStateArr(4) = "Cycle Charging"
    ChargeStateArr(5) = "Float Charging"
    ChargeStateArr(6) = "Battery Test"
    ChargeSourceArr(1) = "None"
    ChargeSourceArr(2) = "Solar"
    ChargeSourceArr(3) = "Continuous"
    CheckBatteryArr(1) = "Normal"
    CheckBatteryArr(2) = "Check Battery"

    'Turn first AM16/32 Multiplexer On
    PortSet(C4,1)
    Delay(0,150,mSec)
    Count=1
    SubScan(0,uSec,4)
      'Switch to next AM16/32 Multiplexer channel
      PulsePort(C3,10000)
      'Geokon 4500 Series Vibrating Wire Piezometer measurement 'Freq()'
      VibratingWire(VW(1),1,U1,1000,4000,1,0.01,"",60,1.4051E-3,2.369E-4,1.019E-7)
      Freq(Count)=VW(1)
      'Amp(Count)=VW(2) 'These measurements are not necessary
      'SNRat(Count)=VW(3)
      'NFreq(Count)=VW(4)
      'DRat(Count)=VW(5)
      TT(Count)=VW(6)
      'Calculate digits 'Digits()'
```

```
      Digits(Count)=Freq(Count)^2/1000
      'Calculate PorePressure (kPa)
      PorePressure(Count)=(Digits(Count)-Digits0(Count))*G_Factor(Count)+(TT(Count)-
TT0(Count))*T_Factor(Count)
      'Calculate WT depth in feet
      WTDepth(Count)=PiezoDepth(Count)-((PorePressure(Count)/9.81)*3.281)
      Count=Count+1
    NextSubScan
    'Turn AM16/32 Multiplexer Off
    PortSet(C4,0)
    Delay(0,150,mSec)

    'Full Bridge Strain
    PortSet(U12,1)
    Delay(0,150,mSec)
    LCount=1
    SubScan(0,uSec,8)
      'Switch to next AM16/32 Multiplexer channel
      PulsePort(C3,10000)
      BrFull(Vr1000(LCount),1,mV200,U7,U5,1,2500,True,True,500,60,1,0)
      'calculate microstrain from calibration factors
      Strain(LCount)=Vr1000(LCount)*GFsRaw(LCount)
      LCount=LCount+1
    NextSubScan
    'turn off multiplexer
    PortSet(U12,0)
    Delay(0,150,mSec)

    'turn on 3rd mux for GS1 measurements
    PortSet(U11,1)
    Delay(0,150,mSec)
    MCount=1
    SubScan(0,uSec,8)
      'Switch to next AM16/32 Multiplexer channel
      PulsePort(C3,10000)
      SW12(1,1)
      Delay(0,150,mSec)
      'GS1 measurements 'VWC()' on the AM16/32 Multiplexer
      VoltSe(RawVWC(MCount),1,mV5000,U9,True,500,60,1,0)
      VWC(MCount)=((3.464*(10^-10))*(RawVWC(MCount)^3))-((1.316*(10^-
6))*(RawVWC(MCount)^2))+((1.878*(10^-3))*RawVWC(MCount))-0.9192
      MCount=MCount+1
      SW12(1,0)
```

```
    NextSubScan
    'turn off multiplexer
    PortSet(U11,0)
    Delay(0,150,mSec)

    'read SDI-12 Sensors
    SW12(2,1)
    Delay(0,1,sec)
    For NCount=1 To 8
      SDI12Recorder(MPS6(NCount,1),C1,NCount,"M!",1,0)
      Delay(0,1,sec)
    Next NCount
    SW12(2,0)

    'read CH200
    SDI12Recorder (CH200_M0(),C1,0,"MC!",1.0,0)
    'Array values start with one. Values for charge state start with -1.
    'Have to shift the value by two to line it up with the correct words
    'in the array.
    ChargeState = ChargeStateArr(Chg_State + 2)
    'Values for charge source start with zero. Have to shift the value
    'by one to line it up with the correct words in the array.
    ChargeSource = ChargeSourceArr(Chg_Source + 1)
    'Values for check battery start with zero. Have to shift the value
    'by one to line it up with the correct words in the array.
    CheckBattery = CheckBatteryArr(Ck_Batt + 1)


    'Call Data Tables and Store Data
    CallTable VertBarriers_Daily
    CallTable VertBarriers_Raw
  NextScan
EndProg
```

Lime Columns Datalogger Program

```
'CR6 Series
'Created by Garrett Wheeler
'for Auburn Univesity Selma project
'
'Modified by Dan Jackson
'
'For DAQ installation
'8 full bridge strain gages Geocomp asphalt gages
'8 SE sensors decagon gs1
'8 decagon mps6 sdi-12
'4 VW piezometers geokon 4500
'30 minute measurements
'daily tables table
'
StationName=LimeColumns

'Declare Variables and Units

'dim variables for default voltage and temp measurement
Public BattV
Public PTemp_C

'dim result for command to get data from other stations
Public Result(10)

'dim variables for VW Piezometers
'Geokon 4500S serial #s: 1603241,1603242,1603243,1603244
Dim Count
Public VW(6)
Public Freq(4)
'Public Amp(4)
'Public SNRat(4)
'Public NFreq(4)
'Public DRat(4)
Public TT(4)
Public Digits(4)
Public PorePressure(4)
Public WTDepth(4)
'depth to each piezometer in feet
Public PiezoDepth(4)={7.4,12.1,7.0,12.3}
'vw gage and temp factors
```

```
Public G_Factor(4)={-0.1171,-0.1153,-0.1059,-0.1082}
Public T_Factor(4)={-0.09278,-0.06385,-0.106,0.007266}
' zero values for digits and temp. Factory zero used for piezo 1 and 2
'(Field zero was not recorded).
'Field zero used for piezo 3 and 4.
Public Digits0(4)={8805,8806,8751.1,8797.7}
Public TT0(4)={20.9,21.5,39.2,40.6}

'dim variables for ASGs
'Geocomp ASGs: A43,A8,A37,A17,A40,A22,A15,A27
Public LCount
Public Vr1000(12) 'full bridge result in mv/V ex.
Public Strain(12) 'strain result in microstrain
'ASG calibration factors in me/mV @ 2.5V Ex.
Public GFsRaw(8)={270.55,286.35,281.92,271.02,276.48,294.10,266.62,227.44}

'dim variables for GS1 (moisture)
'Decagon GS1 serial #s: 02-818,02-846,02-813,02-833,02-801,02-824,02-835,02-792
Public MCount
Public RawVWC(8)
Public VWC(8)

'dim variables for MPS6 (suction)
'Decagon MPS6 serial #s:08-788,08-798,08-797,08-813,08-793,08-808,08-784,08-817
Public NCount
Public MPS6(8,2)

'counter for data collection from other stations
Public i =0

'Dim variables for CH200
Public CH200_M0(9)
'Battery voltage: VDC
Alias CH200_M0(1)=VBatt
Units VBatt = Volts
'Current going into, or out of, the battery: Amps
Alias CH200_M0(2)=IBatt
Units IBatt=Amps
'Current going to the load: Amps
Alias CH200_M0(3)=ILoad
Units ILoad=Amps
'Voltage coming into the charger: VDC
Alias CH200_M0(4)=V_in_chg
```

```
Units V_in_chg = Volts
'Current coming into the charger: Amps
Alias CH200_M0(5)=I_in_chg
Units I_in_chg = amps
'Charger temperature: Celsius
Alias CH200_M0(6)=Chg_TmpC
Units Chg_TmpC = deg C
'Charging state: Cycle, Float, Current Limited, or None
Alias CH200_M0(7)=Chg_State
'Charging source: None, AC, or Solar
Alias CH200_M0(8)=Chg_Source
'Check battery error: 0=normal, 1=check battery
Alias CH200_M0(9)=Ck_Batt

'Arrays to hold the associated words for the charge state, charge source,
'and check battery values.
Dim ChargeStateArr(6) As String
Dim ChargeSourceArr(3) As String
Dim CheckBatteryArr(2) As String

'Variables to hold the words for charge state, charge source, and check
'battery.
Public ChargeState As String
Public ChargeSource As String
Public CheckBattery As String

'dim variables for weather station
Public WXT(7)
Alias WXT(1)=WindDir
Alias WXT(2)=WS_mph
Alias WXT(3)=AirTF
Alias WXT(4)=RH
Alias WXT(5)=BP_kPa
Alias WXT(6)=Rain_in
Alias WXT(7)=HAmount
Units WindDir=Degrees
Units WS_mph=miles/hour
Units AirTF=Deg F
Units RH=%
Units BP_kPa=kPa
Units Rain_in=inch
Units HAmount=hits/cm^2
```

```
Alias MPS6(1,1)=Suction1
Alias MPS6(2,1)=Suction2
Alias MPS6(3,1)=Suction3
Alias MPS6(4,1)=Suction4
Alias MPS6(5,1)=Suction5
Alias MPS6(6,1)=Suction6
Alias MPS6(7,1)=Suction7
Alias MPS6(8,1)=Suction8
Alias MPS6(1,2)=Temp1
Alias MPS6(2,2)=Temp2
Alias MPS6(3,2)=Temp3
Alias MPS6(4,2)=Temp4
Alias MPS6(5,2)=Temp5
Alias MPS6(6,2)=Temp6
Alias MPS6(7,2)=Temp7
Alias MPS6(8,2)=Temp8

Units BattV=Volts
Units PTemp_C=Deg C
Units Freq=Hz
'Units Amp=mV RMS
'Units NFreq=Hz
Units TT=Deg C

Units TT0=Deg C
Units Digits=Digits
Units Digits0=Digits
Units PorePressure=kPa
Units WTDepth=feet

Units Suction1=kPa
Units Suction2=kPa
Units Suction3=kPa
Units Suction4=kPa
Units Suction5=kPa
Units Suction6=kPa
Units Suction7=kPa
Units Suction8=kPa

Units Temp1=Deg C
Units Temp2=Deg C
Units Temp3=Deg C
```

```
Units Temp4=Deg C
Units Temp5=Deg C
Units Temp6=Deg C
Units Temp7=Deg C
Units Temp8=Deg C


Units Strain=microstrain
Units Vr1000=mV/V



'Define Data Tables
'Data table for processed data
DataTable(LimeColumns_Daily,True,-1)
  DataInterval(0,1,Day,10)
  Minimum(1,BattV,IEEE4,False,False)
  Average(1,PTemp_C,IEEE4,False)
  Minimum (6,CH200_M0(),IEEE4,False,False)
  Maximum (6,CH200_M0(),IEEE4,False,False)

  'weather station data
  WindVector(1,WS_mph,WindDir,FP2,False,0,0,0)
  FieldNames("WS_mph_S_WVT,WindDir_D1_WVT,WindDir_SD1_WVT")
  Average(1,WS_mph,FP2,False)
  Average(1,AirTF,FP2,False)
  Maximum(1,AirTF,FP2,False,False)
  Minimum(1,AirTF,FP2,False,False)
  Average(1,RH,FP2,False)
  Average(1,BP_kPa,FP2,False)
  Totalize(1,Rain_in,FP2,False)
  Totalize(1,HAmount,FP2,False)

  'VW Piezometer Data. Record time stamp for max/min temperature
  'pore pressure in kPa, WT depth in feet, temp in celsius
  Average(4,PorePressure(),IEEE4,False)
  Minimum(4,PorePressure(),IEEE4,False,False)
  Maximum(4,PorePressure(),IEEE4,False,False)
  Average(4,WTDepth(),IEEE4,False)
  Minimum(4,WTDepth(),IEEE4,False,False)
  Maximum(4,WTDepth(),IEEE4,False,False)
  Average(4,TT(),IEEE4,False)
  Minimum(4,TT(),IEEE4,False,True)
```

```
  Maximum(4,TT(),IEEE4,False,True)

  'ASG Data. Record time stamp for max/min strain
  'ASG strain in microstrain
  Average(8,Strain(),IEEE4,False)
  Minimum(8,Strain(),IEEE4,False,True)
  Maximum(8,Strain(),IEEE4,False,True)

  'GS1 Data
  'VWC as a decimal
  Average(8,VWC(),IEEE4,False)
  Minimum(8,VWC(),IEEE4,False,False)
  Maximum(8,VWC(),IEEE4,False,False)

  'MPS6 data. Record time stamp for max/min temperature.
  'Suction in kPa,Temp in celsius
  Average(16,MPS6(),IEEE4,False)
  Minimum(16,MPS6(),IEEE4,False,True)
  Maximum(16,MPS6(),IEEE4,False,True)
  TableFile("CRD:LimeColumns_Daily",8,-1,0,1,day,0,0)
EndTable

'Data table for raw data
DataTable(LimeColumns_Raw,true,-1)

  DataInterval(0,1,Day,10)
  'VW Piezometer Raw Data (frequency in Hz)
  Average(4,Freq(),IEEE4,False)
  Minimum(4,Freq(),IEEE4,False,False)
  Maximum(4,Freq(),IEEE4,False,False)
  'ASG Raw Data (full bridge measurements in mV/V,Exicitation=2.5V)
  Average(8,Vr1000(),IEEE4,False)
  Minimum(8,Vr1000(),IEEE4,False,True)
  Maximum(8,Vr1000(),IEEE4,False,True)
  'GS1 Raw Data (single ended measurements in mV)
  Average(8,RawVWC(),IEEE4,False)
  Minimum(8,RawVWC(),IEEE4,False,False)
  Maximum(8,RawVWC(),IEEE4,False,False)
  TableFile("CRD:LimeColumns_Raw",8,-1,0,0,day,0,0)
EndTable

DataTable(Control_Daily,True,-1)
```

```
  DataInterval(0,1,Day,10)
  Minimum(1,BattV,IEEE4,False,False)
  Average(1,PTemp_C,IEEE4,False)
  Minimum (6,CH200_M0(),IEEE4,False,False)
  Maximum (6,CH200_M0(),IEEE4,False,False)


  'VW Piezometer Data. Record time stamp for max/min temperature
  'pore pressure in kPa, WT depth in feet, temp in celsius
  Average(4,PorePressure(),IEEE4,False)
  Minimum(4,PorePressure(),IEEE4,False,False)
  Maximum(4,PorePressure(),IEEE4,False,False)
  Average(4,WTDepth(),IEEE4,False)
  Minimum(4,WTDepth(),IEEE4,False,False)
  Maximum(4,WTDepth(),IEEE4,False,False)
  Average(4,TT(),IEEE4,False)
  Minimum(4,TT(),IEEE4,False,True)
  Maximum(4,TT(),IEEE4,False,True)

  'ASG Data. Record time stamp for max/min strain
  'ASG strain in microstrain
  Average(8,Strain(),IEEE4,False)
  Minimum(8,Strain(),IEEE4,False,True)
  Maximum(8,Strain(),IEEE4,False,True)

  'GS1 Data
  'VWC as a decimal
  Average(8,VWC(),IEEE4,False)
  Minimum(8,VWC(),IEEE4,False,False)
  Maximum(8,VWC(),IEEE4,False,False)

  'MPS6 data. Record time stamp for max/min temperature.
  'Suction in kPa,Temp in celsius
  Average(16,MPS6(),IEEE4,False)
  Minimum(16,MPS6(),IEEE4,False,True)
  Maximum(16,MPS6(),IEEE4,False,True)
  TableFile("CRD:Control_Daily",8,-1,0,1,day,0,0)
EndTable

'Data table for raw data
DataTable(Control_Raw,true,-1)

  DataInterval(0,1,Day,10)
```

```
  'VW Piezometer Raw Data (frequency in Hz)
  Average(4,Freq(),IEEE4,False)
  Minimum(4,Freq(),IEEE4,False,False)
  Maximum(4,Freq(),IEEE4,False,False)
  'ASG Raw Data (full bridge measurements in mV/V,Exicitation=2.5V)
  Average(8,Vr1000(),IEEE4,False)
  Minimum(8,Vr1000(),IEEE4,False,True)
  Maximum(8,Vr1000(),IEEE4,False,True)
  'GS1 Raw Data (single ended measurements in mV)
  Average(8,RawVWC(),IEEE4,False)
  Minimum(8,RawVWC(),IEEE4,False,False)
  Maximum(8,RawVWC(),IEEE4,False,False)
  TableFile("CRD:Control_Raw",8,-1,0,0,day,0,0)
EndTable

DataTable(SandBlanket_Daily,True,-1)

  DataInterval(0,1,Day,10)
  Minimum(1,BattV,IEEE4,False,False)
  Average(1,PTemp_C,IEEE4,False)
  Minimum (6,CH200_M0(),IEEE4,False,False)
  Maximum (6,CH200_M0(),IEEE4,False,False)


  'VW Piezometer Data. Record time stamp for max/min temperature
  'pore pressure in kPa, WT depth in feet, temp in celsius
  Average(4,PorePressure(),IEEE4,False)
  Minimum(4,PorePressure(),IEEE4,False,False)
  Maximum(4,PorePressure(),IEEE4,False,False)
  Average(4,WTDepth(),IEEE4,False)
  Minimum(4,WTDepth(),IEEE4,False,False)
  Maximum(4,WTDepth(),IEEE4,False,False)
  Average(4,TT(),IEEE4,False)
  Minimum(4,TT(),IEEE4,False,True)
  Maximum(4,TT(),IEEE4,False,True)

  'ASG Data. Record time stamp for max/min strain
  'ASG strain in microstrain
  Average(12,Strain(),IEEE4,False)
  Minimum(12,Strain(),IEEE4,False,True)
  Maximum(12,Strain(),IEEE4,False,True)

  'GS1 Data
```

```
  'VWC as a decimal
  Average(8,VWC(),IEEE4,False)
  Minimum(8,VWC(),IEEE4,False,False)
  Maximum(8,VWC(),IEEE4,False,False)

  'MPS6 data. Record time stamp for max/min temperature.
  'Suction in kPa,Temp in celsius
  Average(16,MPS6(),IEEE4,False)
  Minimum(16,MPS6(),IEEE4,False,True)
  Maximum(16,MPS6(),IEEE4,False,True)
  TableFile("CRD:SandBlanket_Daily",8,-1,0,1,day,0,0)
EndTable

'Data table for raw data
DataTable(SandBlanket_Raw,true,-1)

  DataInterval(0,1,Day,10)
  'VW Piezometer Raw Data (frequency in Hz)
  Average(4,Freq(),IEEE4,False)
  Minimum(4,Freq(),IEEE4,False,False)
  Maximum(4,Freq(),IEEE4,False,False)
  'ASG Raw Data (full bridge measurements in mV/V,Exicitation=2.5V)
  Average(12,Vr1000(),IEEE4,False)
  Minimum(12,Vr1000(),IEEE4,False,True)
  Maximum(12,Vr1000(),IEEE4,False,True)
  'GS1 Raw Data (single ended measurements in mV)
  Average(8,RawVWC(),IEEE4,False)
  Minimum(8,RawVWC(),IEEE4,False,False)
  Maximum(8,RawVWC(),IEEE4,False,False)
  TableFile("CRD:SandBlanket_Raw",8,-1,0,0,day,0,0)
EndTable

DataTable(VertBarriers_Daily,True,-1)

  DataInterval(0,1,Day,10)
  Minimum(1,BattV,IEEE4,False,False)
  Average(1,PTemp_C,IEEE4,False)
  Minimum (6,CH200_M0(),IEEE4,False,False)
  Maximum (6,CH200_M0(),IEEE4,False,False)


  'VW Piezometer Data. Record time stamp for max/min temperature
  'pore pressure in kPa, WT depth in feet, temp in celsius
```

```
  Average(4,PorePressure(),IEEE4,False)
  Minimum(4,PorePressure(),IEEE4,False,False)
  Maximum(4,PorePressure(),IEEE4,False,False)
  Average(4,WTDepth(),IEEE4,False)
  Minimum(4,WTDepth(),IEEE4,False,False)
  Maximum(4,WTDepth(),IEEE4,False,False)
  Average(4,TT(),IEEE4,False)
  Minimum(4,TT(),IEEE4,False,True)
  Maximum(4,TT(),IEEE4,False,True)

  'ASG Data. Record time stamp for max/min strain
  'ASG strain in microstrain
  Average(8,Strain(),IEEE4,False)
  Minimum(8,Strain(),IEEE4,False,True)
  Maximum(8,Strain(),IEEE4,False,True)

  'GS1 Data
  'VWC as a decimal
  Average(8,VWC(),IEEE4,False)
  Minimum(8,VWC(),IEEE4,False,False)
  Maximum(8,VWC(),IEEE4,False,False)

  'MPS6 data. Record time stamp for max/min temperature.
  'Suction in kPa,Temp in celsius
  Average(16,MPS6(),IEEE4,False)
  Minimum(16,MPS6(),IEEE4,False,True)
  Maximum(16,MPS6(),IEEE4,False,True)
  TableFile("CRD:VertBarriers_Daily",8,-1,0,1,day,0,0)
EndTable

'Data table for raw data
DataTable(VertBarriers_Raw,true,-1)

  DataInterval(0,1,Day,10)
  'VW Piezometer Raw Data (frequency in Hz)
  Average(4,Freq(),IEEE4,False)
  Minimum(4,Freq(),IEEE4,False,False)
  Maximum(4,Freq(),IEEE4,False,False)
  'ASG Raw Data (full bridge measurements in mV/V,Exicitation=2.5V)
  Average(8,Vr1000(),IEEE4,False)
  Minimum(8,Vr1000(),IEEE4,False,True)
  Maximum(8,Vr1000(),IEEE4,False,True)
  'GS1 Raw Data (single ended measurements in mV)
```

```
  Average(8,RawVWC(),IEEE4,False)
  Minimum(8,RawVWC(),IEEE4,False,False)
  Maximum(8,RawVWC(),IEEE4,False,False)
  TableFile("CRD:VertBarriers_Raw",8,-1,0,0,day,0,0)
EndTable

DataTable(PavedShoulders_Daily,True,-1)

  DataInterval(0,1,Day,10)
  Minimum(1,BattV,IEEE4,False,False)
  Average(1,PTemp_C,IEEE4,False)
  Minimum (6,CH200_M0(),IEEE4,False,False)
  Maximum (6,CH200_M0(),IEEE4,False,False)


  'VW Piezometer Data. Record time stamp for max/min temperature
  'pore pressure in kPa, WT depth in feet, temp in celsius
  Average(4,PorePressure(),IEEE4,False)
  Minimum(4,PorePressure(),IEEE4,False,False)
  Maximum(4,PorePressure(),IEEE4,False,False)
  Average(4,WTDepth(),IEEE4,False)
  Minimum(4,WTDepth(),IEEE4,False,False)
  Maximum(4,WTDepth(),IEEE4,False,False)
  Average(4,TT(),IEEE4,False)
  Minimum(4,TT(),IEEE4,False,True)
  Maximum(4,TT(),IEEE4,False,True)

  'ASG Data. Record time stamp for max/min strain
  'ASG strain in microstrain
  Average(8,Strain(),IEEE4,False)
  Minimum(8,Strain(),IEEE4,False,True)
  Maximum(8,Strain(),IEEE4,False,True)

  'GS1 Data
  'VWC as a decimal
  Average(8,VWC(),IEEE4,False)
  Minimum(8,VWC(),IEEE4,False,False)
  Maximum(8,VWC(),IEEE4,False,False)

  'MPS6 data. Record time stamp for max/min temperature.
  'Suction in kPa,Temp in celsius
  Average(16,MPS6(),IEEE4,False)
  Minimum(16,MPS6(),IEEE4,False,True)
```

```
  Maximum(16,MPS6(),IEEE4,False,True)
  TableFile("CRD:PavedShoulders_Daily",8,-1,0,1,day,0,0)
EndTable

'Data table for raw data
DataTable(PavedShoulders_Raw,true,-1)

  DataInterval(0,1,Day,10)
  'VW Piezometer Raw Data (frequency in Hz)
  Average(4,Freq(),IEEE4,False)
  Minimum(4,Freq(),IEEE4,False,False)
  Maximum(4,Freq(),IEEE4,False,False)
  'ASG Raw Data (full bridge measurements in mV/V,Exicitation=2.5V)
  Average(8,Vr1000(),IEEE4,False)
  Minimum(8,Vr1000(),IEEE4,False,True)
  Maximum(8,Vr1000(),IEEE4,False,True)
  'GS1 Raw Data (single ended measurements in mV)
  Average(8,RawVWC(),IEEE4,False)
  Minimum(8,RawVWC(),IEEE4,False,False)
  Maximum(8,RawVWC(),IEEE4,False,False)
  TableFile("CRD:PavedShoulders_Raw",8,-1,0,0,day,0,0)
EndTable

DataTable(EdgeDrains_Daily,True,-1)

  DataInterval(0,1,Day,10)
  Minimum(1,BattV,IEEE4,False,False)
  Average(1,PTemp_C,IEEE4,False)
  Minimum (6,CH200_M0(),IEEE4,False,False)
  Maximum (6,CH200_M0(),IEEE4,False,False)


  'VW Piezometer Data. Record time stamp for max/min temperature
  'pore pressure in kPa, WT depth in feet, temp in celsius
  Average(4,PorePressure(),IEEE4,False)
  Minimum(4,PorePressure(),IEEE4,False,False)
  Maximum(4,PorePressure(),IEEE4,False,False)
  Average(4,WTDepth(),IEEE4,False)
  Minimum(4,WTDepth(),IEEE4,False,False)
  Maximum(4,WTDepth(),IEEE4,False,False)
  Average(4,TT(),IEEE4,False)
  Minimum(4,TT(),IEEE4,False,True)
  Maximum(4,TT(),IEEE4,False,True)
```

```
  'ASG Data. Record time stamp for max/min strain
  'ASG strain in microstrain
  Average(8,Strain(),IEEE4,False)
  Minimum(8,Strain(),IEEE4,False,True)
  Maximum(8,Strain(),IEEE4,False,True)

  'GS1 Data
  'VWC as a decimal
  Average(8,VWC(),IEEE4,False)
  Minimum(8,VWC(),IEEE4,False,False)
  Maximum(8,VWC(),IEEE4,False,False)

  'MPS6 data. Record time stamp for max/min temperature.
  'Suction in kPa,Temp in celsius
  Average(16,MPS6(),IEEE4,False)
  Minimum(16,MPS6(),IEEE4,False,True)
  Maximum(16,MPS6(),IEEE4,False,True)
  TableFile("CRD:EdgeDrains_Daily",8,-1,0,1,day,0,0)
EndTable

'Data table for raw data
DataTable(EdgeDrains_Raw,true,-1)

  DataInterval(0,1,day,10)
  'VW Piezometer Raw Data (frequency in Hz)
  Average(4,Freq(),IEEE4,False)
  Minimum(4,Freq(),IEEE4,False,False)
  Maximum(4,Freq(),IEEE4,False,False)
  'ASG Raw Data (full bridge measurements in mV/V,Exicitation=2.5V)
  Average(8,Vr1000(),IEEE4,False)
  Minimum(8,Vr1000(),IEEE4,False,True)
  Maximum(8,Vr1000(),IEEE4,False,True)
  'GS1 Raw Data (single ended measurements in mV)
  Average(8,RawVWC(),IEEE4,False)
  Minimum(8,RawVWC(),IEEE4,False,False)
  Maximum(8,RawVWC(),IEEE4,False,False)
  TableFile("CRD:EdgeDrains_Raw",8,-1,0,0,day,0,0)
EndTable

'Main Program
BeginProg
  'Main Scan
```

```
  Scan(30,Min,1,0)
    'Default CR6 Datalogger Battery Voltage measurement 'BattV'
    Battery(BattV)
    'Default CR6 Datalogger Wiring Panel Temperature measurement 'PTemp_C'
    PanelTemp(PTemp_C,60)

    ChargeStateArr(1) = "Regulator Fault"
    ChargeStateArr(2) = "No Charge"
    ChargeStateArr(3) = "Current Limited"
    ChargeStateArr(4) = "Cycle Charging"
    ChargeStateArr(5) = "Float Charging"
    ChargeStateArr(6) = "Battery Test"
    ChargeSourceArr(1) = "None"
    ChargeSourceArr(2) = "Solar"
    ChargeSourceArr(3) = "Continuous"
    CheckBatteryArr(1) = "Normal"
    CheckBatteryArr(2) = "Check Battery"

    'Turn first AM16/32 Multiplexer On
    PortSet(C4,1)
    Delay(0,150,mSec)
    Count=1
    SubScan(0,uSec,4)
      'Switch to next AM16/32 Multiplexer channel
      PulsePort(C3,10000)
      'Geokon 4500 Series Vibrating Wire Piezometer measurement 'Freq()'
      VibratingWire(VW(1),1,U1,1000,4000,1,0.01,"",60,1.4051E-3,2.369E-4,1.019E-7)
      Freq(Count)=VW(1)
      'Amp(Count)=VW(2) 'These measurements are not necessary
      'SNRat(Count)=VW(3)
      'NFreq(Count)=VW(4)
      'DRat(Count)=VW(5)
      TT(Count)=VW(6)
      'Calculate digits 'Digits()'
      Digits(Count)=Freq(Count)^2/1000
      'Calculate PorePressure (kPa)
      PorePressure(Count)=(Digits(Count)-Digits0(Count))*G_Factor(Count)+(TT(Count)-
TT0(Count))*T_Factor(Count)
      'Calculate WT depth in feet
      WTDepth(Count)=PiezoDepth(Count)-((PorePressure(Count)/9.81)*3.281)
      Count=Count+1
    NextSubScan
    'Turn AM16/32 Multiplexer Off
```

```
  PortSet(C4,0)
  Delay(0,150,mSec)

  'Full Bridge Strain
  PortSet(U12,1)
  Delay(0,150,mSec)
  LCount=1
  SubScan(0,uSec,8)
    'Switch to next AM16/32 Multiplexer channel
    PulsePort(C3,10000)
    BrFull(Vr1000(LCount),1,mV200,U7,U5,1,2500,True,True,500,60,1,0)
    'calculate microstrain from calibration factors
    Strain(LCount)=Vr1000(LCount)*GFsRaw(LCount)
    LCount=LCount+1
  NextSubScan
  'turn off multiplexer
  PortSet(U12,0)
  Delay(0,150,mSec)

  'turn on 3rd mux for GS1 measurements
  PortSet(U11,1)
  Delay(0,150,mSec)
  MCount=1
  SubScan(0,uSec,8)
    'Switch to next AM16/32 Multiplexer channel
    PulsePort(C3,10000)
    SW12(1,1)
    Delay(0,150,mSec)
    'GS1 measurements 'VWC()' on the AM16/32 Multiplexer
    VoltSe(RawVWC(MCount),1,mV5000,U9,True,500,60,1,0)
    VWC(MCount)=((3.464*(10^-10))*(RawVWC(MCount)^3))-((1.316*(10^-
6))*(RawVWC(MCount)^2))+((1.878*(10^-3))*RawVWC(MCount))-0.9192
    MCount=MCount+1
    SW12(1,0)
  NextSubScan
  'turn off multiplexer
  PortSet(U11,0)
  Delay(0,150,mSec)

  'read SDI-12 Sensors
  SW12(2,1)
  Delay(0,1,sec)
  For NCount=1 To 8
```

```
  SDI12Recorder(MPS6(NCount,1),C1,NCount,"M!",1,0)
  Delay(0,1,sec)
Next NCount
SW12(2,0)



'read CH200
SDI12Recorder (CH200_M0(),C1,0,"MC!",1.0,0)
'Array values start with one. Values for charge state start with -1.
'Have to shift the value by two to line it up with the correct words
'in the array.
ChargeState = ChargeStateArr(Chg_State + 2)
'Values for charge source start with zero. Have to shift the value
'by one to line it up with the correct words in the array.
ChargeSource = ChargeSourceArr(Chg_Source + 1)
'Values for check battery start with zero. Have to shift the value
'by one to line it up with the correct words in the array.
CheckBattery = CheckBatteryArr(Ck_Batt + 1)


'WXT520 Weather Transmitter measurements 'WindDir', 'WS_mph', 'AirTF',
'RH', 'BP_kPa', 'Rain_in', and 'HAmount'
'make sure SDI12 address is 9
'power to 12V (not switched)

Delay(0,1,Sec)
SDI12Recorder(WXT(),C1,"9","R!",1,0)
'Reset all WXT520 Weather Transmitter measurements if NaN is returned to WXT(1)
If WXT(1)=NaN Then Move(WXT(),7,NaN,1)
If WS_mph<>NaN Then
  WS_mph=WS_mph*2.236936
EndIf
If AirTF<>NaN Then
  AirTF=AirTF*1.8+32
EndIf
If BP_kPa<>NaN Then
  BP_kPa=BP_kPa*0.1
EndIf
If Rain_in<>NaN Then
  Rain_in=Rain_in*0.0394
EndIf
```

```
    Delay(0,1,Sec)

    i=i+1

    If i=48 Then
      i=0
      'get data from other stations
      GetDataRecord(Result(1),ComSDC7,-1,10,0000,2000,2,1+32768,Control_Daily)
      GetDataRecord(Result(2),ComSDC7,-1,10,0000,2000,2,2+32768,Control_Raw)

      GetDataRecord(Result(3),ComSDC7,-1,20,0000,2000,2,1+32768,SandBlanket_Daily)
      GetDataRecord(Result(4),ComSDC7,-1,20,0000,2000,2,2+32768,SandBlanket_Raw)

      GetDataRecord(Result(5),ComSDC7,-1,30,0000,2000,2,1+32768,VertBarriers_Daily)
      GetDataRecord(Result(6),ComSDC7,-1,30,0000,2000,2,2+32768,VertBarriers_Raw)

      GetDataRecord(Result(7),ComSDC7,-1,50,0000,2000,2,1+32768,PavedShoulders_Daily)
      GetDataRecord(Result(8),ComSDC7,-1,50,0000,2000,2,2+32768,PavedShoulders_Raw)

      GetDataRecord(Result(9),ComSDC7,-1,60,0000,2000,2,1+32768,EdgeDrains_Daily)
      GetDataRecord(Result(10),ComSDC7,-1,60,0000,2000,2,2+32768,EdgeDrains_Raw)
    EndIf

    'Call Data Tables and Store Data
    CallTable LimeColumns_Daily
    CallTable LimeColumns_Raw
  NextScan
EndProg
```

Paved Shoulders Datalogger Program

```
'CR6 Series
'Created by Garrett Wheeler
'for Auburn Univesity Selma project
'
'Modified by Dan Jackson
'
'8 full bridge strain gages Geocomp asphalt gages
'8 SE sensors decagon gs1
'8 decagon mps6 sdi-12
'4 VW piezometers geokon 4500
'30 minute measurements
'daily table
'
StationName=PavedShoulders

'Declare Variables and Units

'dim variables for default voltage and temp measurement
Public BattV
Public PTemp_C

'dim variables for vw piezometers
'Geokon 4500S serial #s: 1603245,1603246,1603247,1603248
Dim Count
Public VW(6)
Public Freq(4)
'Public Amp(4)
'Public SNRat(4)
'Public NFreq(4)
'Public DRat(4)
Public TT(4)
Public Digits(4)
Public PorePressure(4)
Public WTDepth(4)
'depth to each piezometer in feet
Public PiezoDepth(4)={7.6,11.8,7.5,11.6}
'vw gage and temp factors
Public G_Factor(4)={-0.1105,-0.1207,-0.1092,-0.1206}
Public T_Factor(4)={0.02419,-0.09639,-0.02278,-0.07591}
' zero values for digits and temp. Factory zero used for piezo 1 and 2
'(Field zero was not recorded).
```

```
'Field zero used for piezo 3 and 4.
Public Digits0(4)={8762,8710,8766,8732.1}
Public TT0(4)={21.2,21.4,37.5,37.0}

'dim variables for ASGs
'Geocomp ASGs: A19,A31,A29,A25,A10,A7,A5,A36
Public LCount
Public Vr1000(8) 'full bridge result in mv/V ex.
Public Strain(8) 'strain result in microstrain
'ASG calibration factors in me/mV @ 2.5V Ex.
Public GFsRaw(8)={270.41,249.48,251.95,252.22,257.77,278.97,269.50,276.40}

'dim variables for GS1 (moisture)
'Decagon GS1 serial #s: 02-817,02-838,02-827,02-839,02-826,02-803,02-784,02-840
Public MCount
Public RawVWC(8)
Public VWC(8)

'dim variables for MPS6 (suction)
'Decagon MPS6 serial #s: 08-814,08-771,08-806,08-785,08-792,08-807,08-804,08-787
Public NCount
Public MPS6(8,2)

'Dim variables for CH200
Public CH200_M0(9)
'Battery voltage: VDC
Alias CH200_M0(1)=VBatt
Units VBatt = Volts
'Current going into, or out of, the battery: Amps
Alias CH200_M0(2)=IBatt
Units IBatt=Amps
'Current going to the load: Amps
Alias CH200_M0(3)=ILoad
Units ILoad=Amps
'Voltage coming into the charger: VDC
Alias CH200_M0(4)=V_in_chg
Units V_in_chg = Volts
'Current coming into the charger: Amps
Alias CH200_M0(5)=I_in_chg
Units I_in_chg = amps
'Charger temperature: Celsius
Alias CH200_M0(6)=Chg_TmpC
Units Chg_TmpC = deg C
```

```
'Charging state: Cycle, Float, Current Limited, or None
Alias CH200_M0(7)=Chg_State
'Charging source: None, AC, or Solar
Alias CH200_M0(8)=Chg_Source
'Check battery error: 0=normal, 1=check battery
Alias CH200_M0(9)=Ck_Batt

'Arrays to hold the associated words for the charge state, charge source,
'and check battery values.
Dim ChargeStateArr(6) As String
Dim ChargeSourceArr(3) As String
Dim CheckBatteryArr(2) As String

'Variables to hold the words for charge state, charge source, and check
'battery.
Public ChargeState As String
Public ChargeSource As String
Public CheckBattery As String

Alias MPS6(1,1)=Suction1
Alias MPS6(2,1)=Suction2
Alias MPS6(3,1)=Suction3
Alias MPS6(4,1)=Suction4
Alias MPS6(5,1)=Suction5
Alias MPS6(6,1)=Suction6
Alias MPS6(7,1)=Suction7
Alias MPS6(8,1)=Suction8
Alias MPS6(1,2)=Temp1
Alias MPS6(2,2)=Temp2
Alias MPS6(3,2)=Temp3
Alias MPS6(4,2)=Temp4
Alias MPS6(5,2)=Temp5
Alias MPS6(6,2)=Temp6
Alias MPS6(7,2)=Temp7
Alias MPS6(8,2)=Temp8

Units BattV=Volts
Units PTemp_C=Deg C
Units Freq=Hz
'Units Amp=mV RMS
'Units NFreq=Hz
Units TT=Deg C
```

```
Units TT0=Deg C
Units Digits=Digits
Units Digits0=Digits
Units PorePressure=kPa
Units WTDepth=feet

Units Suction1=kPa
Units Suction2=kPa
Units Suction3=kPa
Units Suction4=kPa
Units Suction5=kPa
Units Suction6=kPa
Units Suction7=kPa
Units Suction8=kPa

Units Temp1=Deg C
Units Temp2=Deg C
Units Temp3=Deg C
Units Temp4=Deg C
Units Temp5=Deg C
Units Temp6=Deg C
Units Temp7=Deg C
Units Temp8=Deg C


Units Strain=microstrain
Units Vr1000=mV/V



'Define Data Tables
'Data table for processed data
DataTable(PavedShoulders_Daily,True,-1)

  DataInterval(0,1,Day,10)
  Minimum(1,BattV,IEEE4,False,False)
  Average(1,PTemp_C,IEEE4,False)
  Minimum (6,CH200_M0(),IEEE4,False,False)
  Maximum (6,CH200_M0(),IEEE4,False,False)


  'VW Piezometer Data. Record time stamp for max/min temperature
  'pore pressure in kPa, WT depth in feet, temp in celsius
```

```
  Average(4,PorePressure(),IEEE4,False)
  Minimum(4,PorePressure(),IEEE4,False,False)
  Maximum(4,PorePressure(),IEEE4,False,False)
  Average(4,WTDepth(),IEEE4,False)
  Minimum(4,WTDepth(),IEEE4,False,False)
  Maximum(4,WTDepth(),IEEE4,False,False)
  Average(4,TT(),IEEE4,False)
  Minimum(4,TT(),IEEE4,False,True)
  Maximum(4,TT(),IEEE4,False,True)

  'ASG Data. Record time stamp for max/min strain
  'ASG strain in microstrain
  Average(8,Strain(),IEEE4,False)
  Minimum(8,Strain(),IEEE4,False,True)
  Maximum(8,Strain(),IEEE4,False,True)

  'GS1 Data
  'VWC as a decimal
  Average(8,VWC(),IEEE4,False)
  Minimum(8,VWC(),IEEE4,False,False)
  Maximum(8,VWC(),IEEE4,False,False)

  'MPS6 data. Record time stamp for max/min temperature.
  'Suction in kPa,Temp in celsius
  Average(16,MPS6(),IEEE4,False)
  Minimum(16,MPS6(),IEEE4,False,True)
  Maximum(16,MPS6(),IEEE4,False,True)
  TableFile("CRD:PavedShoulders_Daily",8,-1,0,1,day,0,0)
EndTable

'Data table for raw data
DataTable(PavedShoulders_Raw,true,-1)

  DataInterval(0,1,Day,10)
  'VW Piezometer Raw Data (frequency in Hz)
  Average(4,Freq(),IEEE4,False)
  Minimum(4,Freq(),IEEE4,False,False)
  Maximum(4,Freq(),IEEE4,False,False)
  'ASG Raw Data (full bridge measurements in mV/V,Exicitation=2.5V)
  Average(8,Vr1000(),IEEE4,False)
  Minimum(8,Vr1000(),IEEE4,False,True)
  Maximum(8,Vr1000(),IEEE4,False,True)
  'GS1 Raw Data (single ended measurements in mV)
```

```
  Average(8,RawVWC(),IEEE4,False)
  Minimum(8,RawVWC(),IEEE4,False,False)
  Maximum(8,RawVWC(),IEEE4,False,False)
  TableFile("CRD:PavedShoulders_Raw",8,-1,0,0,day,0,0)
EndTable


'Main Program
BeginProg
  'Main Scan
  Scan(30,Min,1,0)
    'Default CR6 Datalogger Battery Voltage measurement 'BattV'
    Battery(BattV)
    'Default CR6 Datalogger Wiring Panel Temperature measurement 'PTemp_C'
    PanelTemp(PTemp_C,60)


    ChargeStateArr(1) = "Regulator Fault"
    ChargeStateArr(2) = "No Charge"
    ChargeStateArr(3) = "Current Limited"
    ChargeStateArr(4) = "Cycle Charging"
    ChargeStateArr(5) = "Float Charging"
    ChargeStateArr(6) = "Battery Test"
    ChargeSourceArr(1) = "None"
    ChargeSourceArr(2) = "Solar"
    ChargeSourceArr(3) = "Continuous"
    CheckBatteryArr(1) = "Normal"
    CheckBatteryArr(2) = "Check Battery"

    'Turn first AM16/32 Multiplexer On
    PortSet(C4,1)
    Delay(0,150,mSec)
    Count=1
    SubScan(0,uSec,4)
      'Switch to next AM16/32 Multiplexer channel
      PulsePort(C3,10000)
      'Geokon 4500 Series Vibrating Wire Piezometer measurement 'Freq()'
      VibratingWire(VW(1),1,U1,1000,4000,1,0.01,"",60,1.4051E-3,2.369E-4,1.019E-7)
      Freq(Count)=VW(1)
      'Amp(Count)=VW(2) 'These measurements are not necessary
      'SNRat(Count)=VW(3)
      'NFreq(Count)=VW(4)
      'DRat(Count)=VW(5)
```

```
    TT(Count)=VW(6)
    'Calculate digits 'Digits()'
    Digits(Count)=Freq(Count)^2/1000
    'Calculate PorePressure (kPa)
    PorePressure(Count)=(Digits(Count)-Digits0(Count))*G_Factor(Count)+(TT(Count)-
TT0(Count))*T_Factor(Count)
    'Calculate WT depth in feet
    WTDepth(Count)=PiezoDepth(Count)-((PorePressure(Count)/9.81)*3.281)
    Count=Count+1
  NextSubScan
  'Turn AM16/32 Multiplexer Off
  PortSet(C4,0)
  Delay(0,150,mSec)

  'Full Bridge Strain
  PortSet(U12,1)
  Delay(0,150,mSec)
  LCount=1
  SubScan(0,uSec,8)
   'Switch to next AM16/32 Multiplexer channel
   PulsePort(C3,10000)
   BrFull(Vr1000(LCount),1,mV200,U7,U5,1,2500,True,True,500,60,1,0)
   'calculate microstrain from calibration factors
   Strain(LCount)=Vr1000(LCount)*GFsRaw(LCount)
   LCount=LCount+1
  NextSubScan
  'turn off multiplexer
  PortSet(U12,0)
  Delay(0,150,mSec)

  'turn on 3rd mux for GS1 measurements
  PortSet(U11,1)
  Delay(0,150,mSec)
  MCount=1
  SubScan(0,uSec,8)
   'Switch to next AM16/32 Multiplexer channel
   PulsePort(C3,10000)
   SW12(1,1)
   Delay(0,150,mSec)
   'GS1 measurements 'VWC()' on the AM16/32 Multiplexer
   VoltSe(RawVWC(MCount),1,mV5000,U9,True,500,60,1,0)
   VWC(MCount)=((3.464*(10^-10))*(RawVWC(MCount)^3))-((1.316*(10^-
6))*(RawVWC(MCount)^2))+((1.878*(10^-3))*RawVWC(MCount))-0.9192
```

```
    MCount=MCount+1
    SW12(1,0)
  NextSubScan
  'turn off multiplexer
  PortSet(U11,0)
  Delay(0,150,mSec)

  'read SDI-12 Sensors
  SW12(2,1)
  Delay(0,1,sec)
  For NCount=1 To 8
    SDI12Recorder(MPS6(NCount,1),C1,NCount,"M!",1,0)
    Delay(0,1,sec)
  Next NCount
  SW12(2,0)


  'read CH200
  SDI12Recorder (CH200_M0(),C1,0,"MC!",1.0,0)
  'Array values start with one. Values for charge state start with -1.
  'Have to shift the value by two to line it up with the correct words
  'in the array.
  ChargeState = ChargeStateArr(Chg_State + 2)
  'Values for charge source start with zero. Have to shift the value
  'by one to line it up with the correct words in the array.
  ChargeSource = ChargeSourceArr(Chg_Source + 1)
  'Values for check battery start with zero. Have to shift the value
  'by one to line it up with the correct words in the array.
  CheckBattery = CheckBatteryArr(Ck_Batt + 1)


  'Call Data Tables and Store Data
  CallTable PavedShoulders_Daily
  CallTable PavedShoulders_Raw
 NextScan
EndProg
```

Edge Drains Datalogger Program

```
'CR6 Series
'Created by Garrett Wheeler
'for Auburn Univesity Selma project
'
'Modified by Dan Jackson
'
'8 full bridge strain gages Geocomp asphalt gages
'8 SE sensors decagon gs1
'8 decagon mps6 sdi-12
'4 VW piezometers geokon 4500
'30 minute measurements
'daily table
'
StationName=EdgeDrains

'Declare Variables and Units

'Dim variables for default voltage and temp measurement
Public BattV
Public PTemp_C

'Dim Variables for VW Piezometers
'Geokon 4500S Piezometers Serial #s: 1603249,1603250,1603251,1603252
Dim Count
Public VW(6)
Public Freq(4)
'Public Amp(4) 'unnecessary for this study
'Public SNRat(4) 'unnecessary for this study
'Public NFreq(4) 'unnecessary for this study
'Public DRat(4) 'unnecessary for this study
Public TT(4)
Public Digits(4)
Public PorePressure(4)
Public WTDepth(4)
'depth to each piezometer in feet
Public PiezoDepth(4)={7.1,11.9,7.5,12.0}
'vw gage and temp factors
Public G_Factor(4)={-0.1026,-0.1128,-0.1126,-0.1044}
Public T_Factor(4)={-0.1609,-0.06741,-0.07937,-0.1325}
' zero values for digits and temp
'Field zero used
```

```
Public Digits0(4)={8744.6,8770.0,8835.1,8768.5}
Public TT0(4)={30.4,30.1,27.0,27.7}

'Dim Variables for ASGs
'Geocomp ASGs: A9,A32,A39,A38,A24,A23,A26,A6
Public LCount
Public Vr1000(8) 'full bridge result in mv/V ex.
Public Strain(8) 'strain result in microstrain
'ASG calibration factors in me/mV @ 2.5V Ex.
'Geocomp ASGs: A9,A32,A39,A38,A24,A23,A26,A6
Public GFsRaw(8)={253.74,263.78,278.23,261.78,269.33,296.85,261.10,246.25}

'Dim Variables for GS1 (Moisture)
'Decagon GS1 Serial #s: 02-816,02-845,02-805,02-806,02-811,02-832,02-802,02-843
Public MCount
Public RawVWC(8)
Public VWC(8)

'Dim Variables for MPS6 (Suction)
'Decagon MPS6 Serial #s: 08-769,08-795,08-786,08-796,08-754,08-777,08-756,08-805
Public NCount
Public MPS6(8,2)


'Dim variables for CH200
Public CH200_M0(9)
'Battery voltage: VDC
Alias CH200_M0(1)=VBatt
Units VBatt = Volts
'Current going into, or out of, the battery: Amps
Alias CH200_M0(2)=IBatt
Units IBatt=Amps
'Current going to the load: Amps
Alias CH200_M0(3)=ILoad
Units ILoad=Amps
'Voltage coming into the charger: VDC
Alias CH200_M0(4)=V_in_chg
Units V_in_chg = Volts
'Current coming into the charger: Amps
Alias CH200_M0(5)=I_in_chg
Units I_in_chg = amps
'Charger temperature: Celsius
Alias CH200_M0(6)=Chg_TmpC
```

```
Units Chg_TmpC = deg C
'Charging state: Cycle, Float, Current Limited, or None
Alias CH200_M0(7)=Chg_State
'Charging source: None, AC, or Solar
Alias CH200_M0(8)=Chg_Source
'Check battery error: 0=normal, 1=check battery
Alias CH200_M0(9)=Ck_Batt

'Arrays to hold the associated words for the charge state, charge source,
'and check battery values.
Dim ChargeStateArr(6) As String
Dim ChargeSourceArr(3) As String
Dim CheckBatteryArr(2) As String

'Variables to hold the words for charge state, charge source, and check
'battery.
Public ChargeState As String
Public ChargeSource As String
Public CheckBattery As String

'Define Alias and units for variables
Alias MPS6(1,1)=Suction1
Alias MPS6(2,1)=Suction2
Alias MPS6(3,1)=Suction3
Alias MPS6(4,1)=Suction4
Alias MPS6(5,1)=Suction5
Alias MPS6(6,1)=Suction6
Alias MPS6(7,1)=Suction7
Alias MPS6(8,1)=Suction8
Alias MPS6(1,2)=Temp1
Alias MPS6(2,2)=Temp2
Alias MPS6(3,2)=Temp3
Alias MPS6(4,2)=Temp4
Alias MPS6(5,2)=Temp5
Alias MPS6(6,2)=Temp6
Alias MPS6(7,2)=Temp7
Alias MPS6(8,2)=Temp8

Units BattV=Volts
Units PTemp_C=Deg C
Units Freq=Hz
'Units Amp=mV RMS
'Units NFreq=Hz
```

```
Units TT=Deg C

Units TT0=Deg C
Units Digits=Digits
Units Digits0=Digits
Units PorePressure=kPa
Units WTDepth=feet

Units Suction1=kPa
Units Suction2=kPa
Units Suction3=kPa
Units Suction4=kPa
Units Suction5=kPa
Units Suction6=kPa
Units Suction7=kPa
Units Suction8=kPa

Units Temp1=Deg C
Units Temp2=Deg C
Units Temp3=Deg C
Units Temp4=Deg C
Units Temp5=Deg C
Units Temp6=Deg C
Units Temp7=Deg C
Units Temp8=Deg C


Units Strain=microstrain
Units Vr1000=mV/V



'Define Data Tables
'Data table for processed data
DataTable(EdgeDrains_Daily,True,-1)

  DataInterval(0,1,Day,10)
  Minimum(1,BattV,IEEE4,False,False)
  Average(1,PTemp_C,IEEE4,False)
  Minimum (6,CH200_M0(),IEEE4,False,False)
  Maximum (6,CH200_M0(),IEEE4,False,False)
```

```
  'VW Piezometer Data. Record time stamp for max/min temperature
  'pore pressure in kPa, WT depth in feet, temp in celsius
  Average(4,PorePressure(),IEEE4,False)
  Minimum(4,PorePressure(),IEEE4,False,False)
  Maximum(4,PorePressure(),IEEE4,False,False)
  Average(4,WTDepth(),IEEE4,False)
  Minimum(4,WTDepth(),IEEE4,False,False)
  Maximum(4,WTDepth(),IEEE4,False,False)
  Average(4,TT(),IEEE4,False)
  Minimum(4,TT(),IEEE4,False,True)
  Maximum(4,TT(),IEEE4,False,True)

  'ASG Data. Record time stamp for max/min strain
  'ASG strain in microstrain
  Average(8,Strain(),IEEE4,False)
  Minimum(8,Strain(),IEEE4,False,True)
  Maximum(8,Strain(),IEEE4,False,True)

  'GS1 Data
  'VWC as a decimal
  Average(8,VWC(),IEEE4,False)
  Minimum(8,VWC(),IEEE4,False,False)
  Maximum(8,VWC(),IEEE4,False,False)

  'MPS6 data. Record time stamp for max/min temperature.
  'Suction in kPa,Temp in celsius
  Average(16,MPS6(),IEEE4,False)
  Minimum(16,MPS6(),IEEE4,False,True)
  Maximum(16,MPS6(),IEEE4,False,True)
  TableFile("CRD:EdgeDrains_Daily",8,-1,0,1,day,0,0)
EndTable

'Data table for raw data
DataTable(EdgeDrains_Raw,true,-1)

  DataInterval(0,1,Day,10)
  'VW Piezometer Raw Data (frequency in Hz)
  Average(4,Freq(),IEEE4,False)
  Minimum(4,Freq(),IEEE4,False,False)
  Maximum(4,Freq(),IEEE4,False,False)
  'ASG Raw Data (full bridge measurements in mV/V,Exicitation=2.5V)
  Average(8,Vr1000(),IEEE4,False)
  Minimum(8,Vr1000(),IEEE4,False,True)
```

```
  Maximum(8,Vr1000(),IEEE4,False,True)
  'GS1 Raw Data (single ended measurements in mV)
  Average(8,RawVWC(),IEEE4,False)
  Minimum(8,RawVWC(),IEEE4,False,False)
  Maximum(8,RawVWC(),IEEE4,False,False)
  TableFile("CRD:EdgeDrains_Raw",8,-1,0,0,day,0,0)
EndTable


'Main Program
BeginProg
  'Main Scan
  Scan(30,Min,1,0)
    'Default CR6 Datalogger Battery Voltage measurement 'BattV'
    Battery(BattV)
    'Default CR6 Datalogger Wiring Panel Temperature measurement 'PTemp_C'
    PanelTemp(PTemp_C,60)

    ChargeStateArr(1) = "Regulator Fault"
    ChargeStateArr(2) = "No Charge"
    ChargeStateArr(3) = "Current Limited"
    ChargeStateArr(4) = "Cycle Charging"
    ChargeStateArr(5) = "Float Charging"
    ChargeStateArr(6) = "Battery Test"
    ChargeSourceArr(1) = "None"
    ChargeSourceArr(2) = "Solar"
    ChargeSourceArr(3) = "Continuous"
    CheckBatteryArr(1) = "Normal"
    CheckBatteryArr(2) = "Check Battery"

    'Turn first AM16/32 Multiplexer On
    PortSet(C4,1)
    Delay(0,150,mSec)
    Count=1
    SubScan(0,uSec,4)
      'Switch to next AM16/32 Multiplexer channel
      PulsePort(C3,10000)
      'Geokon 4500 Series Vibrating Wire Piezometer measurement 'Freq()'
      VibratingWire(VW(1),1,U1,1000,4000,1,0.01,"",60,1.4051E-3,2.369E-4,1.019E-7)
      Freq(Count)=VW(1)
      'Amp(Count)=VW(2) 'These measurements are not necessary
      'SNRat(Count)=VW(3)
      'NFreq(Count)=VW(4)
```

```
    'DRat(Count)=VW(5)
    TT(Count)=VW(6)
    'Calculate digits 'Digits()'
    Digits(Count)=Freq(Count)^2/1000
    'Calculate PorePressure (kPa)
    PorePressure(Count)=(Digits(Count)-Digits0(Count))*G_Factor(Count)+(TT(Count)-
TT0(Count))*T_Factor(Count)
    'Calculate WT depth in feet
    WTDepth(Count)=PiezoDepth(Count)-((PorePressure(Count)/9.81)*3.281)
    Count=Count+1
  NextSubScan
  'Turn AM16/32 Multiplexer Off
  PortSet(C4,0)
  Delay(0,150,mSec)

  'Full Bridge Strain
  PortSet(U12,1)
  Delay(0,150,mSec)
  LCount=1
  SubScan(0,uSec,8)
    'Switch to next AM16/32 Multiplexer channel
    PulsePort(C3,10000)
    BrFull(Vr1000(LCount),1,mV200,U7,U5,1,2500,True,True,500,60,1,0)
    'calculate microstrain from calibration factors
    Strain(LCount)=Vr1000(LCount)*GFsRaw(LCount)
    LCount=LCount+1
  NextSubScan
  'turn off multiplexer
  PortSet(U12,0)
  Delay(0,150,mSec)

  'turn on 3rd mux for GS1 measurements
  PortSet(U11,1)
  Delay(0,150,mSec)
  MCount=1
  SubScan(0,uSec,8)
    'Switch to next AM16/32 Multiplexer channel
    PulsePort(C3,10000)
    SW12(1,1)
    Delay(0,150,mSec)
    'GS1 measurements 'VWC()' on the AM16/32 Multiplexer
    VoltSe(RawVWC(MCount),1,mV5000,U9,True,500,60,1,0)
```

```
    VWC(MCount)=((3.464*(10^-10))*(RawVWC(MCount)^3))-((1.316*(10^-
6))*(RawVWC(MCount)^2))+((1.878*(10^-3))*RawVWC(MCount))-0.9192
     MCount=MCount+1
     SW12(1,0)
   NextSubScan
   'turn off multiplexer
   PortSet(U11,0)
   Delay(0,150,mSec)

   'read SDI-12 Sensors
   SW12(2,1)
   Delay(0,1,sec)
   For NCount=1 To 8
     SDI12Recorder(MPS6(NCount,1),C1,NCount,"M!",1,0)
     Delay(0,1,sec)
   Next NCount
   SW12(2,0)

   'read CH200
   SDI12Recorder (CH200_M0(),C1,0,"MC!",1.0,0)
   'Array values start with one. Values for charge state start with -1.
   'Have to shift the value by two to line it up with the correct words
   'in the array.
   ChargeState = ChargeStateArr(Chg_State + 2)
   'Values for charge source start with zero. Have to shift the value
   'by one to line it up with the correct words in the array.
   ChargeSource = ChargeSourceArr(Chg_Source + 1)
   'Values for check battery start with zero. Have to shift the value
   'by one to line it up with the correct words in the array.
   CheckBattery = CheckBatteryArr(Ck_Batt + 1)


   'Call Data Tables and Store Data
   CallTable EdgeDrains_Daily
   CallTable EdgeDrains_Raw
  NextScan
EndProg
```

Trees Datalogger Program

```
'CR6 Series

'
'Created by Dan Jackson
'
'4 SE sensors decagon gs1
'4 decagon mps6 sdi-12
'30 minute measurements
'daily table
'
StationName=Trees

'Declare Variables and Units

'dim variables for default voltage and temp measurement
Public BattV
Public PTemp_C




'dim variables for GS1 (Moisture)
'Decagon GS1 serial #s:
Public MCount
Public Count
Public RawVWC(4)
Public VWC(4)

'dim variables for MPS6 (suction)
'Decagon MPS6 serial #s:
Public NCount
Public MPS6(4,2)

'Dim variables for CH200
Public CH200_M0(9)
'Battery voltage: VDC
Alias CH200_M0(1)=VBatt
Units VBatt = Volts
'Current going into, or out of, the battery: Amps
Alias CH200_M0(2)=IBatt
Units IBatt=Amps
```

```
'Current going to the load: Amps
Alias CH200_M0(3)=ILoad
Units ILoad=Amps
'Voltage coming into the charger: VDC
Alias CH200_M0(4)=V_in_chg
Units V_in_chg = Volts
'Current coming into the charger: Amps
Alias CH200_M0(5)=I_in_chg
Units I_in_chg = amps
'Charger temperature: Celsius
Alias CH200_M0(6)=Chg_TmpC
Units Chg_TmpC = deg C
'Charging state: Cycle, Float, Current Limited, or None
Alias CH200_M0(7)=Chg_State
'Charging source: None, AC, or Solar
Alias CH200_M0(8)=Chg_Source
'Check battery error: 0=normal, 1=check battery
Alias CH200_M0(9)=Ck_Batt

'Arrays to hold the associated words for the charge state, charge source,
'and check battery values.
Dim ChargeStateArr(6) As String
Dim ChargeSourceArr(3) As String
Dim CheckBatteryArr(2) As String

'Variables to hold the words for charge state, charge source, and check
'battery.
Public ChargeState As String
Public ChargeSource As String
Public CheckBattery As String

Alias MPS6(1,1)=Suction1
Alias MPS6(2,1)=Suction2
Alias MPS6(3,1)=Suction3
Alias MPS6(4,1)=Suction4
Alias MPS6(1,2)=Temp1
Alias MPS6(2,2)=Temp2
Alias MPS6(3,2)=Temp3
Alias MPS6(4,2)=Temp4


Units BattV=Volts
Units PTemp_C=Deg C
```

```
Units Suction1=kPa
Units Suction2=kPa
Units Suction3=kPa
Units Suction4=kPa


Units Temp1=Deg C
Units Temp2=Deg C
Units Temp3=Deg C
Units Temp4=Deg C




'Define Data Tables
'Data table for processed data
DataTable(Trees_Daily,True,-1)

  DataInterval(0,1,Day,10)
  Minimum(1,BattV,IEEE4,False,False)
  Average(1,PTemp_C,IEEE4,False)
  Minimum (6,CH200_M0(),IEEE4,False,False)
  Maximum (6,CH200_M0(),IEEE4,False,False)

  'GS1 Data
  'VWC as a decimal
  Average(4,VWC(),IEEE4,False)
  Minimum(4,VWC(),IEEE4,False,False)
  Maximum(4,VWC(),IEEE4,False,False)

  'MPS6 data. Record time stamp for max/min temperature.
  'Suction in kPa,Temp in celsius
  Average(8,MPS6(),IEEE4,False)
  Minimum(8,MPS6(),IEEE4,False,True)
  Maximum(8,MPS6(),IEEE4,False,True)
  TableFile("CRD:Trees_Daily",8,-1,0,1,day,0,0)
EndTable
```

```
'Data table for raw data
DataTable(Trees_Raw,true,-1)
  DataInterval(0,1,Day,10)
  'GS1 Raw Data (single ended measurements in mV)
  Average(4,RawVWC(),IEEE4,False)
  Minimum(4,RawVWC(),IEEE4,False,False)
  Maximum(4,RawVWC(),IEEE4,False,False)
  TableFile("CRD:Trees_Raw",8,-1,0,0,day,0,0)
EndTable


'Main Program
BeginProg
  'Main Scan
  Scan(30,Min,1,0)
    'Default CR6 Datalogger Battery Voltage measurement 'BattV'
    Battery(BattV)
    'Default CR6 Datalogger Wiring Panel Temperature measurement 'PTemp_C'
    PanelTemp(PTemp_C,60)

    ChargeStateArr(1) = "Regulator Fault"
    ChargeStateArr(2) = "No Charge"
    ChargeStateArr(3) = "Current Limited"
    ChargeStateArr(4) = "Cycle Charging"
    ChargeStateArr(5) = "Float Charging"
    ChargeStateArr(6) = "Battery Test"
    ChargeSourceArr(1) = "None"
    ChargeSourceArr(2) = "Solar"
    ChargeSourceArr(3) = "Continuous"
    CheckBatteryArr(1) = "Normal"
    CheckBatteryArr(2) = "Check Battery"
    Delay(0,1,sec)
    SW12(1,1)
    VoltSe(RawVWC(),4,mV5000,U1,True,500,60,1,0)
    For Count = 1 To 4
      VWC(Count)=((3.464*(10^-10))*(RawVWC(Count)^3))-((1.316*(10^-
6))*(RawVWC(Count)^2))+((1.878*(10^-3))*RawVWC(Count))-0.9192
    Next Count
    SW12(1,0)
    Delay(0,1,sec)


    'read SDI-12 Sensors
```

```
    SW12(2,1)
    Delay(0,1,sec)
    For NCount=1 To 4
      SDI12Recorder(MPS6(NCount,1),C1,NCount,"M!",1,0)
      Delay(0,1,sec)
    Next NCount
    SW12(2,0)

    'read CH200
    SDI12Recorder (CH200_M0(),C1,0,"MC!",1.0,0)
    'Array values start with one. Values for charge state start with -1.
    'Have to shift the value by two to line it up with the correct words
    'in the array.
    ChargeState = ChargeStateArr(Chg_State + 2)
    'Values for charge source start with zero. Have to shift the value
    'by one to line it up with the correct words in the array.
    ChargeSource = ChargeSourceArr(Chg_Source + 1)
    'Values for check battery start with zero. Have to shift the value
    'by one to line it up with the correct words in the array.
    CheckBattery = CheckBatteryArr(Ck_Batt + 1)


    'Call Data Tables and Store Data
    CallTable Trees_Daily
    CallTable Trees_Raw
  NextScan
EndProg
```

APPENDIX D: INITIAL DATA VERSUS TIME

Control

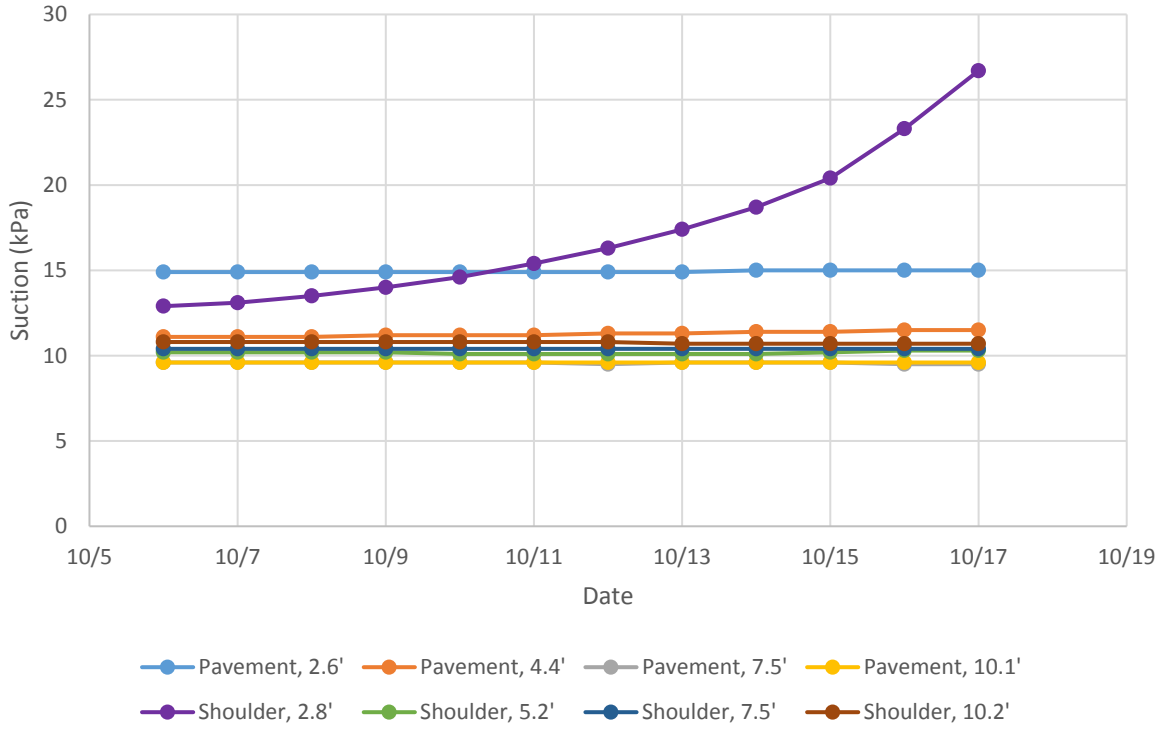

Figure 90: Control, Suction vs. Time

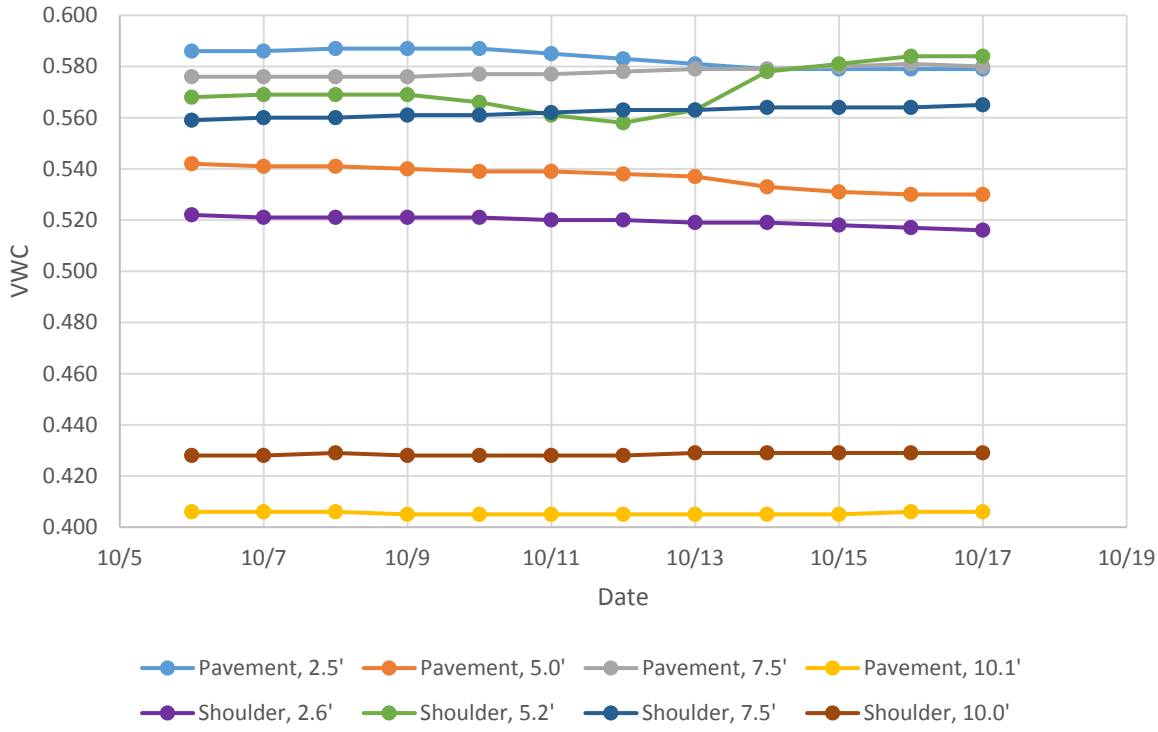

Figure 91: Control, VWC vs. Time

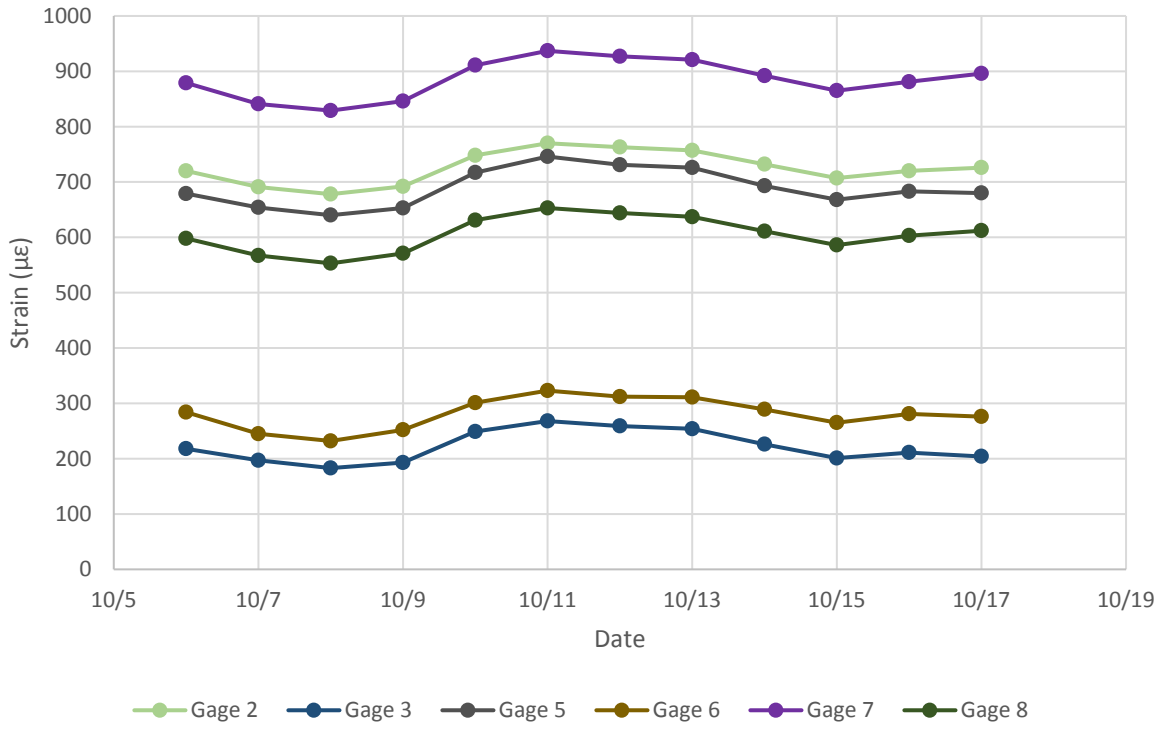

Figure 92: Control, Asphalt Strain vs. Time

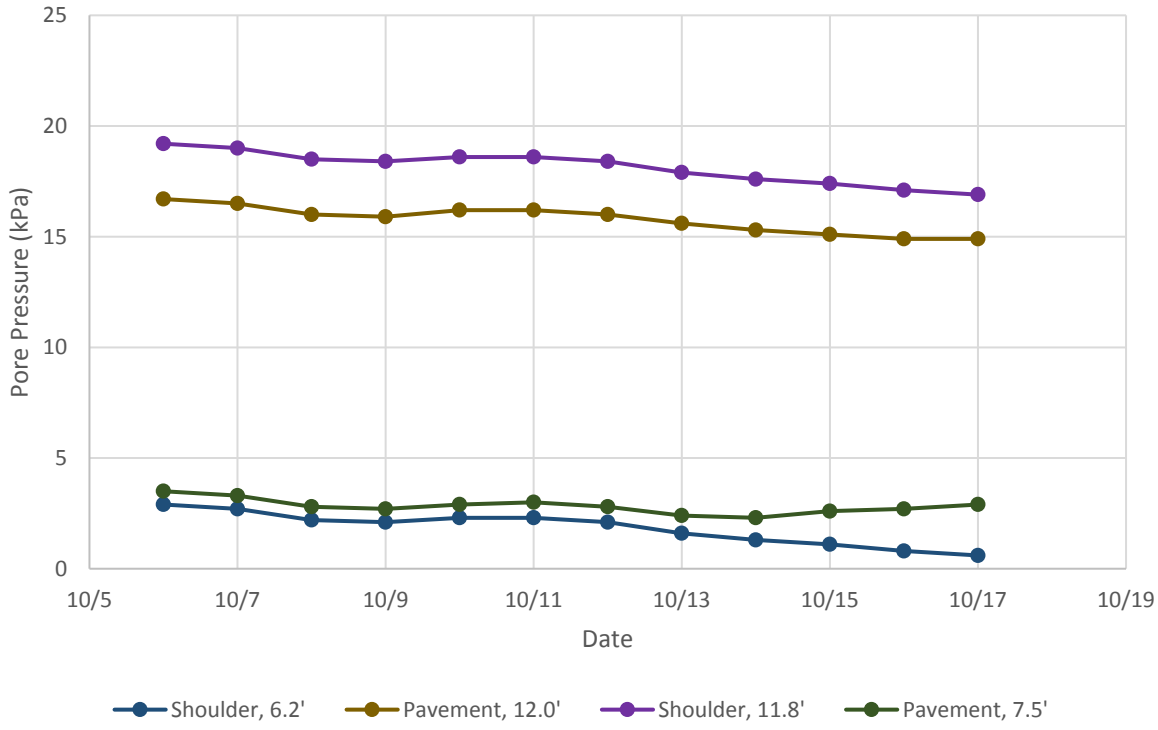

Figure 93: Control, Pore Pressure vs. Time

Sand Blanket

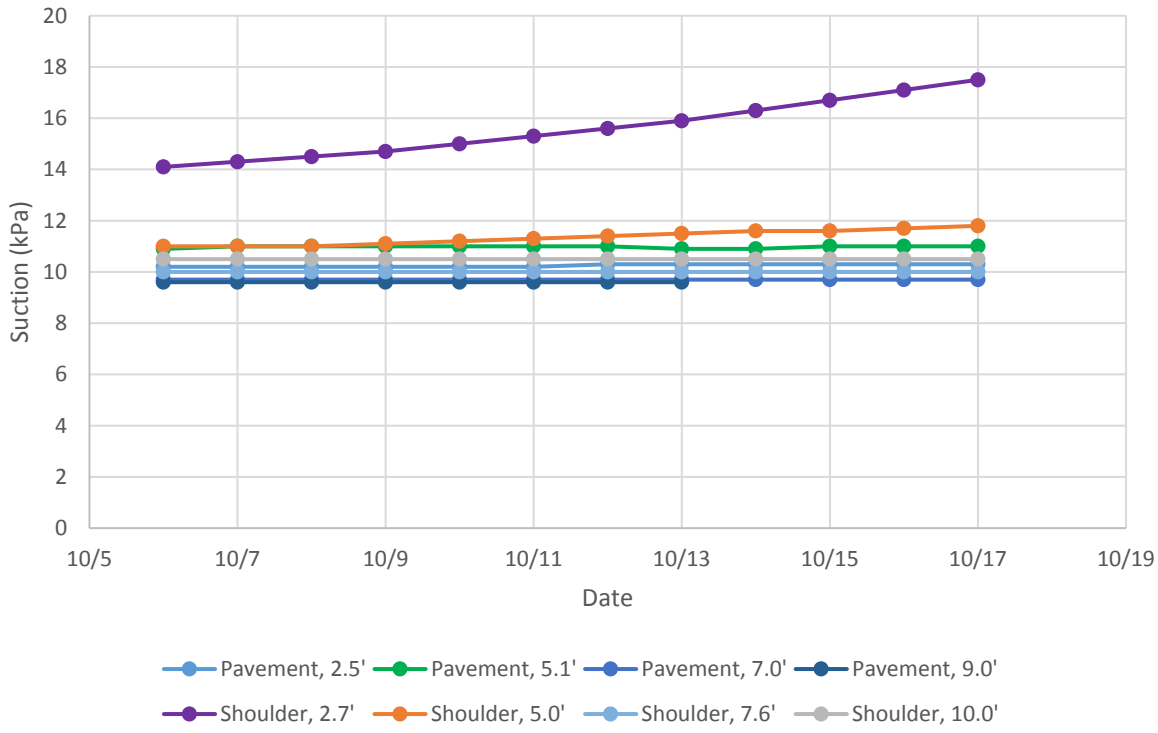

Figure 94: Sand Blanket, Suction vs. Time

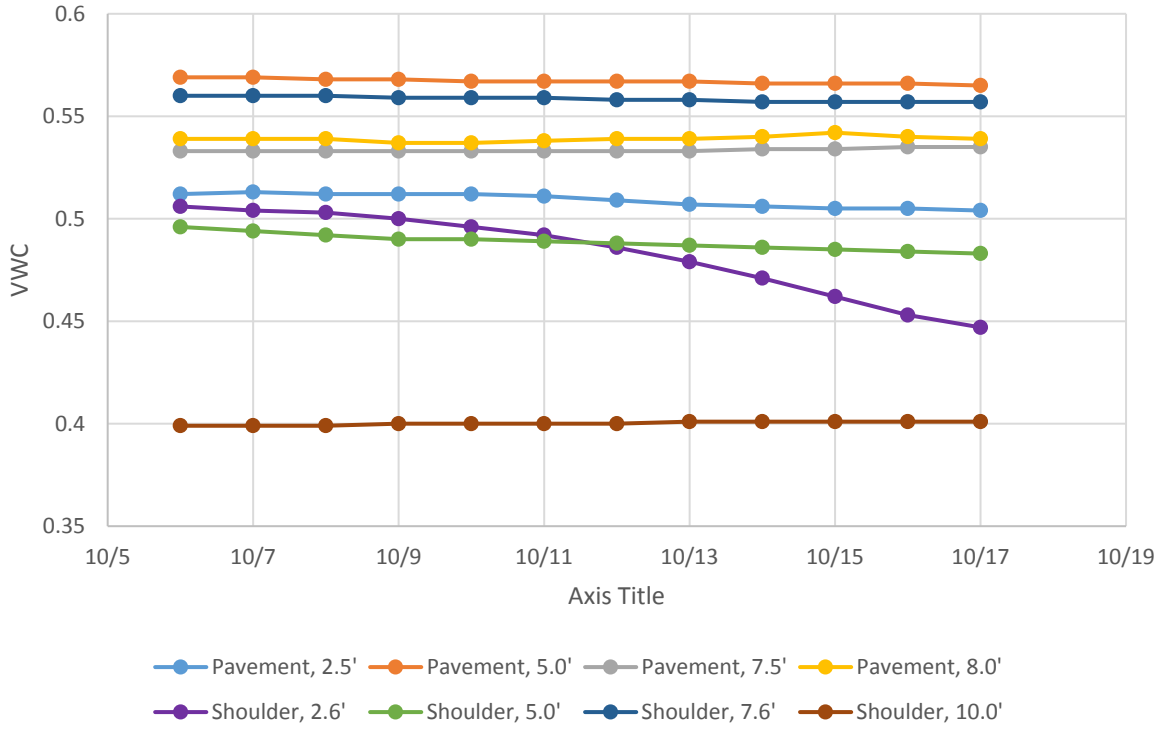

Figure 95: Sand Blanket, VWC vs. Time

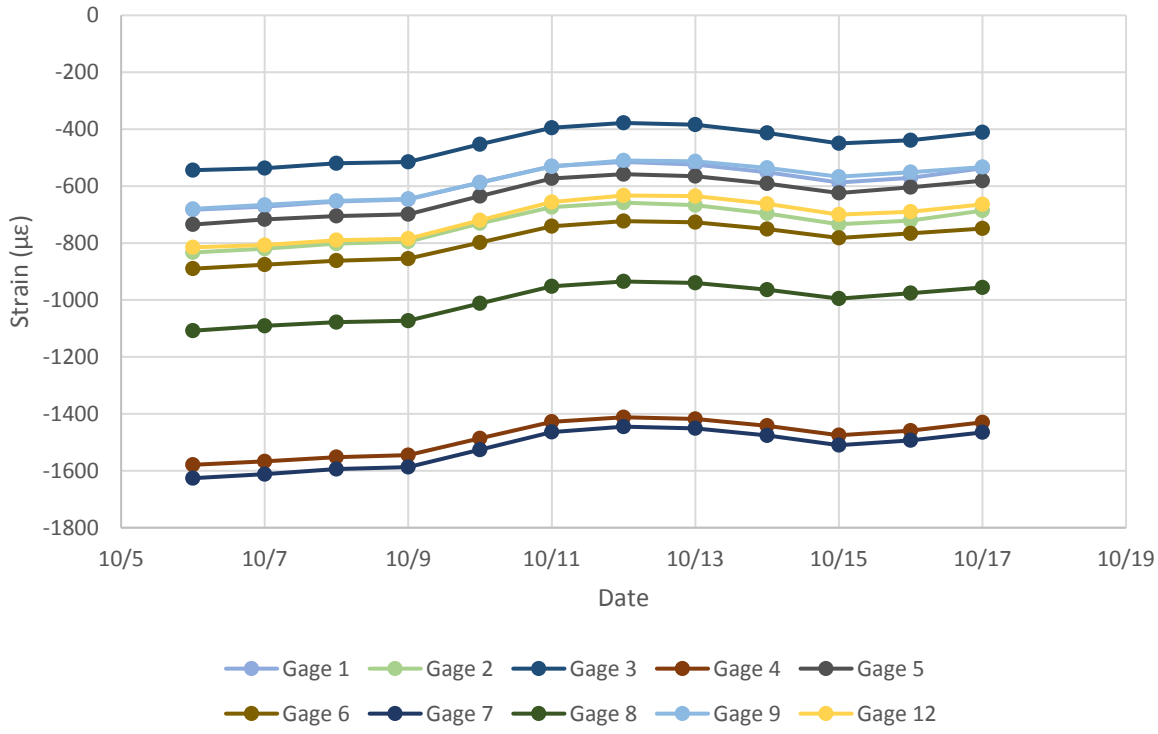

Figure 96: Sand Blanket, Asphalt Strain vs. Time

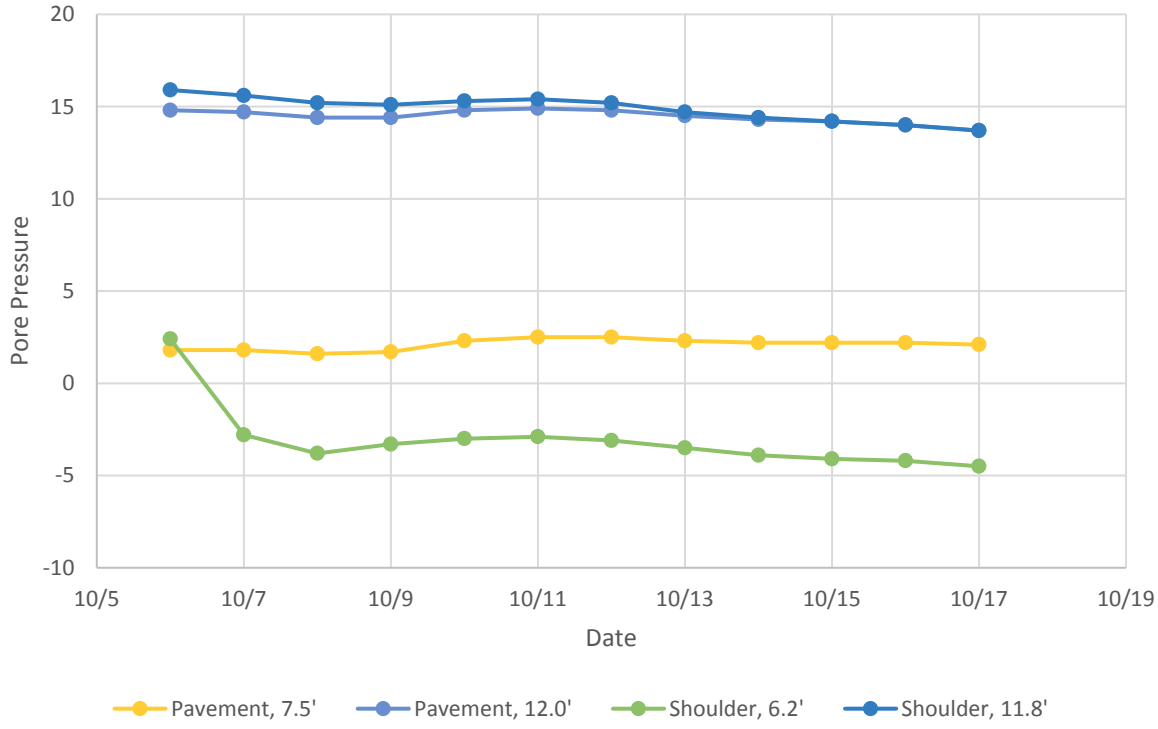

Figure 97: Sand Blanket, Pore Pressure vs. Time

Vertical Moisture Barriers

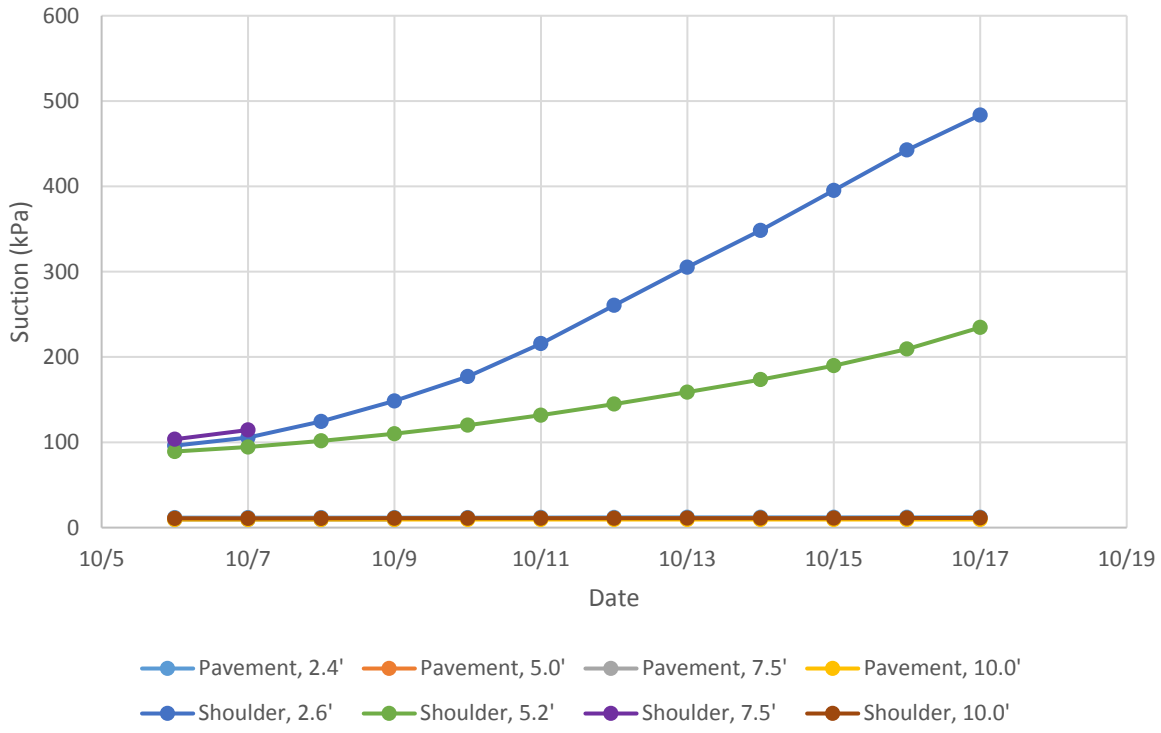

Figure 98: Vertical Moisture Barriers, Suction vs. Time

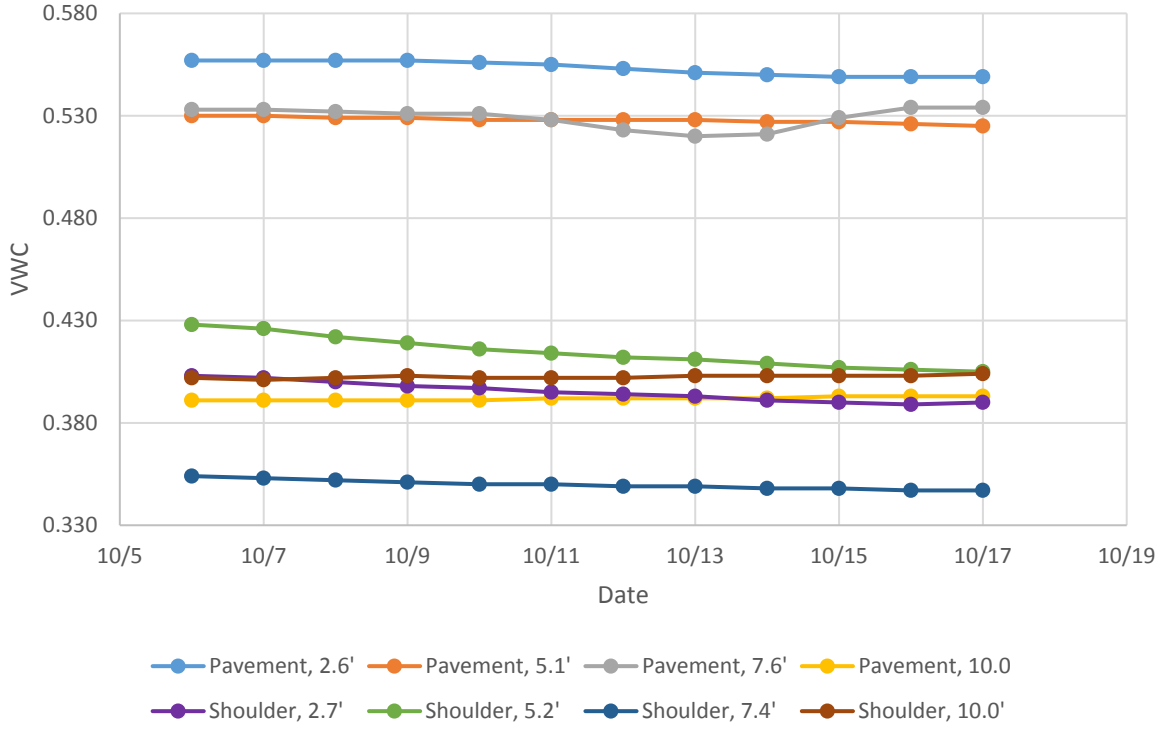

Figure 99: Vertical Moisture Barriers, VWC vs. Time

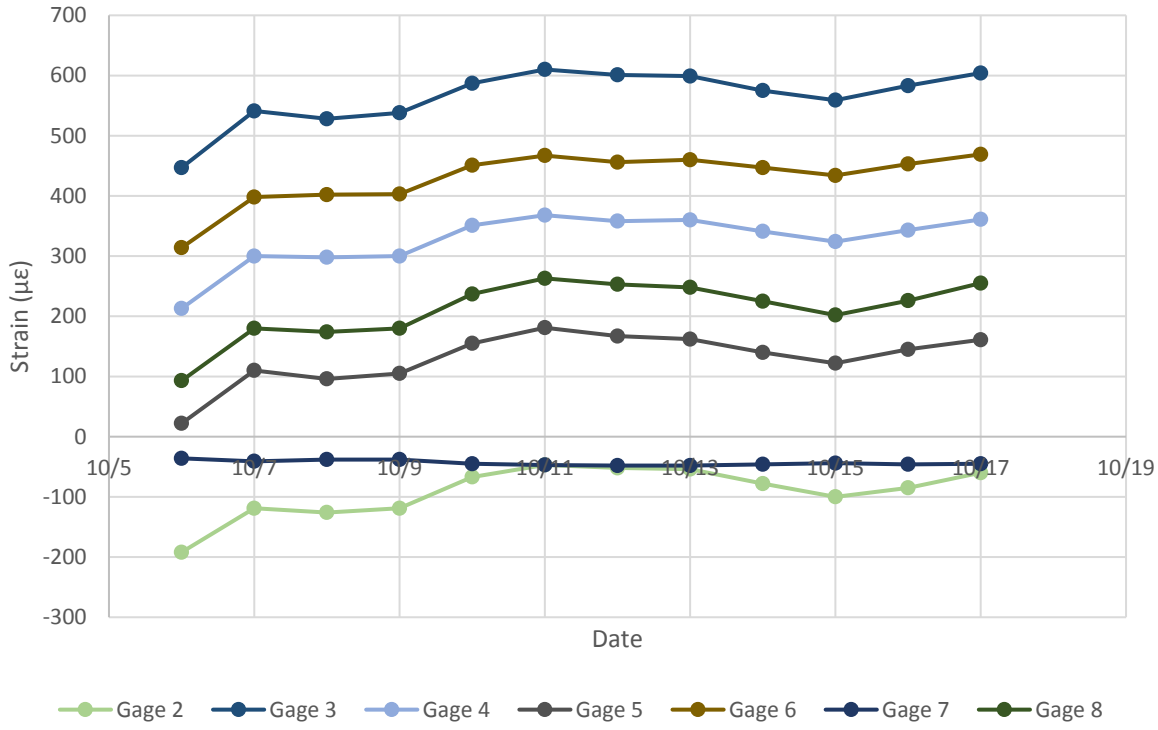

Figure 100: Vertical Moisture Barriers, Strain vs. Time

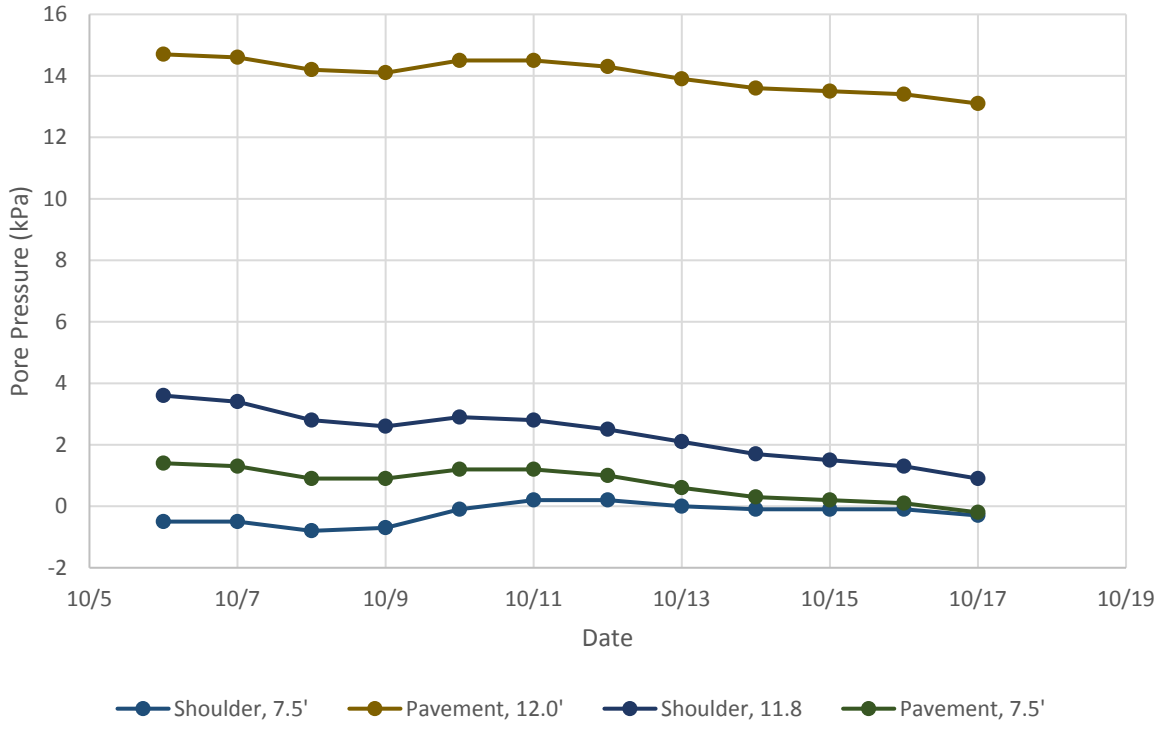

Figure 101: Vertical Moisture Barriers, Pore Pressure vs. Time

Lime Columns

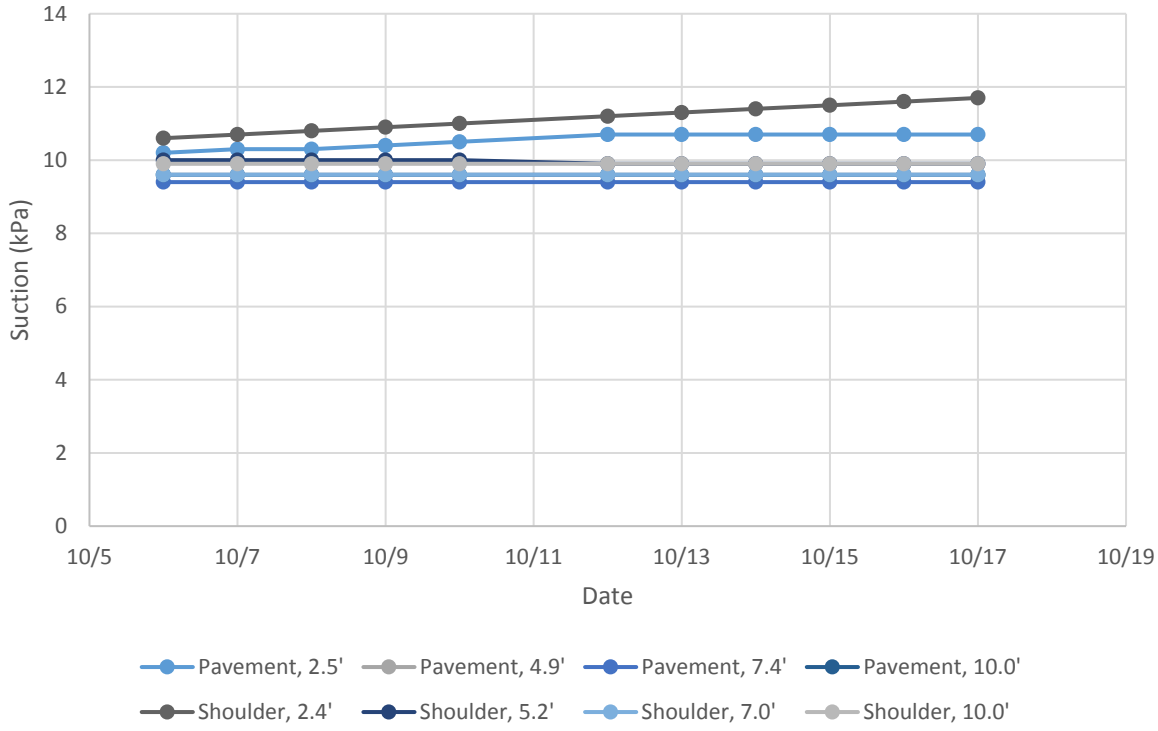

Figure 102: Lime Columns, Suction vs. Time

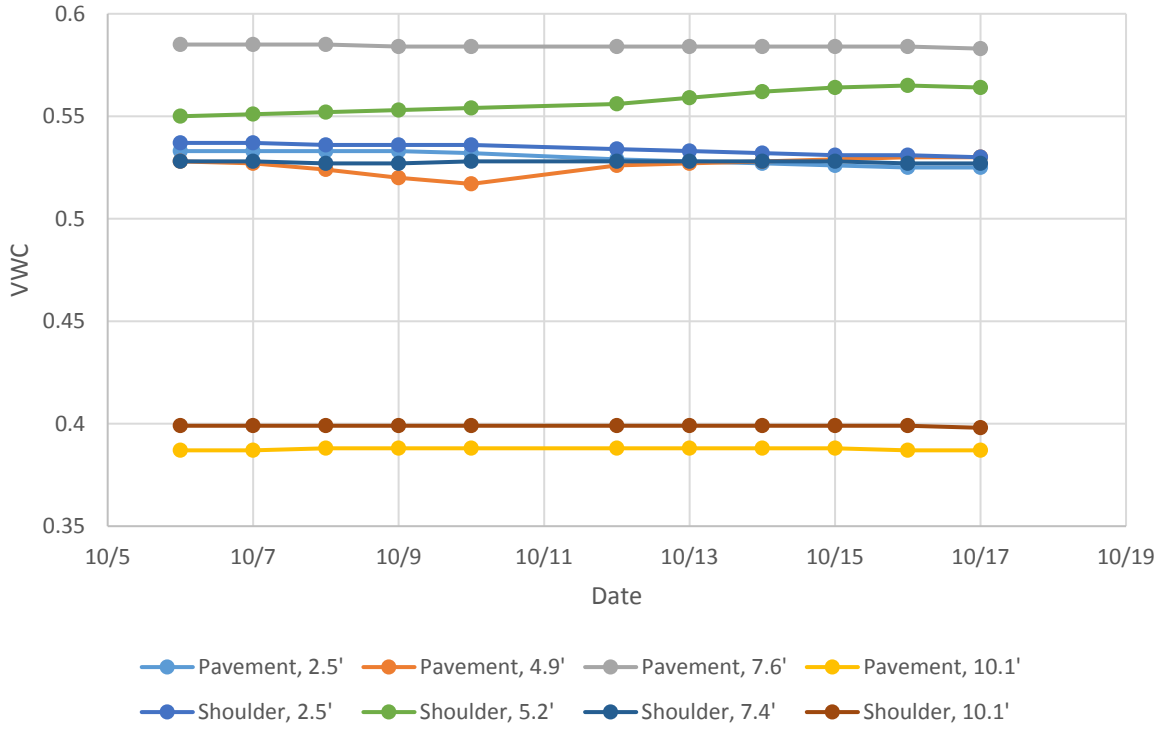

Figure 103: Lime Columns, VWC vs. Time

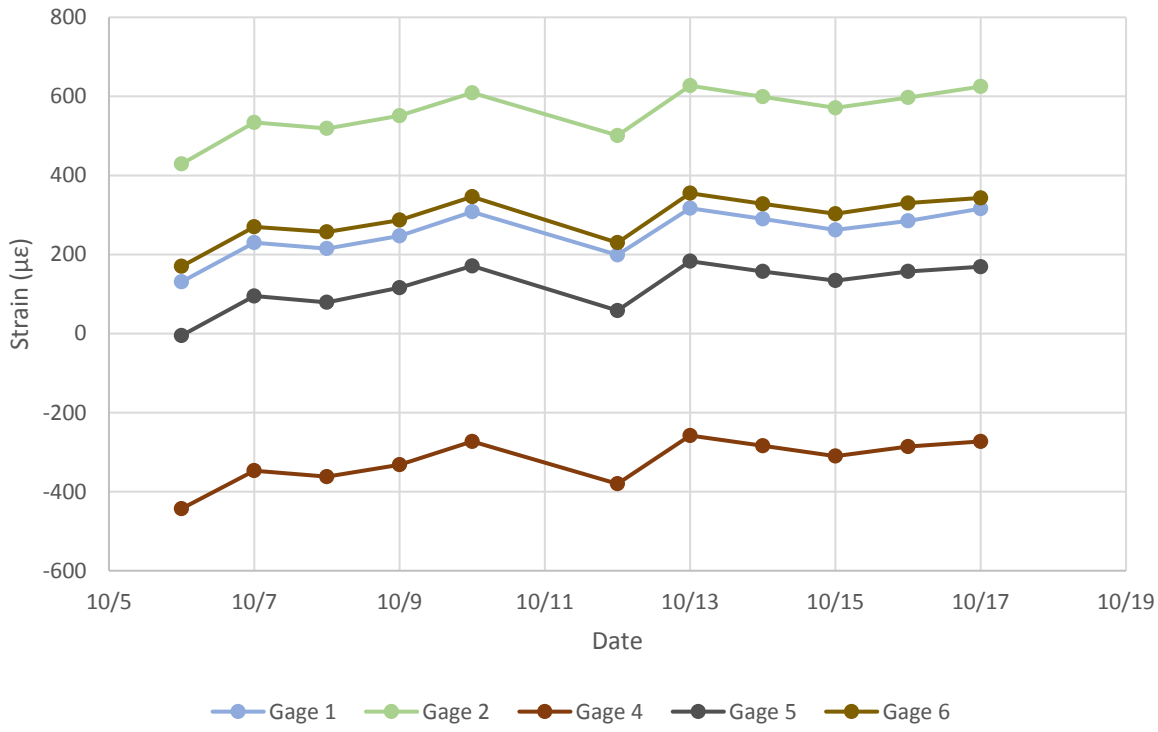

Figure 104: Lime Columns, Asphalt Strain vs. Time

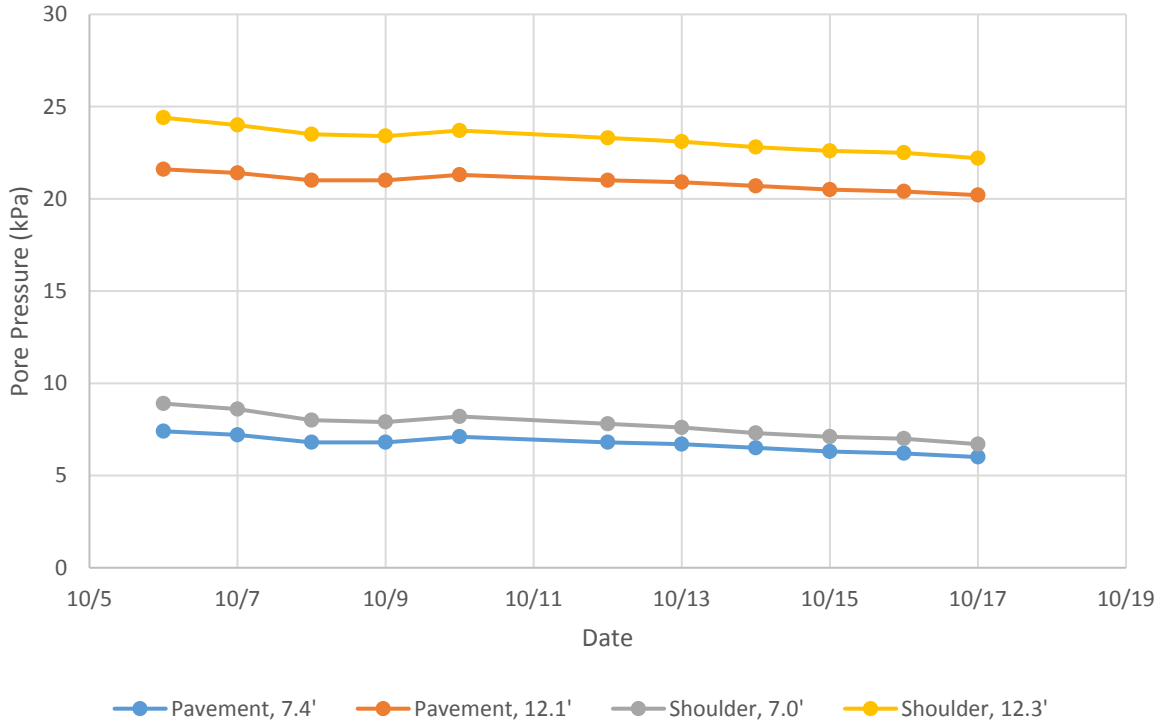

Figure 105: Lime Columns, Pore Pressure vs. Time

Paved Shoulders

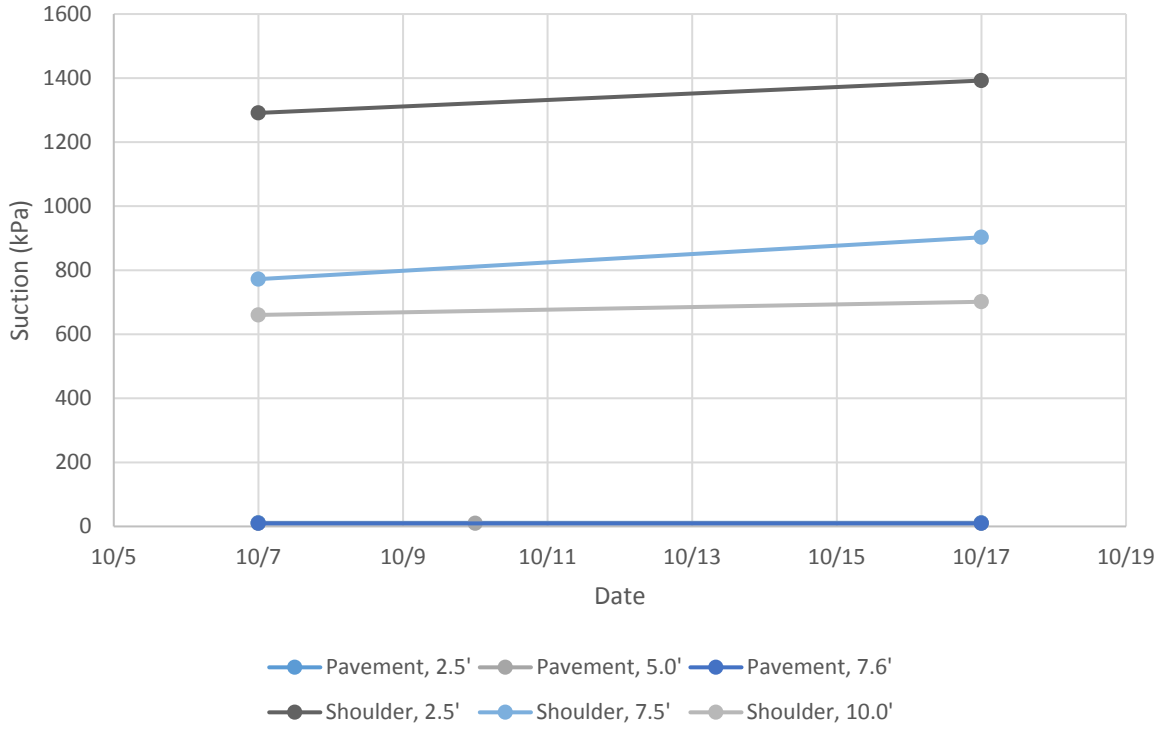

Figure 106: Paved Shoulders, Suction vs. Time

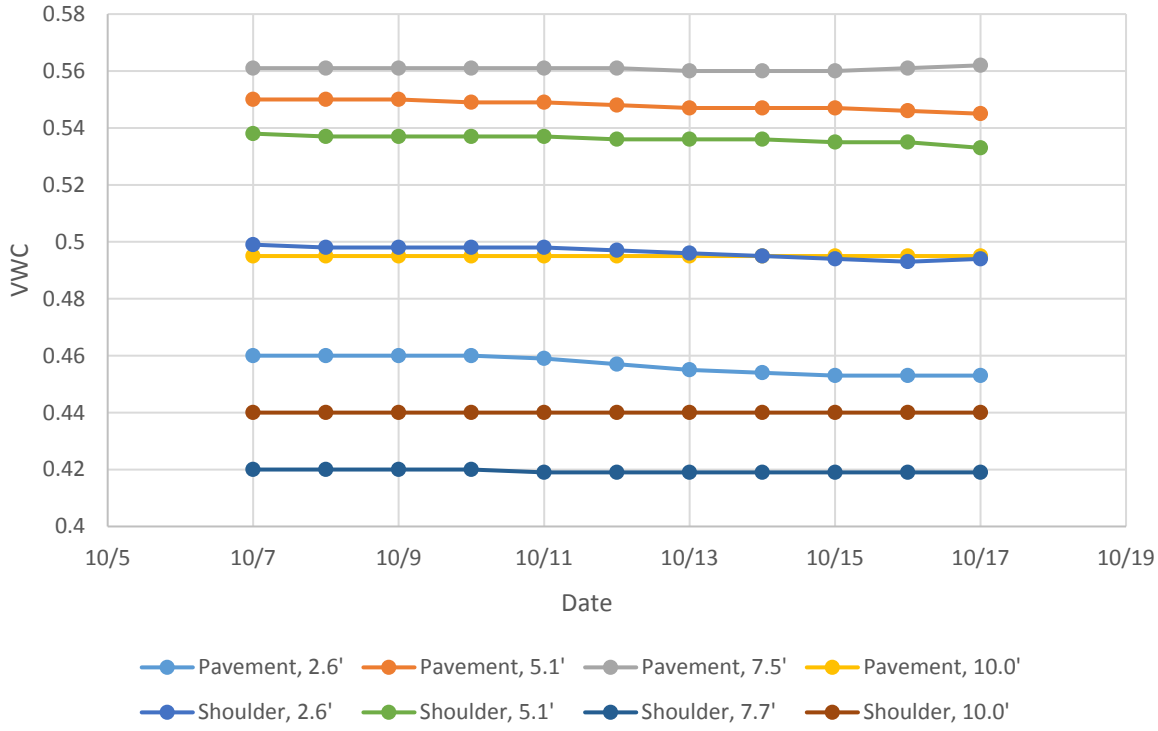

Figure 107: Paved Shoulders, VWC vs. Time

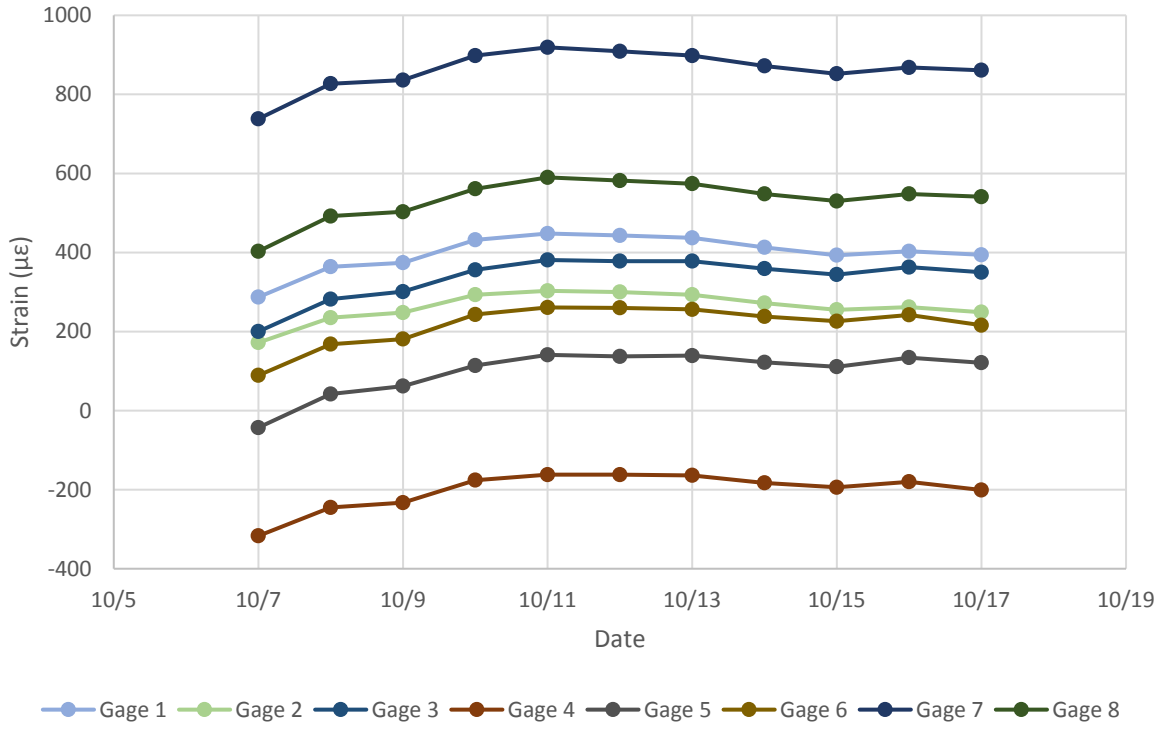

Figure 108: Paved Shoulders, Asphalt Strain vs. Time

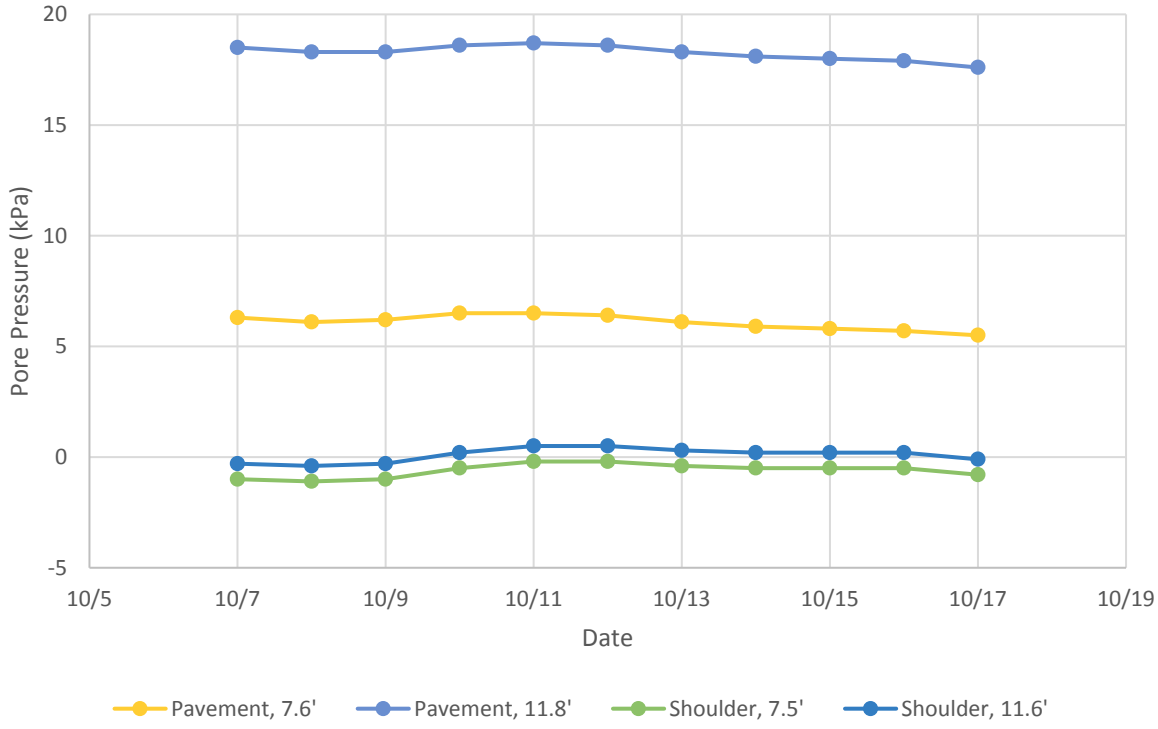

Figure 109: Paved Shoulders, Pore Pressure vs. Time

Edge Drains

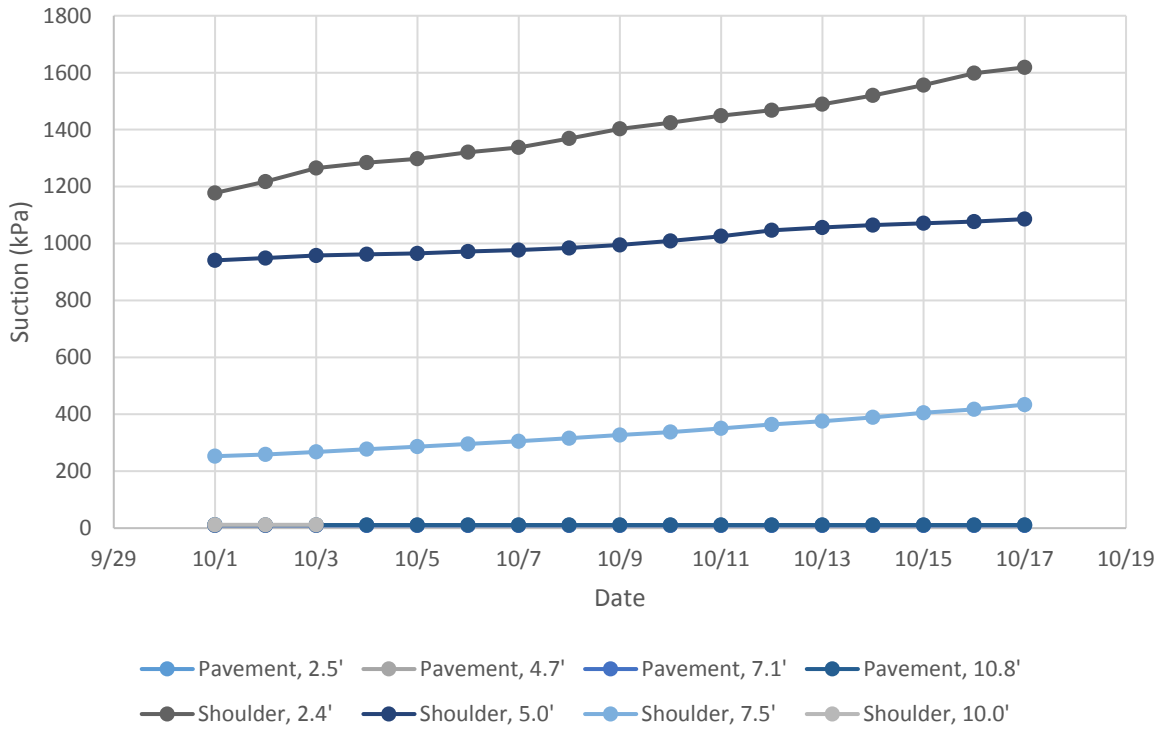

Figure 110: Edge Drains, Suction vs. Time

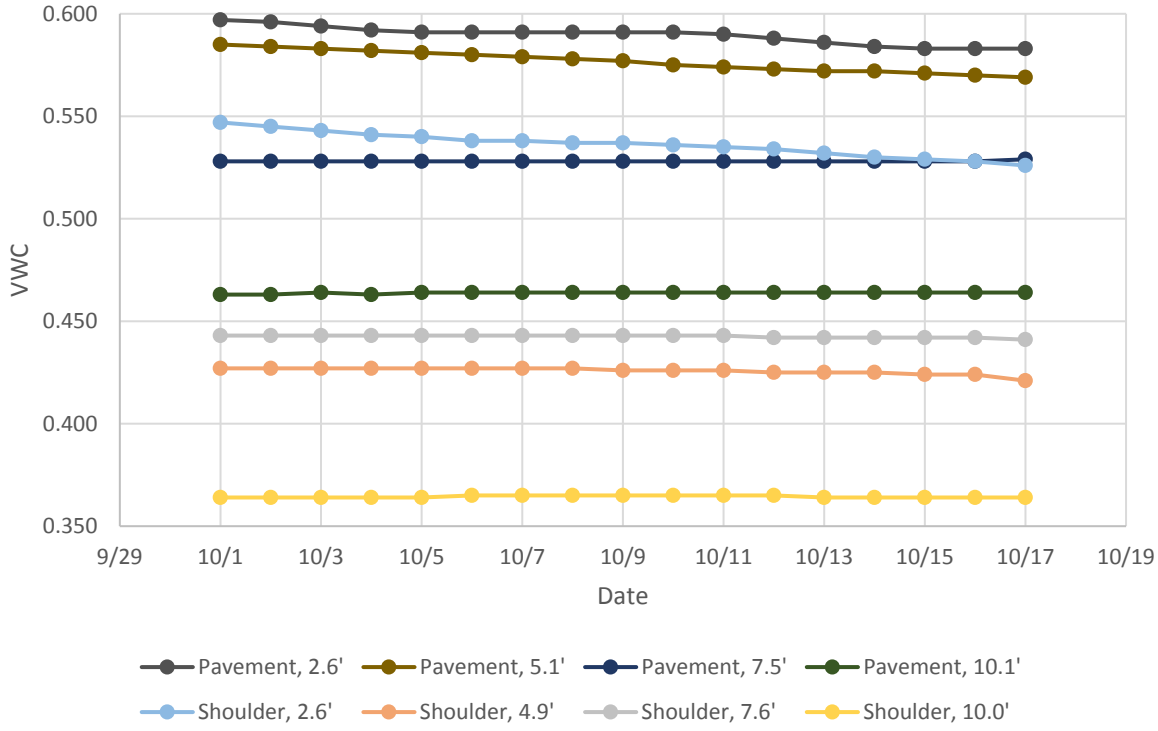

Figure 111: Edge Drains, VWC vs. Time

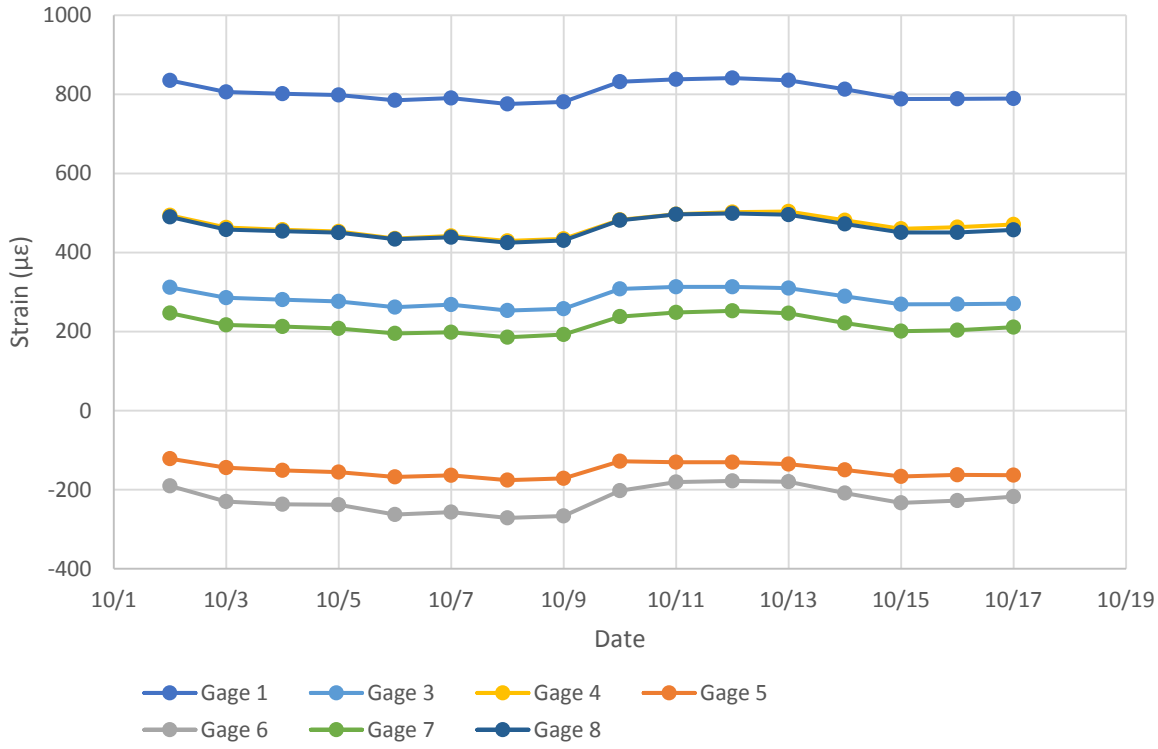

Figure 112: Edge Drains, Asphalt Strain vs. Time

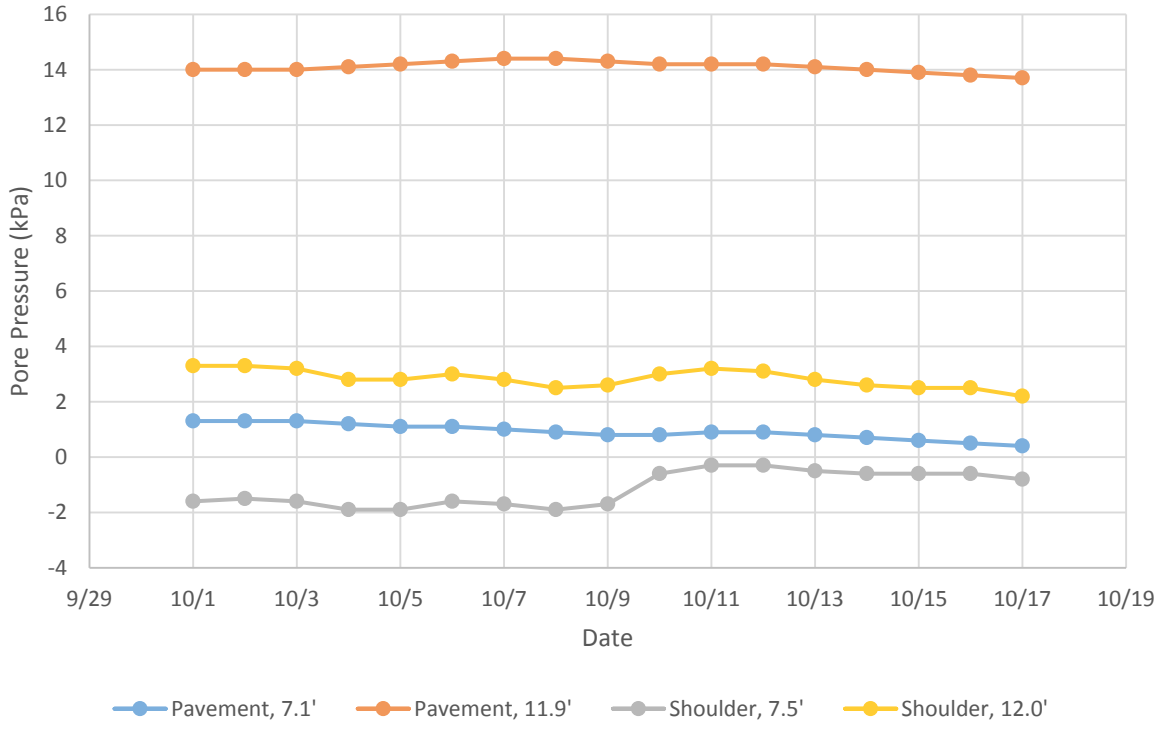

Figure 113: Edge Drains, Pore Pressure vs. Time